LUND UNIVERSITY

Nanowires in Cell Biology

Persson, Henrik

2014

Nanowires in Cell Biology

Exploring Interactions and Applications

Doctoral Thesis

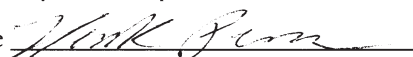Henrik Persson

LUND
UNIVERSITY

Faculty opponent

Jean-François Berret

Université Paris Diderot

Organization LUND UNIVERSITY	Document name Doctoral Dissertation
	Date of issue 2014-07-30
Author: Henrik Persson	Sponsoring organization

Nanowires in Cell Biology – Exploring Interactions and Applications

Abstract

This thesis explores the interactions between cells and nanowires, to increase our understanding of how cells are affected and how they can be manipulated by these one-dimensional, semiconductor crystals (lengths 1-10 µm, diameters <100 nm). These are much smaller than most mammalian cells (10-30 µm in diameter), and it is generally held that nanowires can be interfaced with cells without adverse effects. On this assumption, several nanowire-based applications have been explored, yet few studies investigate how basic cellular functions are affected.

We have studied how the dimensions of nanowires affect fundamental cell behaviour in cells. We found that increasing nanowire length reduces cell migration and interferes with cell division. Cells interfaced with as few as 50 nanowires are inhibited in their migration. Increasing the density of nanowires has minor effects on migration and division until a threshold density is reached when the cells are able to adhere to the tips of the nanowires rather than the substrate, enabling migration. Based on these results, we hypothesize that it is possible to tune nanowire dimensions to control the degree of cell migration and proliferation, enabling experiments where cells are immobilized for continuous observation over several generations. Our results can further be used to limit adverse effects in nanowire-based cell biological applications.

As part of our cell-nanowire interaction studies, we have worked toward a microfluidic injection system based on oxide nanotubes to improve both existing, standard injection systems and nanowire-based experimental versions. We demonstrate the successful fabrication of key parts of this system and its fluidic transport ability, important steps toward a fully functional nanosyringe device, capable of serial injection and retrieval of cell material. To improve future studies regarding the interactions between semiconductor nanowires and cells, we developed inherently fluorescent nanowires and showed that it is possible to fabricate nanowires with alternating fluorescent and non-fluorescent segments, creating a barcode design useful for systematic studies.

These results will prove useful for research groups working towards cell biological applications based on similar nanostructures, both for injections, cell migration and otherwise.

Key words Nanowires, living cells, phase holographic microscopy, cell injection	
Classification system and/or index terms (if any)	
Supplementary bibliographical information	Language English
ISSN and key title	ISBN 978-91-7623-062-6 (print) 978-91-7623-063-3 (electronic)
Recipient's notes	Number of pages 178	Price
	Security classification	

I, the undersigned, being the copyright owner of the abstract of the above-mentioned dissertation, hereby grant to all reference sources permission to publish and disseminate the abstract of the above-mentioned dissertation.

Signature _Henrik Persson_ Date 30/1-2014

Nanowires in Cell Biology

Exploring Interactions and Applications

Doctoral Thesis

Henrik Persson

LUND
UNIVERSITY

Division of Solid State Physics
Department of Physics
Lund University

Front cover: Scanning electron micrograph showing mouse fibroblasts cultured on a dense array of gallium phosphide nanowires.

Backside cover: Scanning electron micrograph showing nanowires clinging together, as seen from above.

Preface

In this thesis, we have studied the fundamental interactions between cells and nanowires in an effort to improve nanowire-based applications, such as cell injections, in cell biology. The thesis is of a highly interdisciplinary nature, dealing with physics and cell biology in the form of advanced nanofabrication, cell culturing and microscopy. The work described herein was carried out during the years 2009-2014 at two separate laboratories at Lund University. The nanofabrication was performed at Lund Nanolab at the Division of Solid State Physics, Department of Physics, while the biological experiments were conducted at the Division of Functional Zoology at the Department of Biology. The microscopy-based evaluations of the results were carried out in both locations.

I hope you will enjoy reading this work at least half as much as I have enjoyed conducting the research.

/Henrik

Malmö 30/7-2014

Abstract

This thesis explores the interactions between cells and nanowires, in order to increase our understanding of how cells are affected by, and how they can be manipulated by these one-dimensional, semiconductor crystals (lengths 1-10 μm, diameters <100 nm). Since nanowires are much smaller than most mammalian cells (10-30 μm in diameter), it is generally held that these can be interfaced with cells without adverse effects. On this assumption, several nanowire-based applications have been explored, yet few studies investigate how basic cellular functions are affected.

Here, we have studied how the dimensions of nanowires affect fundamental cell behaviour in cells. We found that increasing nanowire length reduces cell migration and interferes with cell division. Cells interfaced with as few as 50 nanowires are inhibited in their migration. Increasing the density of nanowires has minor effects on migration and division until a threshold density (around 2000 nanowires per cell) is reached when the cells are able to adhere to the tips of the nanowires rather than the substrate, enabling migration. Based on these results, we hypothesize that it is possible to tune nanowire dimensions to control the degree of cell migration and proliferation, enabling experiments where cells are immobilized for continuous observation over several generations. Our results can further be used to limit adverse effects in nanowire-based cell biological applications.

As part of our cell-nanowire interaction studies, we have worked toward a microfluidic injection system based on oxide nanotubes to improve both existing, standard injection systems and nanowire-based experimental versions. We demonstrate the successful fabrication of key parts of this system and its fluidic transport ability, important steps toward a fully functional nanosyringe device, capable of serial injection and retrieval of cell material. To improve future studies regarding the interactions between semiconductor nanowires and cells, we developed inherently fluorescent nanowires and showed that it is possible to fabricate nanowires with alternating fluorescent and non-fluorescent segments, creating a barcode design useful for systematic studies.

These results will prove useful for research groups working towards cell biological applications based on similar nanostructures, both for injections, cell migration and otherwise.

Acknowledgements

The research I have been involved in over the past five years has involved a lot of people without whom it would neither have been possible nor as enjoyable as it (mostly) has been. Most important for the research has of course been my advisors, Jonas Tegenfeldt, Christelle Prinz, Stina Oredsson and Lars Samuelson, who have lent me part of their expansive knowledge and experience. In the beginning, Jonas, assigned me a master's project working with Christelle on cell cultures in PDMS devices together with Martin Kanje at the biology department, setting me on the path to biophysics and cell-surface interactions. Christelle must have been content as Jonas later chose to hire me as a grad student. From the oxide nanotubes we initially had in mind, the project soon changed direction toward cell-nanowire interactions. Expanding into a more biology-heavy research field, I felt some assistance wouldn't be amiss, and luckily I managed to recruit Stina to aid us with her endless knowledge. Together, the five of us, with a lot of help from a variety of collaborators and co-workers, have conducted the research described in these pages.

This research has been greatly aided by our co-authors. Jason Beech, whose insights into microfluidics were of great use in the cell injection project. Kalle Adolfsson, Jesper Wallentin and Magnus Borgström who made the fluorescent nanowires possible. The assistance we received from across Öresund, where Carsten Købler and Kristian Mølhave helped study the intimate and abusive relationship between cells and nanowires. I have also had the pleasure of assisting Cassandra Niman and Aleksandra Dabkowska in our work on lipid-coated nanowires and to help Farnaz Yadegari and Susanne Norlén during their master projects.

Not only our collaborators have contributed to the research in this thesis. A lot of good ideas, constructive feedback and important assistance have come from the people around me. The occasionally weekly meetings in the biogroup together with Stefan Holm, Mercy Lard, Zhen Li, Dmitry Suyatin, Heiner Linke, Martina Balaz, Johanna Generosi, Waldemar Hällström and Gaëlle Piret as well as several students. At the biology department, John Stegmayr and Xiaoli Huang have aided me with their biological expertise. Alexander Berg and Sebastian Lehman have always been keen to share their MOVPE related experience with me and Alexander has more than once donated precious Aixtron tool time to Kalle and me which has been greatly appreciated. Of course, a special mention should go to Dmitry who once upon a time taught me to run the machine and the countless hours Kalle, Mercy and I have spent growing nanowires together.
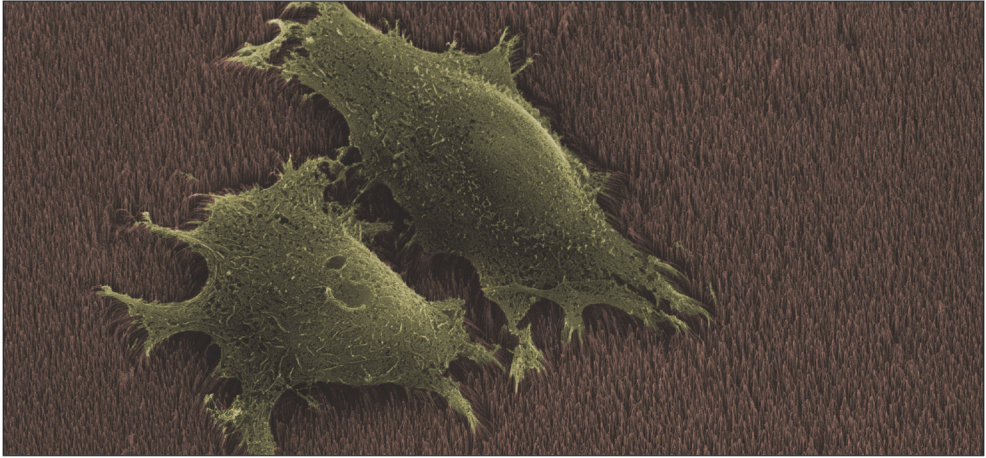
Nanotrådar som cellbiologiska verktyg

Ett nytt verktyg håller på att utvecklas inom cellbiologin. Ett verktyg baserat på nanospikmattor. Spikmattorna består av så kallade nanotrådar vilka undersöks för tillämpningar inom elektronikindustrin, med allt från solceller till transistorer i visionerna. För ca tio år sedan fick forskare även upp ögonen för möjliga tillämpningar inom cellbiologi, vilket är vad denna avhandling handlar om. Närmare bestämt har vi jobbat med att utveckla ett nanoinjektionssystem och studerat hur celler samverkar med nanotrådar.

Cellbiologi – grunden till allt liv

Allt levande vi ser omkring oss är uppbyggt av celler. Precis som alla varelser är väldigt olika så är även celler det. Både mellan olika arter men även inom enskilda djur. Generellt för nästan alla djurceller är att de omges av ett flexibelt cellmembran och har en kärna i mitten som innehåller djurets DNA. Cellerna innehåller också en mängd olika proteiner som likt maskiner i en fabrik utför alla jobb som gör att cellen fungerar.

Vad gäller forskning på dessa komplexa system så kan man betrakta en cell som en svart låda och cellbiologens jobb är att peta på lådan, se vad som händer och försöka gissa hur lådan ser ut inuti. För att kunna stimulera cellerna har flera olika verktyg utvecklats. Det är just inom detta område som nano-trådarna kommer in i bilden: idén är att dessa små strukturer enkelt kan reta cellerna utan att påverka för mycket.

Endimensionella kristaller

I Lund används ordet "*nanopinnar"* eller *"nanotrådar"* för att beskriva avlånga nano-kristaller som har växts fram, ett atomlager i taget. Denna noggranna process gör att man har god kontroll över nanotrådarnas elektriska egenskaper vilket möjliggör både solceller och lysdioder.

Inom cellbiologi är man intresserad av nanotrådarnas ringa storlek. Tanken är att de är tillräckligt små för att man ska kunna manipulera cellerna utan att skada dem. Vad nanopinnarna kommer att användas till inom biologin är inte helt klart. Några forskargrupper använder nanotrådarna som elektriska kontakter medan andra studerar styrning av nervceller, stamcellsdifferentiering och kraft-mätningar.

Nanoinjektioner

Ett vanligt experiment inom cellbiologi går ut på att introducera främmande substanser som DNA, proteiner och läkemedel i celler. Denna typ av experiment försöker många forskar-grupper nu genomföra med nano-pinnar. Ett sätt att göra detta är att härma förgiftade pilar: man fäster molekyler på nanopinnarna och sen lägger man dit cellerna. Tanken är att cellerna spetsas på nanotrådarna och att molekylerna då tar sig in i cellerna. Med denna taktik har flera grupper lyckats föra in molekyler i olika typer av djurceller.
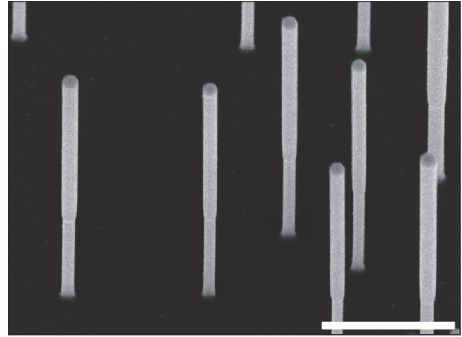
Elektronmikroskopbild av nanotrådar.
Med hjälp av epitaxi kan man få nanotrådar att växa rakt upp från en yta. Skalstreck är 1 μm.

En stor begränsning med denna metod är att det inte är möjligt att genomföra flera injektioner vid olika tidpunkter. Denna begränsning är något vi försöker åtgärda i denna avhandling genom att omvandla nanopinnarna till ihåliga nanorör. Tanken är att nanorören kan fungera mer som de sprutor med ihåliga nålar vi är vana vid från sjukhus. Detta skulle möjliggöra injektion av flera olika molekyler vid olika tidpunkter. Det skulle också bli möjligt att ta ut material från cellerna och analysera detta.
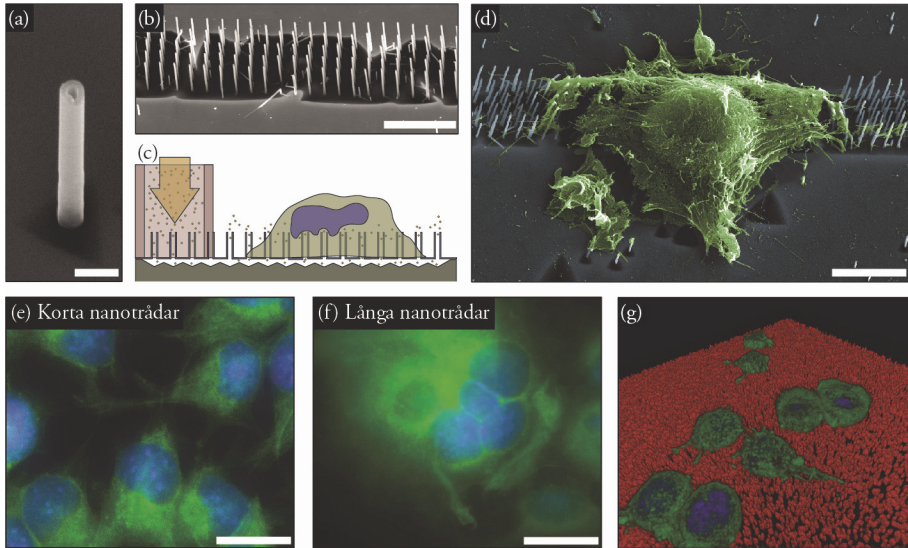
Avhandlingskollage. I det här arbetet har vi lyckats koppla ihop nanorör (a) med en mikrokanal under provets yta (b-c). Här visas också en cell som fäst sig vid nanorören (d). Den stora, gröna cellen med fyra blå cellkärnor (f), missformad kärna visar hur snett det kan gå om cellerna odlas på för långa nanotrådar, jämfört med kortare trådar (e). Här visas en 3D bild av grönfärgade celler som odlats på rödlysande nanopinnar (g). Skalstreck är 250 nm (a), 5 μm (b, d), och 20 μm (e, f).

Hur påverkas cellerna?

Om vi ska använda nanotrådar för att studera celler måste vi förstå hur nanopinnarna själva påverkar cellerna. Genom att filma våra celler har vi sett att när de odlas på ytorna ändras deras normala beteende beroende på hur tätt pinnarna står och på deras längd. Om trådarna är för långa blir cellerna intrasslade och kan inte längre krypa runt. Celldelningen påverkas också, med stora, vanskapta celler som resultat. Om cellerna däremot odlas på korta nanopinnar så kan de röra sig och dela sig nästan normalt. Vi fann också att om nanotrådarna stod tillräckligt tätt så uppstod en spikmatte-effekt och cellerna kunde krypa ovanpå trådarna istället för att nålas fast.

Cellbiologernas nya verktyg

Det verkar som att cellbiologin håller på att få ett nytt verktyg baserat på ytor med nanotrådar. En av de många lovande tillämpningarna är att föra in främmande material i celler. I denna avhandling har vi arbetat mot detta mål och även studerat hur nanotrådar påverkar celler, viktig kunskap oavsett vilka försök som görs med nanotrådar i slutändan. När vi har lärt oss mer om hur nanotrådar kan användas kommer dessa nya verktyg kunna bidra med ökad kunskap om cellers funktioner. Kunskap som kan leda till nya läkemedel och medicinska behandlingar.

List of publications

This thesis is based on the work presented in the following papers, denoted as Papers I-IV in the text.

I. Vertical oxide nanotubes connected by subsurface microchannels

Persson Henrik, Beech Jason P., Samuelson Lars, Oredsson Stina, Prinz Christelle N., Tegenfeldt Jonas O.

Nano Research, 2012, *5*(3), 190–198

Together with my coauthors, I adapted previously published fabrication protocols to a new material system and explored new fabrication methods. I carried out the nanofabrication as well as the experiments, both with cell cultures and fluidics. I wrote the paper.

II. Fibroblasts cultured on nanowires exhibit low motility, impaired cell division, and DNA damage

Persson Henrik, Købler Carsten, Mølhave Kristian, Samuelson Lars, Tegenfeldt Jonsas O., Oredsson Stina, Prinz Christelle N.

Small, 2013, *9*(23), 4006–16, 3905.

I performed the experiments after initial design together with my coauthors, with the exception of the focused ion beam milling experiments, which were carried out by Købler in Copenhagen. I carried out data analysis and wrote the majority of the paper.

III. Fluorescent nanowire heterostructures as a versatile tool for biology applications

Adolfsson Karl[†], <u>Persson Henrik</u>[†], Wallentin Jesper, Oredsson Stina, Samuelson Lars, Tegenfeldt Jonas O., Borgström Magnus T., Prinz Christelle N.

[†]These authors contributed equally to the work.

Based on an initial recipe by Wallentin and Borgström, Adolfsson and I developed the recipe further through a series of growth related experiments and evaluations, using input from our coauthors. Adolfsson and I fabricated the nanowires and carried out characterisation of these with assistance from Wallentin. I performed the cell biological experiments while Adolfsson worked with Drosophila.

IV. From immobilized cells to motile cells on a bed of nails: effects of vertical nanowire array density on cell behaviour

<u>Persson Henrik</u>, Tegenfeldt Jonas O., Oredsson Stina, Prinz Christelle N.

Submitted

Together with my coauthors, I designed the study. I performed the experiments and carried out data analysis and wrote the initial manuscript.

Related publications

The following publications fall outside the scope of this thesis.

I. Nanofluidics in hollow nanowires

Sköld Niklas, Hällström Waldemar, <u>Persson Henrik</u>, Montelius Lars, Kanje Martin, Samuelson Lars, Prinz Christelle N., Tegenfeldt Jonas O.

Nanotechnology, 2010, 21(15), 155301-155304

II. Fluid and highly curved model membranes on vertical nanowire arrays

Dabkowska Aleksandra P., Niman Cassandra S., Piret Gaëlle, <u>Persson Henrik</u>, Wacklin Hanna P., Linke Heiner, Prinz Christelle N., Nylander Tommy

Nano Letters, 2014, published online 2014-06-27

III. Enhanced laminin adsorption on nanowires compared to flat surfaces

Hammarin Greger, <u>Persson Henrik</u>, Dabkowska Aleksandra P., Prinz Christelle N.

Colloids and Surfaces B, 2014, 122, 85-89

List of abbreviations

A list of abbreviations used in this thesis.

ACS	American Chemical Society
AFM	Atomic force microscopy
ALD	Atomic layer deposition
BS	Back scatter
Calcein AM	Calcein-acetomethoxyl
CLSM	Confocal laser scanning microscopy
CPD	Critical point drying
dsDNA	Double-stranded DNA
DTU	Denmark's Technical University
EBL	Electron beam lithography
ECM	Extra cellular matrix
EDTA	Ethylene-diamine-tetraacetic acid
EthD-1	Ethidium homodimer-1
FITC	Fluorescein isothiocyanate
GFP	Green fluorescent protein
MOVPE	Metal organic vapour phase epitaxy
MTT	3-(4,5-dimethylthiazol-2-yl)-2,5-diphenyltetrazolium bromide
PBS	Phosphate buffered saline
PCR	Polymerase chain reaction
PDMS	Poly-dimethyl-siloxane
PI	Propidium iodide
PS	Polystyrene
RIE	Reactive ion etching
ROS	Reactive oxygen species
SEM	Scanning electron microscopy
siRNA	Short interfering RNA
SLB	Supported lipid bilayer
SPM	Scanning probe microscopy
STED	Stimulated emission depletion

STORM	Stochastic optical reconstruction microscopy
TEM	Transmission electron microscopy
TMAl	Trimethyl-aluminium
TMGa	Trimethyl-gallium
TMIn	Trimethyl-indium
UVL	UV-lithography
VLS	Vapour-liquid-solid

Table of contents

1 Introduction

The interdisciplinary work in this thesis was carried out with two aims:

Aim 1: Explore fundamental interactions between mammalian cells and nanowires to further the field of nanowire-based applications in cell biology by improving both device design and the interpretation of the results obtained.

Aim 2: Improve existing nanowire-based injection systems by exploring the use of nanotubes incorporated into a fluidic system for cell injection.

To fulfil these two aims, we have cultured mammalian cells on GaP nanowires (Figure 1.1 d) and we have worked toward converting these nanowires into hollow, oxide nanosyringes. To describe this work, this thesis is divided into four main chapters. Following this introductory chapter, the second chapter describes the most important experimental methods used, such as nanofabrication and microscopy. The third chapter discusses applications of nanowires in cell biology, those found in the literature and those explored by us, with a focus on nanowire-based cell injection, the topic of Paper I. The fourth chapter describes cell-nanowire interactions and consists of an extensive literature study along with our results from Paper II and IV and attempts to shed light on how cells interact with nanowires. The fourth chapter also deals with our work on developing fluorescent nanowires for improved cell-nanowire interaction studies, as described in Paper III.

1.1 Nanotechnology and nanowires

The field of nanotechnology is often said to have started with the words *"There's plenty of room at the bottom"*, spoken by Richard P. Feynman during an after-dinner speech at the annual meeting of the American Physical Society in 1959 [1]. Since then, the field of nanotechnology has grown tremendously, keeping pace with the development of new tools to observe and manipulate matter on the nanoscale. Today, nanotechnology is used extensively in everyday life, particularly in the computer industry where the defining features are rapidly shrinking; Samsung's and Apple's latest

phones (Galaxy 5 and iPhone 5) [2], for instance, uses chipsets with a gate size* of 28 nm, or approximately 100 atoms. Nanotechnology is not only confined to the computer industry but is finding an increased use in other everyday applications such as sun screens [3], anti-fouling coatings in the shipping industry [4] and stronger materials through nanocomposites [5] to name a few.
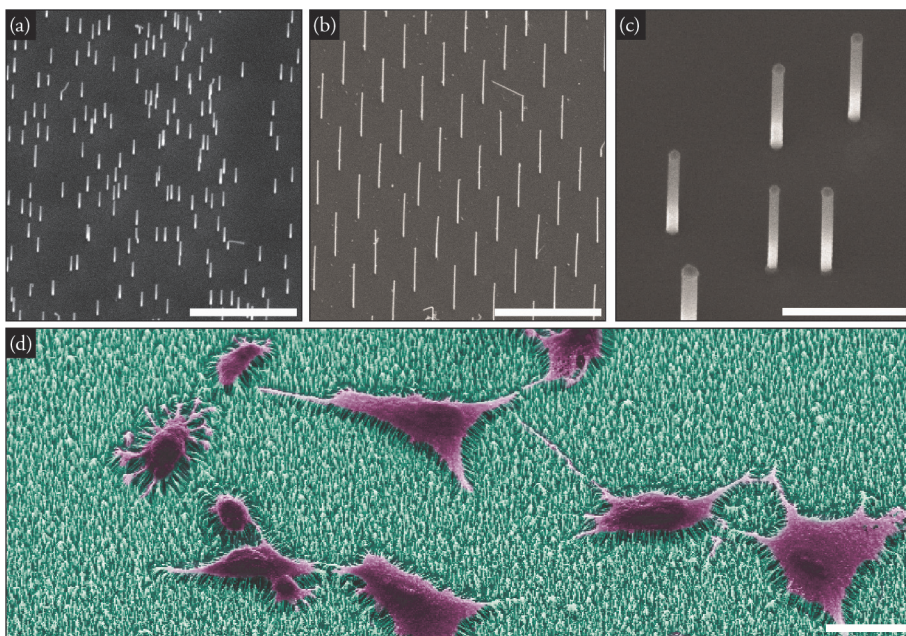
Figure 1.1 The GaP nanowires used in this thesis are long, thin crystals, standing vertically on a substrate from which they are grown. They can be grown in a random distribution (a) or in ordered arrays (b). The close up (c) shows the gold particles on the tips of the nanowires, used to control their diameter and location. When cells are cultured on top of arrays of nanowires they create a tight interface with these (d). This interaction is what has inspired many researchers to investigate potential applications of nanowires in cell biology. Scale bars are 5 μm (a, b), 1 μm (c) and 20 μm (d). Tilt 30 ° for all images.

In the 1960s, a method to grow semiconductor nanowires [6] was discovered. These nanostructures (Figure 1.1 a-c) are typically 1-10 μm long, have diameters below 100 nm and are fabricated in a self-assembly process: a sample is placed in a reactor and by tuning conditions, such as the chemical environment and the temperature, the nanowires form spontaneously. Historically, the field started with the growth of silicon nanowires but around thirty years ago, the field expanded to include III-V nanowires.

---

* A gate is the key component in a transistor, the heart of any computer. The smaller the gate, the more transistors you can have per unit area, enabling more and faster computations.

The roman numerals III and V refer to group 13 and 15 in the periodic table which include elements like Al, Ga and In (group 13), and N, P and As (group 15). One of the most important properties of these nanowires is the possibility to combine different semiconductor materials[*] into a single, nanoscale structure (referred to as a heterostructure). Different semiconductors have different optical and electrical properties. Using nanowires, these properties can be tailored to create nanoscale light emitting diodes [7], solar cells [8] or transistors [9]. The high degree of control over geometry and electrical properties also make nanowires uniquely suited to conduct basic quantum mechanical research around the behaviour of electrons [10], [11] and other subatomic particles [12], [13].

1.2 Cells and nanowires

Physicists and biologists working across the border between the two disciplines are investigating medical applications of nanotechnology such as implants [14], cancer treatment [15]–[17] and neural interfaces [18]. In 2007, the field of nanobiotechnology expanded to include semiconductor nanowires [19], [20]. The idea is that, since the diameters of nanowires are much smaller than mammalian cells (<100 nm compared to 10-30 μm), these could be used to manipulate and probe cellular behaviour. In general, these applications are solely based on the nanowires' physical dimensions, allowing nanowires to closely interface with the cells (Figure 1.1 d). These intimate interactions have been used to create neuronal networks [21], [22], control stem cell differentiation [23] or measure the electric activity of cells [24], [25]. In this thesis, we have explored the use of nanotubes derived from nanowires as a base for cellular injection (Paper I), a topic receiving attention by other groups as well [26]–[28].

With the multitude of applications being explored, the fundamental question of the status of the cells is often neglected. It is assumed that since the cells are present and the application appears to work, the cells are intact and maintain normal behaviour, an assumption which does not always hold (Papers II and IV). In this thesis, we have explored the interactions between cells and nanowires to learn more about this system which is of great importance for both interpreting results and for minimizing any potential impact nanowires might have on cells. These studies have relied heavily on microscopy-based techniques. Different versions of optical microscopy have been used to visualize the cells and characterize their behaviour while electron microscopy has been used to investigate the physical interface between the cells and the nanowires.

---

[*] Combining different semiconductor materials is not always possible in microscale structures due to lattice mismatch, i.e. the difference in atomic spacing creates defect forming strain between the two materials.

1.3 Microscopy

This thesis relies heavily on microscopy to study the interactions between cells and nanowires and for routine imaging during nanofabrication. The optical microscope was first introduced by Hans and Zacharias Janssen in 1595 and later popularized by Robert Hooke and Antonie van Leeuwenhoek [29], [30]. Hooke used the microscope to study the microscopic structures of life and published the book Micrographia for the general public, in which he coined the phrase "cell" to describe the compartmentalization he observed in plants [31] (Figure 1.2 b) (it should be noted that these structures were not living cells but rather the cell walls of plant cells, i.e. their dead remains [29], [32]). Leeuwenhoek has been dubbed the "father of microbiology" and the "father of microscopy" for his leading role in creating high quality microscopes, leading to his discoveries of both bacteria and single cells [30], [33]. The extensive study of quantum mechanics in the late 19th and early 20th centuries eventually led to Ernst Ruska's invention of the electron microscope in the 1930s, for which he received the Nobel Prize in Physics, 1986 [34]. The prize was shared with Gerd Binning and Heinrich Rohrer who invented scanning probe microscopy (SPM)[*], a technique capable of imaging and physically manipulating single atoms.

The inventions of and subsequent advances in optical and electron microscopy have enabled scientists to study the cellular structure of living organisms which has led to many breakthroughs in medicine, including the discovery of bacteria [33] and cellular organelles like the endoplasmic reticulum [35]. Medicine and biology have been greatly aided by the invention of the electron microscope, but it is its use in nanotechnology, along with SPM, where it is really indispensable. Without electron microscopy or SPM, nanoscientists would not be able to observe their work.

---

[*] SPM uses a sharp tip is moved across a surface similar to how the blind read brail. The tip is capable of both measuring Angstrom differences in height and pushing single atoms across a surface.
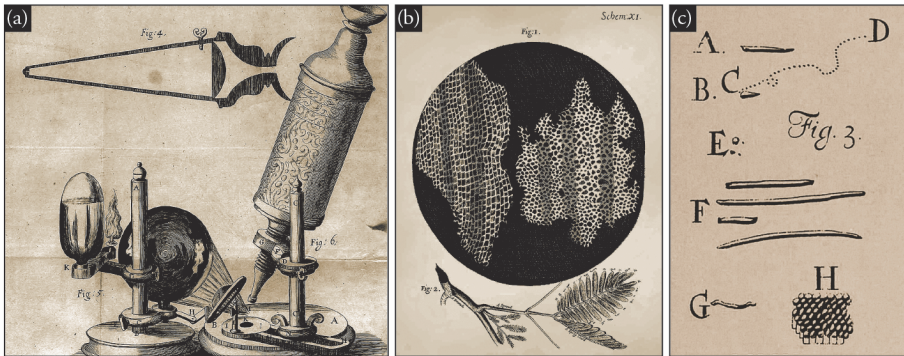
Figure 1.2 Hooke introduced microscopy to a wide audience through his book Micrographia based on observations through his microscope [31] (a). Among other discoveries, he introduced the concept of compartmentalised life, coining the phrase "cell" to describe what he saw (b) [31]. Leeuwenhoek was the first person to observe bacteria which he retrieved from his teeth and described in letters to the Royal Society in England (c) [33].

1.4 Cell biology and cell cultures

The invention of the microscope soon led to Leeuwenhoek's discovery of the cell [31], [33] and 150 years later, Schwann and Scheidler discovered that *all* living things consisted of cells [32]. Together with Remak [36], Virchov [32] and others, they laid the foundations for cell theory, describing how all beings consist of cells and how all cells are created from other cells (as opposed to the notion that life could spontaneously arise from non-living matter (e.g. horse hair turning into eels if dropped in water [37])).

Since this pioneering work, our knowledge and understanding of cells and their functions have grown tremendously. We now know that in a multicellular organism, there is a vast number of specialized cell types with different fundamental functions. In the human body, there are more than 200 kinds of cells, such as the easily recognisable neurons and red blood cells along with the white blood cells guarding us from diseases and the bone building osteoblasts. Animal cells (Figure 1.3), are bounded by a lipid cell membrane, responsible for regulating what enters and exits the cells. In order to fulfil its functions, the cell produces proteins that carry out almost all tasks in an organism, from relaying electrical signals to muscle contraction and oxygen transport. The proteins are created from blue prints stored in the cell's genetic code: the DNA stored in the cell nucleus, which is surrounded by the nuclear membrane or nuclear envelope. The cell contains a number of organelles with specific tasks. The mitochondria are responsible for converting sugar into fuel for proteins, lysosomes degrade objects and the ribosomes in the endoplasmic reticulum manufacture proteins.

Studying cells often involves keeping them alive outside of their host organism in a procedure called cell culturing. Animal cell culturing can trace its roots to the early 20th century, when Harrison [38], [39] and Carrel [39], [40] independently managed to keep animal cells alive and functioning outside the body. In 1952, Scherer, Syverton and Gey established the first, indefinitely dividing human cell line from a cervical cancer from their patient, Henrietta Lacks [39], [41], [42]. These advances established cell culturing as a research tool, which has proved immensely important for modern medicine by furthering our understanding of basic cell functions and aiding us in the development of new drugs. Today, cell culturing is a routine practice where animal cells are kept alive in an artificial *in vitro** system, mimicking the physiological *in vivo* environment from which they are derived. In the case of mammalian cells, this is usually performed by keeping the cells at 37 °C in flasks containing cell culture medium, a liquid with all components needed by cells such as amino acids, ions, sugars and various proteins. Under the correct conditions, the cells will multiply, generating a surplus of cells which can be used for medical and biological experiments, such as the nanotechnology-based investigations in this thesis.
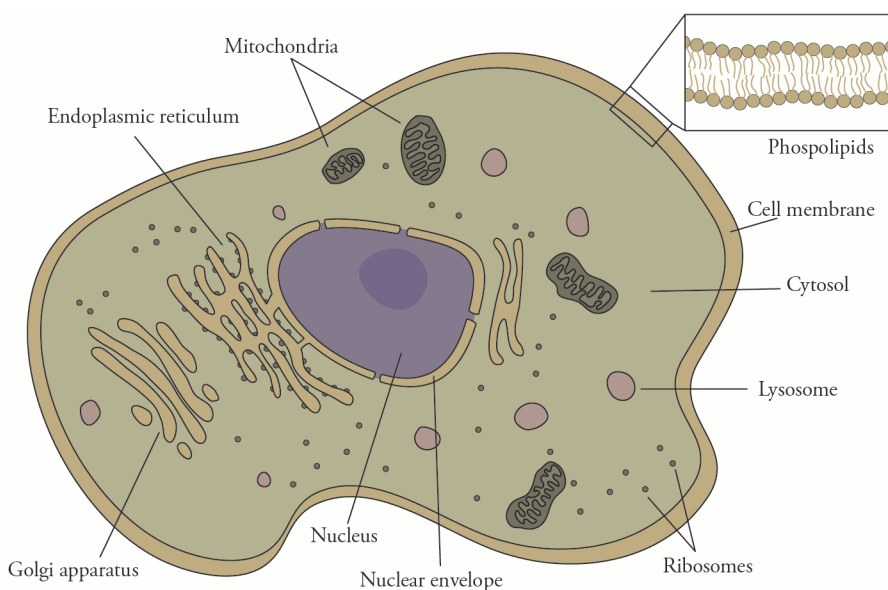
Figure 1.3 The animal cell is a highly complex entity, packed with structures, organelles and proteins necessary to maintain everyday function. A few of these structures are shown in this figure.

---

* *In vitro* and *in vivo* mean "in glass" and "in the living", respectively. These terms are used to differentiate between events taking place in a test tube, Petri dish or similar system (previously made of glass but the term has been transferred to plastic systems) and events in a living organism, respectively.

2 Experimental methods

The interdisciplinary work involving physics, and biology in this thesis relies on nanofabrication and characterization, concerning the former, and cell culturing and biological evaluation methods, concerning the latter. This chapter will describe a selection of methods that are of particular importance for the work presented in Chapters 3 and 4.

2.1 Methods in nanofabrication

Nanostructures can be generated in a multitude of different processes, from naturally formed carbon black generated in a candle flame [43] to the advanced nanoelectronics in a smartphone, carefully designed in elaborate, multistep processing [44]. In this thesis, advanced cleanroom[*] fabrication methods have been used to generate the structures studied. These methods include epitaxial growth of nanowires from gold nanoparticles, lithographic techniques to precisely control the location of the gold nanoparticles, deposition of metal and oxide films as well as wet and dry etching.

Creating arrays of nanowires such as those found in Paper I, relies on using lithography and gold deposition to control the location of the gold nanoparticles used to seed nanowire growth. These techniques are outlined below and summarized in Figure 2.1. In short, electron beam lithography (EBL) is used to create openings in a polymer layer (Figure 2.1 a, b). These openings can be filled with gold (Figure 2.1 c) and by subsequently removing the polymer layer and the surplus gold (Figure 2.1 d), the openings defined by the electron beam can be converted into gold nanoparticles on the substrate. The sample is then transferred into the growth chamber and nanowires are grown from the gold seed particles by supplying growth material and carefully controlling the environment (Figure 2.1 e).

---

[*] A cleanroom is a lab environment commonly used in micro- and nanofabrication. Precautions like circulating, filtered air and special clothing is used to minimize the amount of dust particles present as a single dust particle in the wrong place can ruin many days of work.
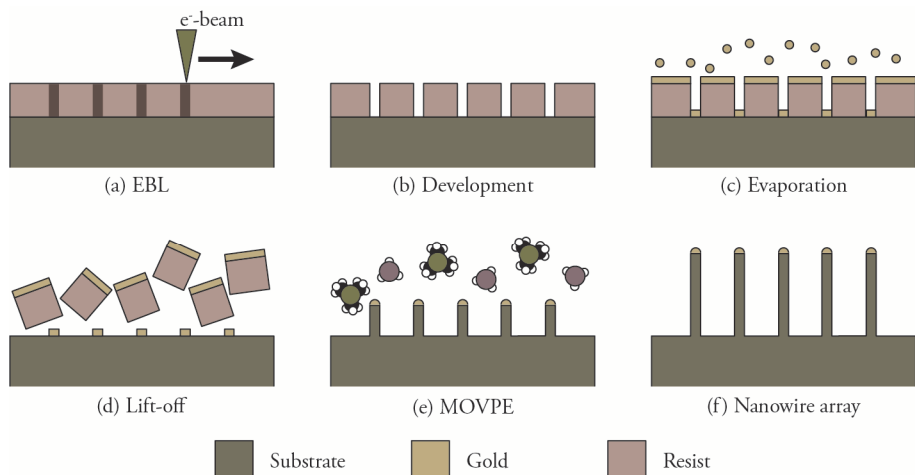
Figure 2.1 To create ordered arrays of nanowires, a series of techniques have to be combined. In this thesis, a polymer resist is exposed using EBL (a) and exposed parts are removed by a solvent (b). The sample is then coated with gold (c) and the resist is removed (d), leaving gold nanoparticles on the surface in a pattern defined by EBL. These gold nanoparticles are then used as catalysts for nanowire growth using MOVPE (e), resulting in well-defined arrays of nanowires (f).

Nanowire growth

The nanowires studied in this thesis are fabricated using particle-assisted metal organic vapour phase epitaxy (MOVPE), a bottom-up[*] process where the reactor environment is precisely controlled to promote the self-assembly of these vertical nanocrystals from metal seed particles. The growth process has been known since the 1960s when it was used to manufacture silicon nanowires [6], a process later expanded to grow III-V nanowires, similar to the nanowires in this thesis [45]. A number of different top-down and bottom-up methods produce similar nanowires (see e.g. review by Dick [46]). In this section, the specific process used to grow the GaP nanowires for Paper I, II and IV is described. In Paper III we developed an MOVPE growth recipe to generate fluorescent GaInP nanowires.

---

[*] In nano- and microfabrication, a distinction is made between top-down and bottom-up methods. Bottom-up refers to self-assembling systems that create themselves, similar to growing plants. Top-down is the opposite, where the nanostructure are created by removing material, like carving a statue from a block of marble.

The starting point of nanowire growth in this thesis is a GaP (111)B* substrate with gold nanoparticles deposited either randomly using aerosol particles from a spark discharge particle generator [47], or in designed patterns using electron beam lithography (Figure 2.1 and 2.3). The original growth recipe used in this thesis was developed by Suyatin et al. [48] and has been slightly modified during this work. In short, the substrate is transferred to a growth chamber where it is heated to between 400 and 500 °C. In order to prevent evaporation of phosphorous (which has a higher vapour pressure than gallium), phosphine (PH_3) is introduced along with the hydrogen used to control chamber pressure. Prior to growth, the substrate is annealed at a high temperature in order to remove any native oxide, reshape the gold particles into droplets and ensure the Au seed particles create a liquid alloy with the substrate. To initiate nanowire growth, the metal organic compound trimethyl-gallium (TMGa) is introduced into the chamber and the nanowires start to grow from the gold nanoparticles, as described by the vapour-liquid-solid (VLS) model [6], [46], [49] (Figure 2.2). The precursors in the vapour phase will decompose in the reaction chamber, a reaction enhanced by the interaction between the precursors, the GaP substrate and, in particular, the gold particle. The decomposition will release methane and create free Ga and P atoms that can diffuse across the sample. Free Ga atoms will be incorporated into to liquid gold particle. This liquid will become supersaturated and Ga will precipitate underneath the gold particle, forming a solid nanowire. Phosphorous has a very low solubility in the gold particle and is thought to diffuse along the interface between the gold and the growing nanowire. The VLS model of growth derives its name from the triple phase mechanism, where precursors enter the system in vapour phase, get incorporated into a liquid alloy and precipitate as a solid. The VLS model has been used to describe nanowire growth for 50 years [6] and has been studied extensively. However, some details are not entirely understood and there are material systems where the model cannot be used to describe nanowire growth, such as nanowires growing from solid seed particles [50], [51] and growth without any seed particles [52], which are described by other models.

To minimize surface energies, most nanowires tend to grow in the (111) direction [53]. By using GaP substrates polished to reveal this crystal facet, it is possible to grow vertical GaP nanowires. Had another crystal facet terminated the growth substrate, the nanowires would preferentially grow at a non-vertical angle to conform to the (111) crystal plane. The gold particles directing growth are used to control both location and diameter of the nanowires while the growth time controls the final nanowire length.

---

* The orientation of a crystal structure is described using a set of numbers. Here (111) refers to the particular crystal surface, or facet, exposed when the GaP substrate was cut from a larger piece. The letter B refers to the terminating group. In this case, the surface is terminated by phosphorous atoms (as opposed to gallium atoms).
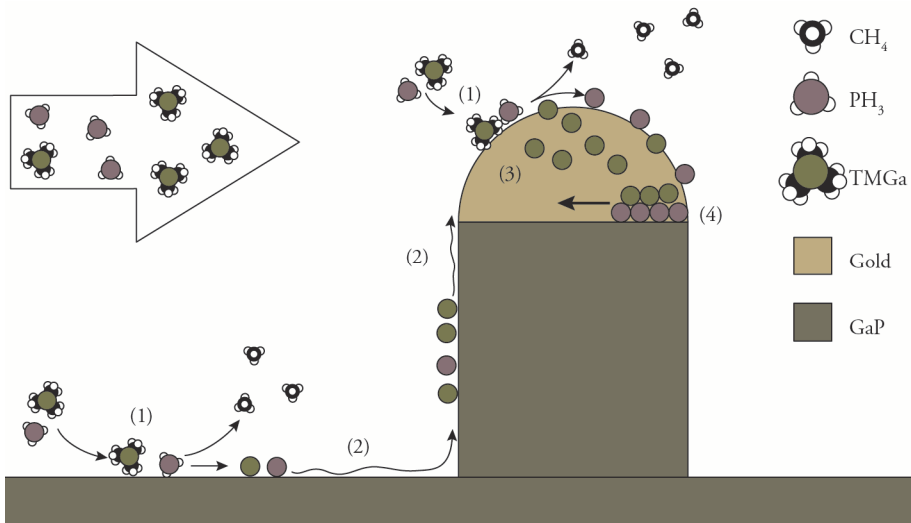
Figure 2.2 GaP nanowires can be grown on a GaP substrate using gold nanoparticles as a catalyst for MOVPE growth. The precursor molecules phosphine (PH₃) and trimethyl-gallium (TMGa) are introduced into the heated chamber. These will loosely adhere to the substrate, the nanowires and the gold particles where they will react, resulting in the release of methane and generation of free Ga and P atoms (a) which will diffuse across the substrate until they reach the gold particles (b).Here, the Ga atoms will be incorporated into the gold particle (c). When the gold particle has become supersaturated, GaP will precipitate adding another layer to the nanowire (d). Nucleation of this layer occurs at the triple phase boundary between the solid nanowire, the liquid Ga/Au alloy and the vapour phase precursors (d). P atoms have low solubility in the gold particle and are incorporated into the nanowire through rapid diffusion between the growing nanowire and the gold particle.

Lithography

In nano- and microfabrication, lithography is the collective name of methods used to transfer patterns to surfaces, typically through the use of a masking material. In the electronics industry, the most common methods are UV lithography (UVL) and electron beam lithography (EBL) [44], summarised in Figure 2.3. As outlined above and in Figure 2.1, EBL was used in Paper I to create ordered arrays of gold nanoparticles, subsequently used to seed nanowire growth. As UVL has not been used in this thesis, it will not be discussed further. Sufficient to say is that UVL is almost identical to EBL but relies on UV radiation through a mask instead of a beam of electrons and, apart from replacing the chemical compounds used, the rest of the procedure is identical.

In EBL, a polymer solution called a resist is deposited on a substrate using spin coating to ensure reproducible and uniform thickness. The polymer solution is heated to remove the solvent, creating a solid polymer network. Depending on the resist, one of

two things will happen when it is exposed to an electron beam. Either the polymer chains in the exposed regions will crosslink (negative resist) or a catalyst included in the polymer solution will initiate the breakdown of the polymer chain into oligomers (positive resist). After exposure, the substrate with the resist is submerged in a developer, a solvent that selectively dissolves either the unexposed, non-cross-linked regions (for the negative resist) or the exposed oligomer regions (for the positive resist). This development will reveal the underlying substrate and expose it to further treatment, such as deposition of material or etching.

In order to create the gold seed particles necessary for the nanowire arrays in Paper I, gold is evaporated onto the resist (Figure 2.1 c) (evaporation is described in the next section). Following gold evaporation, the sample is submerged in a solvent which will remove the remaining resist and the excess gold in a process called lift-off (**Figure 2.1** d). The end result is a substrate with a precisely defined gold pattern.
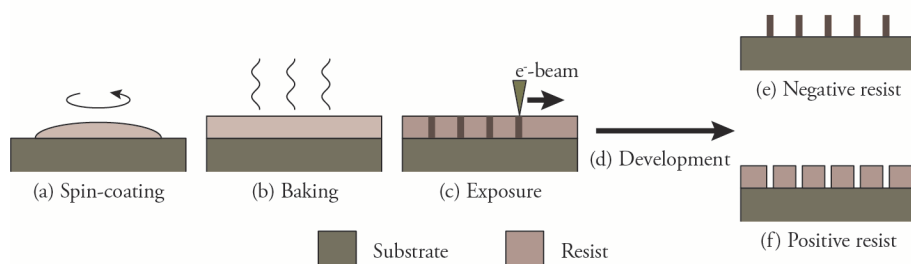
Figure 2.3 The basic steps in sample patterning using EBL, as outlined in the text. First, the substrate is coated with a polymer in a solvent (a). The sample is baked to remove the solvent (b), creating a hard polymer layer, which is then exposed to an electron beam (c). By immersing the sample in another solvent (d), either unexposed (negative resist (e)) or exposed (positive resist (f)) areas can be selectively removed.

Surface coating

A common motif in micro-and nanofabrication is to deposit materials such as gold or oxides on a surface, both with and without prior patterning [44], [54]. In this thesis, three different approaches have been used depending on the material deposited and the intended application: thermal evaporation, sputter coating and atomic layer deposition (ALD). Thermal evaporation was used in Paper I to deposit gold on EBL-patterned resist for nanowire growth as described above. In Paper I, ALD was instrumental in depositing the Al_2O_3 that ultimately formed the nanotubes described in the paper. ALD was also employed in Paper III to change the surface chemistry of the fluorescent nanowires described there. Sputter coating has been used in all four papers to deposit conductive Au or Au/Pt layers for improved SEM imaging.

When discussing different surface coating techniques, a distinction is made between physical and chemical deposition methods. In physical deposition methods, a source material is used to generate free atoms of the material to be deposited. These atoms deposit on all surfaces inside the reactor housing both the source and the sample(s). When using thermal evaporation to deposit gold films for instance, a gold nugget is heated to above its melting point, causing it to evaporate (Figure 2.4 a). In sputter coating, the source material is instead evaporated using plasma, where the plasma ions are accelerated toward the source causing atoms to be sputtered (Figure 2.4 b). Both of these methods are highly directional; coating occurs on surfaces that can trace a line of sight to the source material. The two techniques have a few important differences. Thermal evaporation requires a source material which can be melted without changing composition and works best for metals, though the use of electron beams, as opposed to the resistive heating often used, can be used to evaporate oxides. Sputter coating does not have this restriction and can be used to deposit both metals and oxides.

ALD is a chemical deposition method which relies on the reaction between precursor compounds to generate a film, as opposed to evaporating an existing material [55]–[57]. Here the substrate is placed in a heated, evacuated reaction chamber into which precursor chemicals are introduced (Figure 2.4 c). In order to coat a substrate with Al_2O_3 as in Paper I and III, trimethyl-aluminium (TMAl) and water are used as precursors and when these react at a temperature of 250 °C, Al_2O_3 will form and methane is released [58]. A uniform layer can be deposited by introducing first one precursor and allowing it to create a monolayer covering all surfaces in the reactor before introducing the second precursor. This process is repeated for several cycles, depositing the final film layer by layer. In Paper I, 500 process cycled were used to create an approximately 55 nm thick Al_2O_3 coating. ALD can create a high quality, homogenous film and, importantly, is isotropic, i.e. film thickness is identical on both vertical and horizontal surfaces. One drawback of ALD is the common requirement to heat the sample to create a high quality film as some materials (e.g. many resists) are not compatible with high temperatures, a drawback being addressed by ongoing research [59]. Another weakness is purity: for the physical methods, the film will consist of only the source material, but for ALD, remnants from the precursors (such as carbon and hydrogen) might be embedded in the final film [60].
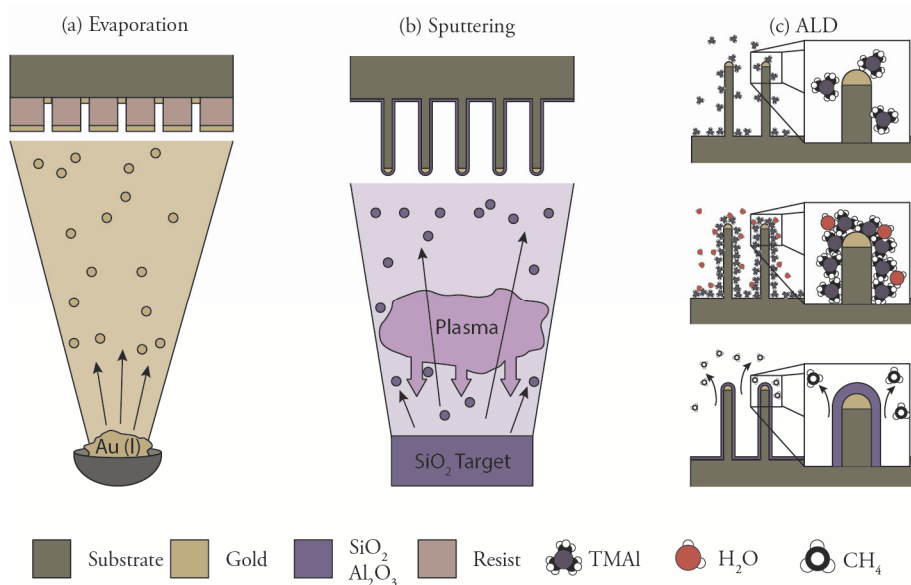
Figure 2.4 Surface coating can be achieved by several different methods. In this thesis, thermal evaporation (a) sputtering (b) and ALD (c) have been used, as described in the text.

Etching

In Paper I, the removal of material from our samples was key to the creation of the oxide nanotubes. In the paper, we employed both wet etching and reactive ion etching (RIE, also known as dry etching) in different stages of the processing. During wet etching, the sample is immersed in an etchant solution, which will react with and dissolve one or more of the materials in the sample. Wet etching relies on chemical reactions and can be highly selective, preferentially removing e.g. semiconductor material while leaving oxides intact. In Paper I, aqua regia (HCl and HNO_3) was used to selectively remove GaP while leaving the Al_2O_3 coating intact. In RIE, plasma is generated in an evacuated chamber containing the sample. The etching process can rely on both chemical and physical methods [61], [62]: either the plasma ions diffuse passively around the chamber, reacting chemically with the substrate, or a bias can be used to accelerate the ions toward the substrate, physically sputtering material from the sample. Depending on the sample and the desired etch profile, one or both of the mechanisms can be used [61], [62]. In paper I, we used a mainly physical approach by accelerating argon ions towards a sample with oxide-coated nanowires embedded in a resist layer. Though physical in nature, the plasma would remove the nanowires at a higher rate than surrounding resist layer owing to the mechanical differences between the two. Following the argon sputtering, oxygen plasma was used to selectively remove the resist, its chemical mode of action enabling high specificity and leaving the oxide coated nanowires intact.

Both wet and dry etching can etch in all directions at the same rate, isotropic etching, or at different rates in different directions, anisotropic etching. For wet etching, anisotropic etching typically follows crystal planes (some planes take longer to remove than others) and the resulting etch profile is determined by these facets [62]. For RIE, etching parameters such as plasma composition and bias can be fine-tuned to generate specific etch slopes by balancing physical and chemical reaction mechanisms [61], [63]. On the other hand, it is not straight forward to use RIE to create e.g. overhang structures such as those described in Paper I.

2.2 Microscopy

The basic function of a modern, optical microscope is very similar to the original versions from the 16th and 17th centuries described in Chapter 1: light is still transmitted through a specimen, collected by an objective and directed to a camera or eye piece. This basic function is in most cases modified to include some means of contrast enhancement which can rely on either physical properties inherent to the sample, such as index of refraction, or the addition of dyes (most often fluorescent) that stain certain parts of the specimen.

Microscopy is vital for both cell biology and nanofabrication and as such, has been used extensively in this thesis. The results presented in Papers II and IV have been almost exclusively obtained using fluorescence microscopy and phase holographic microscopy. Fluorescence microscopy was also used to in Paper III and to some extent in Paper I. SEM is an integral part of nanofabrication and has been used in Papers I-IV, both to characterize nanostructures and to study the interactions between cells and nanowires. At the end of this chapter, example images of the different techniques described here can be found in Figure 2.9, pages 28-33.

Phase holographic imaging

In order to improve contrast in an optical image, several different methods have been explored, some of which rely on the physical properties of a sample such as light scattering or index of refraction. Phase holographic imaging has been extensively used in this thesis (Papers II and IV) and relies on differences in phase induced by differences in index of refraction and sample thickness as light passes through a sample with cells. By illuminating the sample with a laser, collecting the light that passes through the sample and combining it with a reference laser (Figure 2.5), an interference pattern is generated [64], [65]. This pattern contains height information about the specimen and can be used to restore a three-dimensional model of the sample (Figure 2.5). The method does not require any labelling (which might interfere with cell function) and the low intensity, long wavelength laser is not affecting the cells. The image

reconstruction algorithm yields an image with very high contrast and can accommodate for a slightly out-of-focus sample. This inherent focus correction makes phase holographic microscopy superior to many standard microscopy systems: it can adjust for the slight focus drift that often occurs over long imaging sessions. Together, these traits enable extended time-lapse imaging (>96 h) without any adverse effects on the cells.
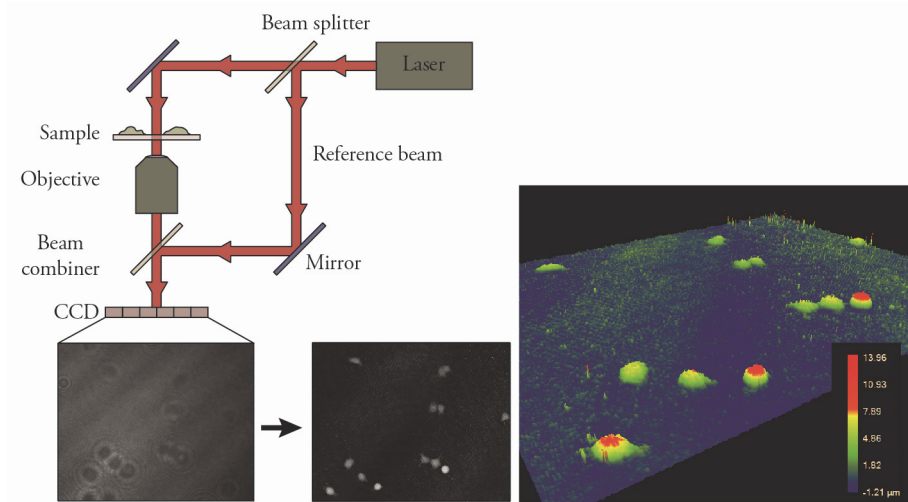
Figure 2.5 Phase holographic microscopy uses a laser beam which is split into a reference beam and a sample beam. After the sample beam has passed through the specimen, the two beams are recombined, giving rise to an interference pattern based on the phase changes the sample beam underwent on its path through the sample. This interference pattern can be used to construct a model of the sample and contains height information, enabling 3D reconstructions of the sample.

For our studies of cells cultured on GaP substrates with Gap nanowires, phase holographic microscopy is especially useful as it can be used to image cells on these surfaces (Figure 2.6). Normally, semiconductor materials are non-transparent to visible light, owing to a low band gap energy. For example, GaAs and InP have band gap energies around 1.5 eV, meaning they will absorb light with wavelengths below ~830 nm[*] while the ubiquitously used silicon has a bandgap of 1.12 eV [44], absorbing light with wavelengths below 1.1 μm. However, GaP has a relatively high band gap energy of 2.26 eV [66], allowing all light with a wavelength longer than 549 nm to pass unabsorbed. This transparency to long wavelengths means that it is possible to use transmitted light-based microscopy methods granted that the light used has a wavelength longer than 549 nm. Standard light based methods such as phase contrast microscopy, commonly uses full spectrum white light (including wavelengths above 549 nm) but, as seen in the phase contrast image of cells cultured on nanowires (Figure 2.6 a and c), this is not always enough. The poor image quality seen here is likely owing to scattering and absorption of shorter wavelengths of light in both the substrate and in the nanowires.

The commercial implementation of phase holographic microscopy provided by the company Phase Holographic Imaging, (PHI AB, Lund, Sweden), utilizes a red laser (633 nm [67]) to acquire image data, making it suitable to image cells on GaP. This long wavelength alone is not enough to image cells on our substrates because the rough backside of the samples will scatter the light, making image restoration impossible. When we instead fabricated our nanowires on substrates that had been polished on both sides, it was possible to image the cells, as shown in Figure 2.6 (b and d). The high bandgap of GaP has enabled us to capture time-lapse images for up to 96 h of unlabelled cells on our nanowire surfaces, forming the backbone of Paper II and Paper IV. Note that, depending on the physical properties such as density and length, it was sometimes possible to use phase contrast microscopy (short and less dense nanowire arrays being preferable). We have also observed a decrease in image quality for phase holography related to nanowire geometry: increasing either nanowire density or nanowire length reduces image quality and it was not possible to image cells on nanowire arrays with a density of 10 nanowires μm^{-2} or more.

---

[*] Visible light has wavelengths in the range 400-700 nm.
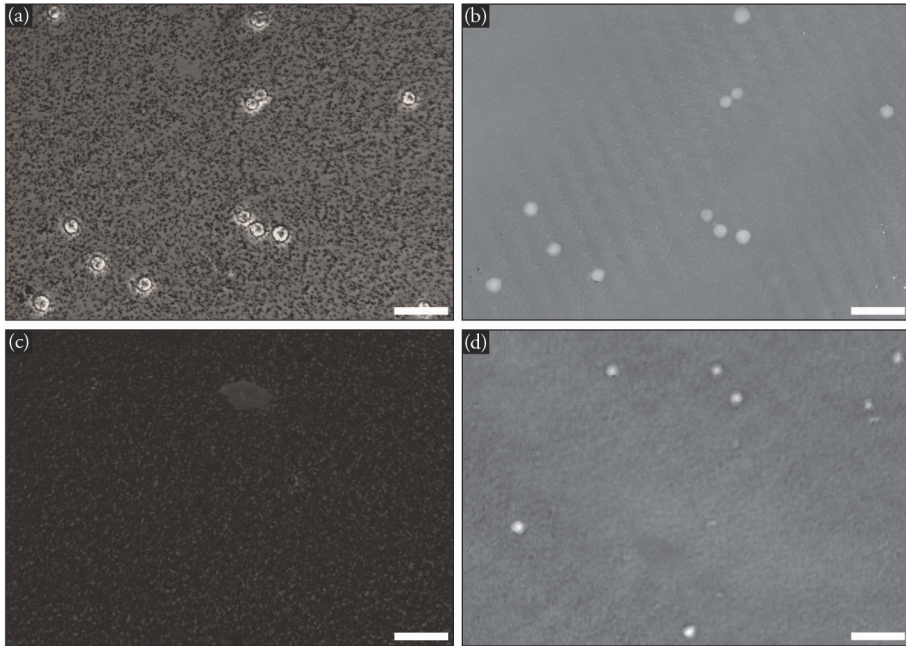
Figure 2.6 Comparison between phase contrast microscopy (a, c) and phase holographic microscopy (b, d). Mouse fibroblasts (L929) cultured on GaP nanowires with a density of 0.1 μm^{-2} (diameter 80 nm, length 4 μm,) (a, b) and similar nanowires with a density of 1 μm^{-2} (diameter 80 nm, length 3.8 μm) (c, d). Phase holographic microscopy vastly improves the image quality; without it, imaging cells on many of the nanowire substrates would not be possible (depending on nanowire geometry). Scale bars are 50 μm.

Fluorescence microscopy

Instead of relying on physical properties of cells to improve contrast in a biological sample as in phase holographic microscopy, it is common to add different fluorescent dyes that bind to specific cellular structures, enabling visualisation of these. The fluorescently labelled sample is imaged in a fluorescence microscope where the dyes are excited using light of a certain wavelength. If the incident photons have an energy corresponding to the difference between energy levels in the fluorophore, the photon energy can be absorbed by an electron, exciting the fluorophore (Figure 2.7 a). The excited electrons will lose a low amount of energy before relaxing to the ground state through the emission of a photon. Due to the energy loss, the emitted photon will have a longer wavelength than the photon used for excitation. This change in wavelength is referred to as Stoke's shift (Figure 2.7 b) and is at the heart of fluorescence microscopy: by using filters it is possible to illuminate the sample with excitation light while only collecting emitted light (Figure 2.7 c). When illumination and light capture occurs on the same side of the sample, the setup is referred to as an epifluorescence microscope (Figure 2.7 c), in contrast to a diafluorescence microscope where light source and collection are at opposite sides of the sample (not shown).

Fluorescence confocal microscopy is a common version of fluorescence microscopy used to collect 3D data from a sample. In this work, confocal microscopy was used in Papers I-III. In contrast to standard fluorescence microscopes, where all emitted light is collected, for confocal microscopy light is only collected from specific optical planes or slices, resulting in a much sharper image. By capturing several such optical slices by means of scanning in the vertical direction, it is possible to create a 3D reconstruction of the sample. The removal of the out-of-focus light is achieved by the insertion of a metal disc into the optical path. A small pinhole in the disc will ensure that only light from a specific focal plane can pass (Figure 2.7 d). The disc will also block light in the XY-plane, improving lateral resolution but imposing the need to scan across the sample, collecting emission light from one point at a time. This scanning is often implemented by scanning an excitation laser across the sample, collecting the emitted light one pixel at a time (confocal laser scanning microscopy (CLSM)). Another variant is the spinning disc confocal system where light from the sample is passed through an array of pinholes, collecting light from several points of a sample at once. By rotating the disc, light can be collected from the entire field of view using a CCD, greatly improving the acquisition rate at the cost of signal to noise ratio.

Fluorophores

Fluorescence microscopy is based around the use of fluorophores, which come in a large variety and can be organic molecules adapted from plants and animals, semiconductor quantum dots, metal nanoparticles or fluorescent proteins among others [68]. Some dyes bind to specific structures such as proteins, DNA or cell membrane. Those dyes that do not possess a high binding affinity are often attached to structures such as antibodies or toxins that do. It is not only this very specific labelling but also dyes that react to their surroundings that give rise to the great versatility of fluorescence based microscopy. Some dyes react to pH, transmembrane voltage or certain ions while other dyes are activated by unique enzymes, indicating their presence and function. Owing to all the research related to the development of genetic techniques and fluorescent dyes, fluorescence microscopy has truly become a workhorse in cell biology [29], [68]–[70]. In this thesis, we have used dyes to stain cell structures such as DNA and actin filaments (Paper I-IV) and we have explored the use of functional dyes to assess cell respiration and generation of reactive oxygen species (ROS) (Paper II).
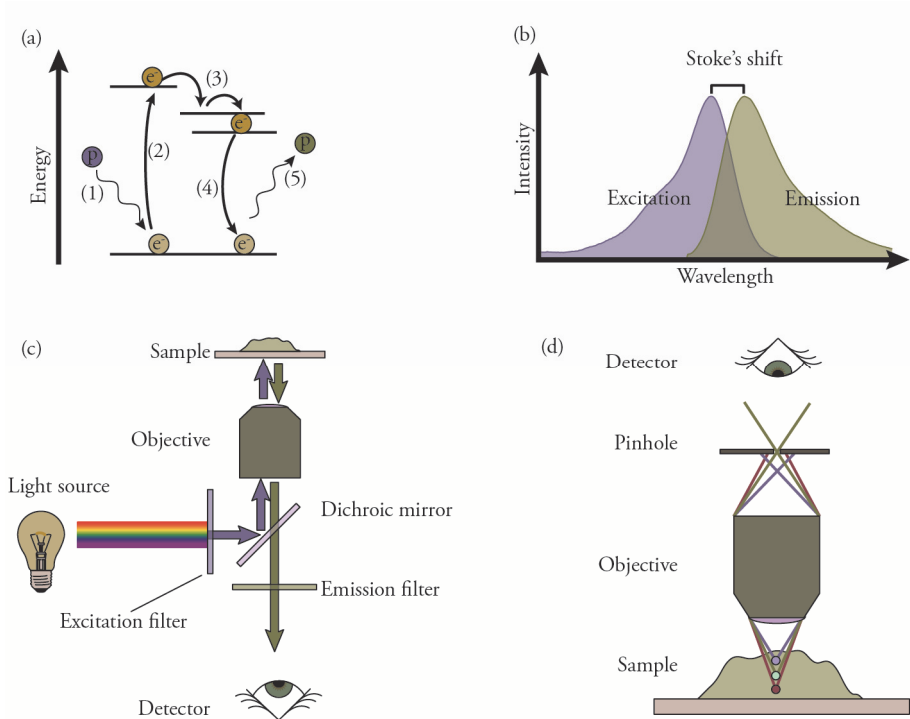
Figure 2.7 In fluorescence microscopy, the electrons in a fluorophore are excited by illumination with light (a). The excited electrons will lose a portion of their energy before relaxing to the ground state via the emission of a photon. This energy loss causes the emitted photon to have a longer wavelength than the incident light. This can be seen in the excitation and emission spectra (b) and is referred to as the Stoke's shift. This shift is capitalized on in fluorescence microscopy (c). The use of filters makes it possible to illuminate a stained sample with short wavelength light (here blue) and only collect emitted, long wavelength light (here green). The excitation light is reflected toward the objective and sample by a dichroic mirror (a mirror which transmits light with wavelengths above or below a cut-off wavelength). The excitation light will excite the fluorophores in the sample and the emitted light is collected by the objective and passes through the dichroic mirror. An emission filter ensures only emitted light can pass to the detector. In confocal microscopy a pinhole is placed in the light path to ensure a narrow focal depth (d) and scanning in the x- and y-directions ensures imaging of the entire sample. This is often combined with z-direction scanning to create 3D reconstructions of the specimen.

One major drawback of using dyes to investigate cell behaviour is phototoxicity [71], [72]. Ideally, the excited electrons will lose their energy through radiative processes (i.e., the emission of a photon) but the high energy make these electrons very reactive. Hence, excited dyes are prone to react with nearby molecules, in particular with oxygen. This often leads to the generation of ROS, which then interacts with e.g. proteins and DNA, causing damage to the cells. These reactions limit the usefulness of dyes in living cells, even if the phototoxicity does not outright induce cell death, it can affect cell

behaviour such as mitosis [71]. If studying living cells, the phototoxicity of fluorescent dyes need to be minimized by e.g. reducing dye concentration, exposure time, using oxygen scavengers or limiting staining and relying on white light, e.g. phase contrast microscopy, for the majority of the imaging [71]–[73]. In our work on time-lapse microscopy (Paper II and IV), we opted to remove fluorescence microscopy completely by using phase holographic microscopy, as outlined above.

In our work, several dyes have been used to assess aspects of cell behaviour, as summarised in Table 2.1. To visualize cells and investigate their morphology, the DNA stain bisbenzimide (Hoechst 33342) has been used together with phalloidin* conjugated to the dye fluorescein isothiocyanate (FITC) in Papers I-IV to label cell nuclei and the actin cytoskeleton, respectively. In Paper II, functional dyes were used to assess ROS generation, double-strand DNA (dsDNA) breaks and cell respiration. ROS was detected using the fluorescein derived compound carboxy-H2DCFDA. Upon entering cells, intracellular esterases will remove two carboxyl groups, rendering the compound membrane impermeable [74]. In the presence of ROS, the altered carboxy-H2DCFDA will be converted to native fluorescein, a membrane impermeable fluorophore, thereby labelling cells with high ROS content. Resazurin, commonly referred to by its trade name AlamarBlue™, is used to study cell respiration. When added to a cell culture, resazurin will enter the cells and be reduced to resorufin via interactions with the electron transport chain in the mitochondria [75], converting it from a weak, blue fluorophore to a strong, red fluorescent compound. In this case, both compounds are membrane permeable, i.e. resorufin is able to leave the cells, giving the medium a visible pink hue. By measuring the red fluorescence from a cell culture, the level of respiration can be assessed. In Paper II, we investigated dsDNA breaks using antibody labelling. When a dsDNA break is detected by the cell, the histone subunit H2AX will be phosphorylated, forming γ-H2AX, triggering the assembly of a DNA repair complex [76]. The γ-H2AX can be selectively labelled using antibodies, enabling an assessment of the ongoing level of DNA repair and, by association, DNA damage.

Propidum iodide (PI) and ethidium homodimer-1 (EthD-1) are two membrane impermeable dyes that are often used to stain the DNA of cells with disrupted membranes [77]. These dyes are often combined with calcein-acetomethoxy (calcein AM) to assess the viability of cells in a culture. Similar to carboxy-H2DCFDA, calcein AM is a modified version of the fluorophore calcein, where several ester groups have been attached, turning the dye non-fluorescent and membrane permeable [78]. Upon entering a cell with enzymatic activity, the ester groups are removed by enzymes, returning calcein to its natural, fluorescent, membrane impermeable state. Adding both

---

* Phalloidin is a toxin extracted from death cap mushrooms which binds strongly to cytoskeletal actin filaments.

20

PI or EthD-1 and calcein AM to a cell culture has the combined effect of turning living cells green (calcein) while dead or dying cells turn red or orange (PI or EthD-1, respectively).

Table 2.1 Fluorophores used in this thesis and cited literature to visualize cells and evaluate their function.

Dye	Target	Description	Used in
FITC/phalloidin	Actin filaments	Membrane impermeable. Used after fixation and permeabilization.	Paper I-IV
Bisbenzimide (Hoechst 33342)	DNA	Membrane permeable. Used to label live or fixed cells.	Paper I-IV
carboxy-H2DCFDA	ROS	Activated to a fluorescent compound by ROS generated in live cells.	Paper II
AlamarBlue™	Electron transport chain	Cell respiration converts resazurin to resorufin, causing a shift in emission wavelength and intensity	Paper II
Antibodies against γ-H2AX	γ-H2AX	Phosphorylated version of histone H2AX, indicative of DNA repair	Paper II
Propidium iodide	DNA	Membrane impermeable	[28], [79]–[82]
EthD-1	DNA	Membrane impermeable	[83]–[85]
Calcein AM	Cytosol	Becomes membrane impermeable and fluorescent upon modification by intracellular enzymes	[26], [28], [79], [81], [83], [85], [86]

Scanning electron microscopy

Though incredibly versatile and extensively used, optical microscopy suffers from one major drawback: the resolution limit. As light from the sample travels through the microscope towards the detector, it will be refracted and the minimum focus spot is limited to approximately half the wavelength of the light[*] used [87], in practice around 200-300 nm. This limit means it is not possible to resolve structures that are closer to each other than this distance without using emerging super resolution techniques like STORM [88] or STED [89] (though limited by diffraction, special procedures enable position determination with greater accuracy, circumventing the resolution limit).

To circumvent the problem of the resolution limit, electron microscopes have been developed. These microscopes do suffer from the same limitations but the wavelength of electrons can be much shorter than that of (visible) light, and a higher resolution is

---

[*] Diffraction limits resolution to approximately $\lambda/2 \cdot n \cdot \sin(\theta)$, where λ is the wavelength of light, n is the refractive index of the medium between objective and specimen and θ is the collection angle of the objective.

readily obtainable. In a standard SEM operating with an accelerating voltage of 20 kV, the wavelength of the electrons is 0.001 nm. In practice, the resolution in SEM is limited by the poor quality of the electron lenses but can reach values down to single nanometres [90]. The improvement in resolution compared to optical microscopy makes electron microscopy an indispensable tool in nanofabrication and is used on a daily basis. In this thesis, SEM has been used to evaluate the results of nanowire growth, nanofabrication (Papers I-IV) and to image the interactions between cells and nanowires (Papers I, II and IV).

In SEM, free electrons are generated from an electron source (such as a heated tungsten filament) and accelerated over a voltage (typically 1-20 kV) [91]. The electrons pass through electromagnetic lenses that shape the beam into a circular cross section and focus it onto the sample. As the electrons impinge on the specimen, secondary electrons are generated and collected by an electron detector. Alternately, electrons from the incident beam that have scattered back toward the electron source can be collected using a back-scatter (BS) detector. To generate an image of the specimen, a set of electromagnetic coils are used to scan the beam across the sample while recording the signal in each position. The strength of the recorded signal is proportional to the number of electrons, either secondary or back-scattered, that reach the detector. This number depends on material composition, topography and location of the detector. For BS electrons, the atomic weight of the sample plays a major role, enabling image contrast based on atomic species; heavy atoms such as the gold used for nanowire growth will appear very bright and can even be seen through lighter materials, such as those composing biological material (Figure 2.9 c, d)

SEM sample preparation

A sample imaged using SEM needs to be conductive in order to prevent charge up: the accumulation of electrons which will deflect the incident beam, giving rise to artefacts and poor image quality. Further, the SEM needs to operate in vacuum to prevent the electrons from scattering and reacting with air molecules. For semiconductor samples, these restrictions pose no problem but cell cultures need special sample preparation. First the sample is dehydrated and then it is coated with a conductive layer. The dehydration typically proceeds by replacing the liquid covering the fixed cells with ethanol at increasing concentrations up to ≥99.5%. The final ethanol solution can either be allowed to evaporate under ambient conditions or replaced with liquid CO_2 using a critical point dryer (CPD). By heating the liquid CO_2 under pressure, the system will reach a critical point in the phase diagram of CO_2 from which the liquid CO_2 can evaporate without an increase in volume. For many samples, CPD is a means of avoiding sample deformations that can be caused by the expansion of an evaporating liquid [92]. For monolayer cell cultures, such sample distortions are minor, but when studying cells on nanowires, CPD can help prevent nanowires from adhering to one

another. If allowed to dry in air, the receding ethanol often causes nanowires to bend and cling together and sometimes even break, depending on the nanowires' physical properties such as density, diameter and length (Figure 2.8). After dehydration, the sample is placed in a sputter coater (see Section 2.1) and a thin, conducting layer of metal is deposited on top to improve imaging by preventing charge up.
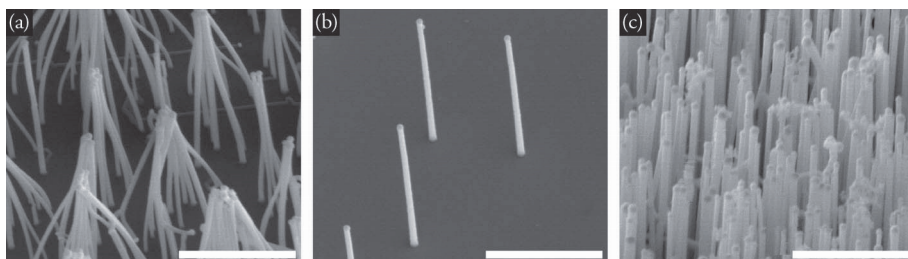
Figure 2.8 If nanowire samples are dehydrated by allowing ethanol to evaporate under ambient conditions, the nanowires may cling together (a), though for certain geometries, such as sparse (b) or short nanowires, this will not happen. To prevent nanowire clinging, the ethanol can be replaced with CO_2 (l) which is then heated until it evaporates in a CPD (c). Scale bars are 2µm, tilt is 30 ° (a, b) or 60 ° (c).

One of the strengths of optical microscopy is the use of dyes to improve contrast. Since contrast in SEM is based on geometry and atomic weight, fluorescent dyes do not work here. Instead, dedicated contrast enhancing fixatives and dyes based on heavy atomic species have been developed for electron microscopy, such as osmium tetroxide and uranyl acetate which were used in Paper II. Osmium tetroxide is primarily incorporated into fatty tissue like the cell membrane while uranyl acetate reacts with phosphates and amine groups, thereby labelling nucleic acids and many proteins [93]. To improve specificity, antibodies labelled with metal nanoparticles are manufactured, making it possible to locate specific cellular structures in electron microscopy [94].

Focused ion beam tomography

In SEM, only the surface of a sample is imaged and, though this gives useful information, it is occasionally of interest to investigate the interior of a sample. For biological samples, sectioning tools such as microtomes are used to cut tissue into thin sections, which can then be imaged. For cells cultured on brittle semiconductor substrates, such as those studied in this thesis, this is not an option since the sample shatters, preventing the creation of thin sections. In Paper II, we circumvented this issue by using focused ion beam (FIB) tomography to section cells on nanowire substrates inside an SEM during operation, experiments carried out by our collaborators Carsten Købler and Kristian Mølhave at Denmark's Technical University. In some commercial SEM systems, an ion source has been installed, enabling the use of a FIB to manipulate a sample using e.g. FIB-assisted material

deposition [95]. Alternately, the FIB can be used to sputter material from a precisely defined region of a sample. That is, the sample can be imaged in SEM and a small area of the specimen can be selected for removal *in situ* [96], [97]. In Paper II, Købler and Mølhave combined FIB tomography with heavy metal stains to generate cross sectional images of cells cultured on nanowires with nanometre resolution, allowing us to study the intracellular cell-nanowire interactions with nanoscale resolution.

2.3 Cell culturing

From its roots in the early 20th century, cell culturing has become an indispensable, routine procedure in cell biology and has been used throughout this thesis (Paper I-IV). Cell culturing is the art of keeping cells alive outside its original organism by mimicking the *in vivo* environment with as much fidelity as required for cells to survive and reproduce [39], [98]. For mammalian cells, this is typically performed by keeping them in culture flasks or Petri dishes together with culture medium, a liquid containing all components such as proteins, salts and sugars that the cells need to survive and function. The container is stored in an incubator, kept at 37 °C. The incubator often houses an atmosphere designed to stabilize the medium's pH and prevent evaporation.

A distinction is made between primary cells, which are retrieved from a patient or animal in connection with an experiment and kept alive for a shorter period of time, and immortal cell lines. Immortal cell lines are cells which have acquired the ability to divide indefinitely and are kept alive for extended periods of time and used in different experiments. Cells can be grown in suspension culture or monolayer culture, where monolayer culture implies that the cells are attached to a substrate and surrounded by medium. For suspension cultures, the cells are floating in the medium. During routine culture of monolayer cells, the cells are seeded at low densities, which stimulates the cells to proliferate and prevents them from entering hibernation. Cell division causes the cell density to increase and when the substrate is confluent with cells (i.e. when cells cover the entire culture surface), the cells are dislodged from the culture vessel and reseeded at a low density in a new culture vessel. To dislodge the cells, the culture can be treated with trypsin and EDTA[*] to remove proteins and divalent ions which are important for cell attachment. To determine cell concentration, a fraction of the suspended cells are counted in a haemocytometer, a specially designed glass chamber.

---

[*] The digestive enzyme trypsin breaks down proteins non-specifically and will degrade all proteins on a cell's surface, including the proteins the cells use to adhere to the substrate. The chelating agent EDTA binds to divalent, positive ions, removing them from solution. Divalent ions are used by some cell types to improve the binding to the substrate via electrostatic interactions.

One major advantage apart from the reduction of animal experiments offered by immortal cell lines is their commercial availability. They are very well characterized and different research groups across the world use exactly the same cell lines, improving the possibility to compare results. The major drawback of immortal cell lines is that they have been altered from their natural state. Apart from the "immortality" they have gained, they have often acquired other behavioural differences compared to primary cells of the same kind [99].

The work in this thesis (Paper I-IV) has revolved around the adherent, immortal fibroblast cell line L929, first established from a mouse in 1948 [100]. This cell line was chosen because it is a non-malignant cell line, easy to cultivate and has a population doubling time around 24 h, which is convenient for time-lapse imaging, Furthermore, the cells have good migratory ability (since they are derived from fibroblasts) and single cells are easily distinguishable. The cells are e.g. used in regulatory toxicology and thus well known in many laboratories. For routine culture, the cells were kept in a 37 °C, humidified incubator, and passaged (i.e. suspended and reseeded at a low density) twice a week using trypsin and EDTA. To carry out cell culture experiments on our nanowire-covered substrates, the substrates were first sterilized overnight by UV-irradiation (Paper II and IV) or submersion in 70% ethanol for ≥10 minutes (Paper I and III). To prevent nanowires from bending or breaking (Figure 2.8), the samples were never allowed to dry and thus kept in sterile PBS prior to culturing. For the fluorescent nanowires, only ethanol sterilisation was used to reduce the risk of bleaching the samples. Cells were seeded on the samples which were kept either in cell culture flasks (for time-lapse microscopy, where the ability to close the flasks to keep the incubator's atmosphere is essential), in Petri dishes or in well plates.

2.4 Chapter summary

This chapter has summarized most of the experimental procedures used in this work, from nanofabrication and MOVPE to cell culturing and microscopy. The two following chapters will outline how we have combined these different methods to obtain the results presented in Papers I-IV.

Figure 2.9 (The following four pages). Example images of L929 mouse fibroblasts on nanowire substrates. SEM is a great way to visualise cell-nanowire interactions (a-f, h). SEM inherently lacks colour information but often, false colours are applied to distinguish certain regions of interest, such as cells (a, b). It is also possible to assign colours using images captured with different detectors (e). Here the secondary electron detector (c) and the BS detector (d) have been assigned different colours and overlain one-another [101]. In the BS image (d), the heavy gold nanoparticles at the tips of the nanowires are clearly visible through the light material of the cell. Confocal microscopy can be used to create 3D images of cells. Here, L929 cultured on fluorescent nanowires from Paper III are shown (g). Phase holographic microscopy contains height information and as such is capable of 3D reconstructions, as shown by the L929 cultured on low density GaP nanowires (Paper IV) (i). Even an SEM can be adapted to record generate 3D data using e.g. beam deflection to emulate different viewing angles (f, h). These L929 cells on GaInP nanowires (f) and on collapsed GaP nanowires on a cover slip (h) were imaged using a Hitachi SU3500. Scale bars are 10 μm (a-f, h). Tilt is 30° (a-f) and 80 (h). Imaged areas are 142x142 μm (g) and 419x337μm (i).

(a)

(b)

#Cells<3NW

28

(f)

(g)

30

(h)

(i)

31
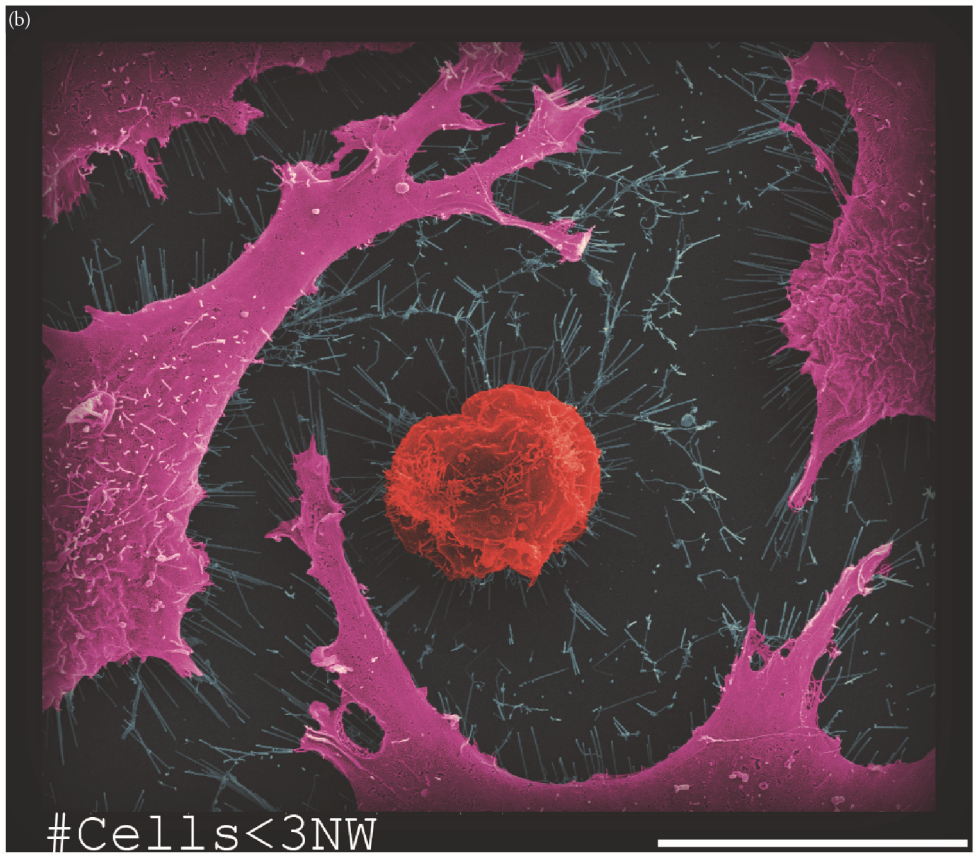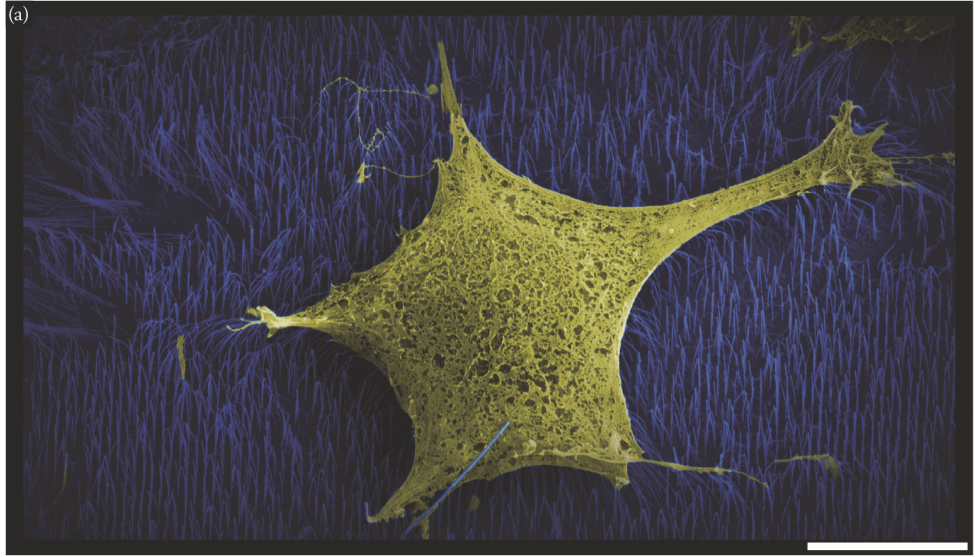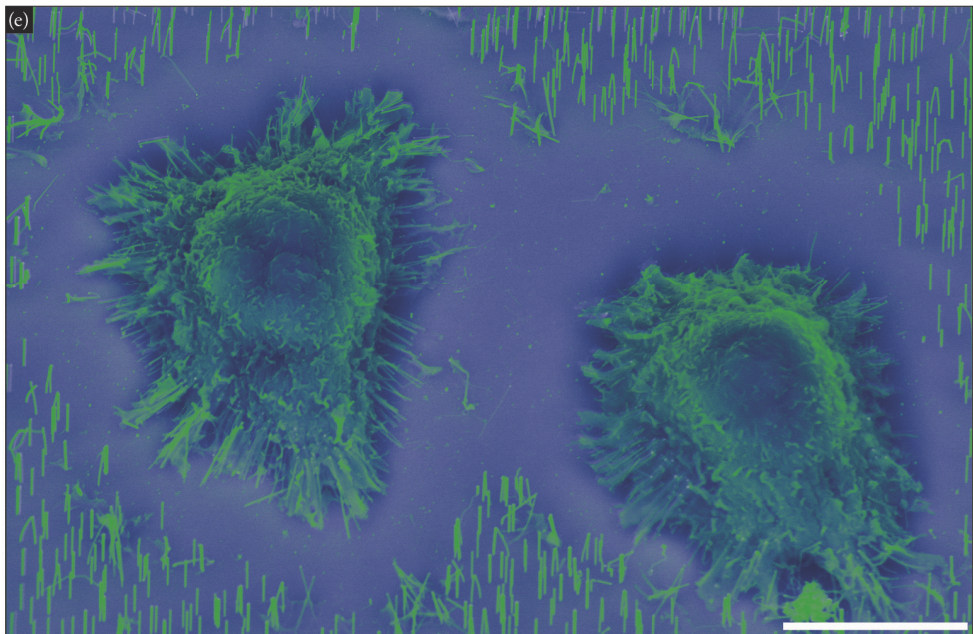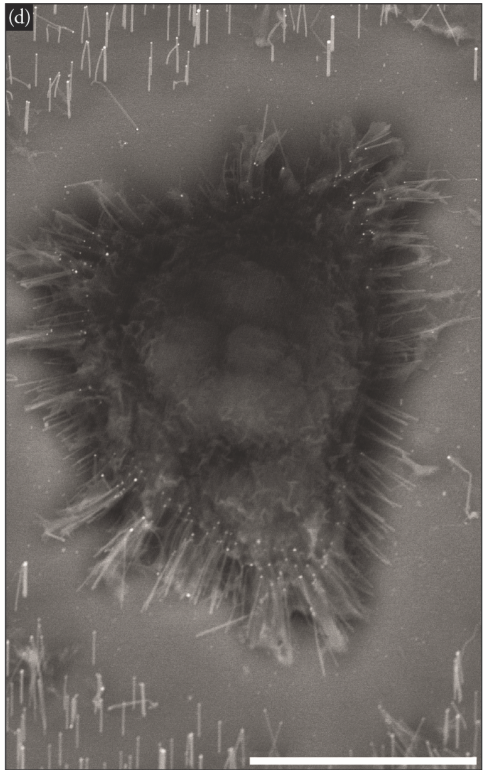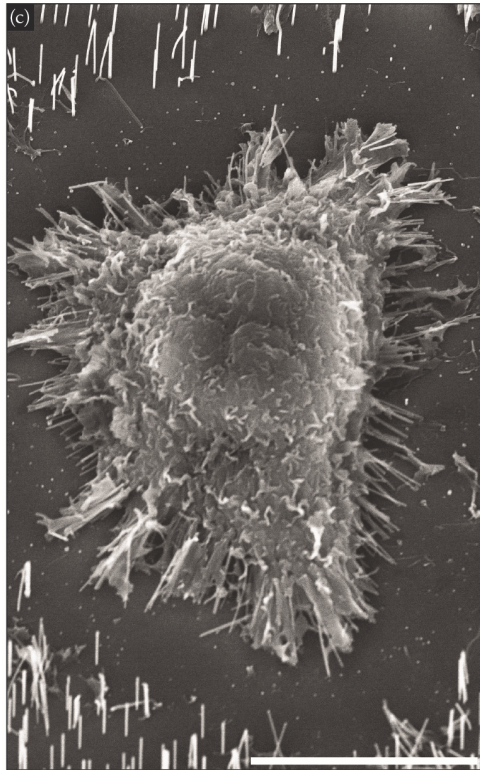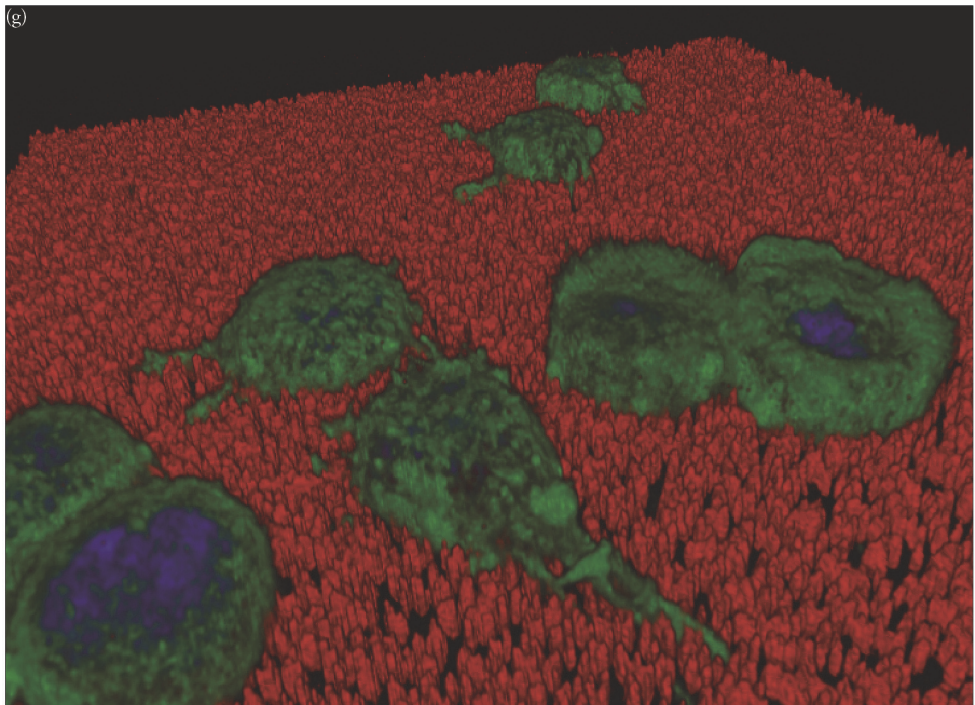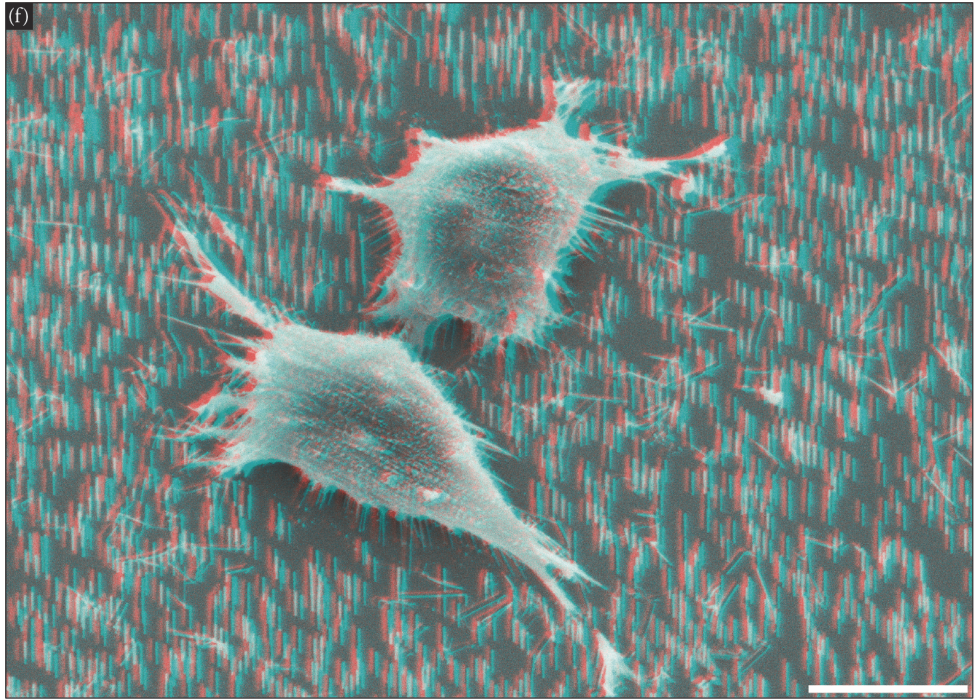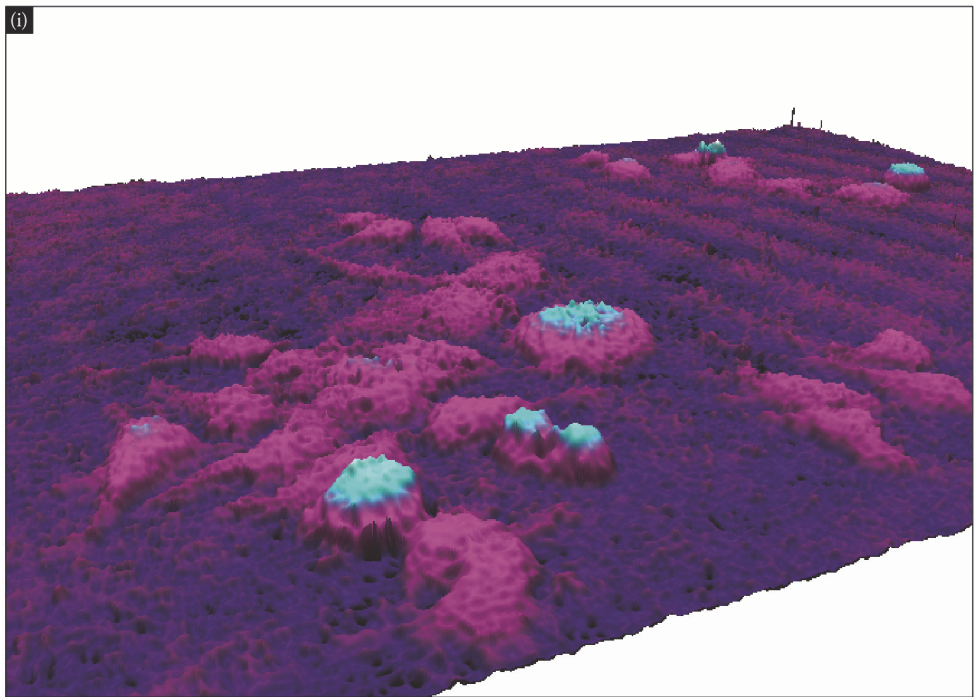
3 Nanowire applications in cell biology

The small size of nanowires has sparked an interest among physicists and biologists working on the border between the two disciplines and several groups have begun exploring the possibilities that these interesting structures give rise to. The whole field of semiconductor nanowires in cell biology started very recently with the first papers appearing in 2007, showing proof-of-principle applications by investigating neuronal growth [19] and an injection system [20]. This chapter will outline some experimental applications of nanowires in cell biology and focus on the application we have explored in paper I, namely nanowire-based cell injections.

3.1 Previous work in the field

There are several different applications being explored where nanowires are interfaced with cells. In this overview, focus will be on substrate adhering, vertical, high aspect ratio nanostructures similar to our epitaxial nanowires. There are other forms of potential nanowire applications, such as using suspended nanowires for cell rheology [102] or cancer therapy by means of drug delivery [103], [104] and hyper-thermal treatment [105]. A large number of cell biological experiments using other nanostructured surfaces such as nanopits, nanoporous substrates and nanoridges exist but fall outside the scope of this thesis. For a review see e.g. Bettinger et al. [106] or Martínez et al. [107].

One recent application of nanowires in biology is their use as electrodes for probing the membrane potential of neurons and other cell types [24], [25], [108]. These nanotechnology-based measurements enable an improved electrical seal between cells and electrodes compared to planar electrodes, leading to better signal-to-noise ratios. The small size of the electrodes makes it possible to place them closer to one another improving the spatial resolution of the system, which is also much simpler to operate than a conventional patch clamp system. Nanowires have also been employed to guide cell growth. Aizenberg et al. reported progress toward geometrically controlled stem cell differentiation [23]. By varying the distance between nanowires, they could control

the morphology of stem cells cultured on these EBL-defined arrays, a first step toward controlling differentiation. Working towards artificial, neuronal networks, nanowires have been employed to act as fences to guide axonal protrusions [21], [22], [109]. In this work, Hällström et al. used vertical, ordered arrays of nanowires to guide the outgrowth of axons and create one-way "streets" by positioning the nanowires in rows at an angle to the axonal bundles. Typically, contact guidance systems are based on microstructures such as ridges or channels. Employing nanowires in this fashion led to a large degree of cell guidance from a relatively small level of perturbations. By culturing cells on top of nanowires and tracking nanowire deflection as cells migrate and grow on these, it is possible to determine the forces exerted on the substrate by the cells [110]. Using nanowires improved both the spatial resolution and the resolution in the force measurements, compared to similar systems based on larger, less dense polymer micropillars [111], [112]. One of the very first nanowire-based applications in cell biology employed these structures as needles in order to transfect human kidney cells with DNA coding for green fluorescent protein (GFP) [20], building on previous work based on similar, conical carbon-based nanostructures [113]. This very promising application is something we explored and improved on in Paper I by creating hollow nanoneedles.

3.2 Cell injection experiments

When performing cell biological experiments, it is often of interest to introduce different molecules or compounds into cells in order to e.g. alter cell behaviour, track cellular components or stain the whole cell or parts thereof. Such molecules and compounds include short interference RNA (siRNA)[*] [114], tracking molecules (e.g. quantum dots that bind to specific organelles) [115], [116], membrane impermeable dyes to stain subcellular components in living cells, drug candidates, peptides, proteins [117] and of course, DNA encoding specific proteins such as the famous GFP [118], [119].

The large interest in the translocation of compounds into cells has led to several methods being developed to accomplish this task, for reviews see e.g. Stephens and Pepperkok [118] or Zhang and Yu [119]. The different methods are based on a variety of mechanisms, from biological and chemical to physical. One method derived from nature is to use viral vectors [99], [120],where a virus has had its DNA replaced by other genetic material, causing the virus to deliver this new genetic cargo as it infects a cell culture. Apart from being limited to injecting genetic material, viral transfection can trigger an immune response, altering cell behaviour. A popular chemistry-based

---

[*] SiRNA is an RNA molecule that will bind to specific mRNA sequences, triggering its degradation and thus blocking translation of that particular protein.

approach, called lipofection, uses lipids to coat proteins or genetic material [121]. These lipid aggregates can fuse with the cell membrane and deliver the load into the cells, though the lipid metabolism of the cells may be disrupted [122]. Some methods rely on creating pores in the membrane through which molecules can diffuse [118]. This can be achieved using surfactants, toxins or applied electric voltages (electroporation) [123]. The pores created not only allow the diffusive uptake of the target compounds but will also cause the cells to lose cytosolic components which might have adverse effects, especially if the pores remain for some period of time [118]

One of the most widely used injection systems is the most straightforward in its design: it is simply a microscopic syringe [119]. This method, dubbed microinjection, has been around since the 1970s and is today used not only in research facilities but also for *in vitro* fertilization in fertility clinics. The method is very versatile since it doesn't place any restrictions or requirements on the injected molecule or compound; it is even possible to inject cellular organelles [124]. A major drawback of microinjection is the need for a trained operator but with experience, 100% delivery efficiency and cell viability can be achieved. A more serious drawback is the serial injection approach, where one cell is injected at a time [118], [119]. Several attempts have been made to increase the rate, using e.g. robotics [125], microfluidics [126] or arrays of microneedles [127], [128]. In recent years, nanoscale injection systems, aiming to minimize cell perturbations, have started to emerge, using e.g. atomic force microscopes (AFM) with fluidic tips [129], carbon nanotubes mounted on glass capillaries [130] or on AFM tips [131] and, as outlined over the following pages and explored in Paper I, vertical nanowire-based injection systems [20], [26]–[28], [84], [113], [132]–[139].

Nanowire-based injection systems

Trying to address the short-comings of existing injection methods, scientists have turned to exploring nanowire-based injection systems. The whole field started in 2003 when McKnight, working together with Simpson, transfected Chinese hamster ovary cells (CHO) with GFP encoding DNA [113]. In short, McKnight, Simpson et al. coated conical carbon nanofibers (Figure 3.1 a) with GFP encoding DNA plasmids and cultured CHO cells on these. The group used two different approaches when attaching DNA to the fibres: in the first case DNA was simply adsorbed to the structures and transfected cells expressed GFP for more than 3 weeks after being removed from the substrate. When DNA instead was covalently bound to the nanostructures, GFP expression would cease shortly after the cells were removed from the substrate, demonstrating temporary and reversible transfection. The group has continued to explore different DNA immobilization strategies, such as letting DNA dry on the structures [113], [137] or using cleavable linkers attached to the DNA backbone at random locations [135], [137] or specifically at the end of the DNA strand [140]. The group has also demonstrated the injection of siRNA [136] and developed a

procedure to transfer the nanofibers into a flexible PDMS sheet while maintaining vertical alignment and injection capabilities [141], an important step towards *in vivo* injection experiments.
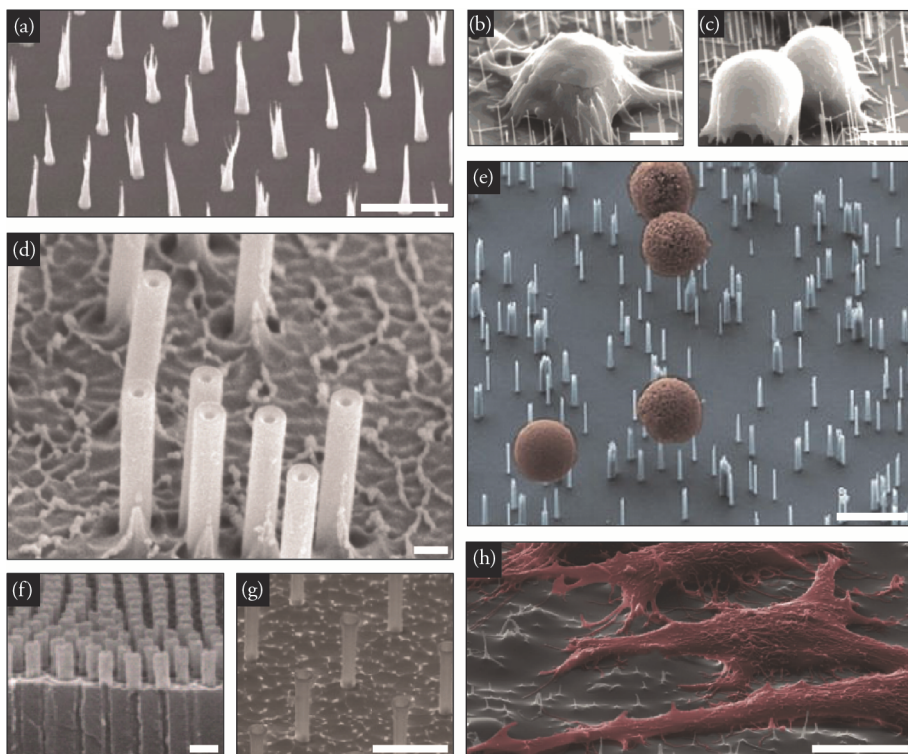
Figure 3.1 Examples of nanostructures used for cell injections in literature[*]. (a): Nanofibers used by McKnight et al. [113] to transfect Chinese hamster ovary cells, scale bar 5 µm. (b-c): Si nanowires from Kim et al. [20]. (d): Alumina nanostraws by VanDersarl et al. [133]. (e) Si nanowires used by Shalek et al. [84]. (f): Carbon nanosyringes used by Jon et al. [132]. (g): Silicon oxide nanoneedles by Peer et al. [27].(h): PDMS coated CuO nanowires from Mumm et al. [81]. Scale bars are 5 µm (a-c, e), 100 nm (d, f), 3 µm (g) and 10 µm (h). Figures have been cropped and scale bars have been adjusted.

The first cell injection application using epitaxial semiconductor nanowires to inject molecules into cells was carried out by Kim working with Yang 2007 [20] who used silicon nanowires (Figure 3.1 b) to inject GFP encoding plasmids into human kidney cells, HEK293, achieving a 1% transfection efficiency. Park's group has continued these nanowire-based injection experiments. In their first paper on the topic, Shalek showcased the high versatility of their simple silicon nanowire-based injection system (Figure 3.1 c) by successfully injecting dyes, DNA plasmids, peptides, proteins, histones, siRNA as well as drugs into HeLa cells as well as primary fibroblasts and neurons [26]. To promote nonspecific binding of reagents, the nanowires were coated with aminosilanes before the sample was submerged in a solution containing the reagent to be injected. Using this approach, they reported a 95-100% delivery efficiency for all the injected compounds and they demonstrate the ability to inject two different compounds into the same cells. While the work of McKnight and Simpson as well as Park's group is very extensive, other groups have explored nanostructure injection systems using e.g. carbon nanosyringes (Figure 3.1 d) [132] or PDMS-coated CuO nanowires on a transparent substrate (Figure 3.1 e) [81].

Until recently, most publications exploring nano-based injection systems have been proof-of-principle, but Hongkun Park and his collaborators are changing this. In one study, Shalek et al. used their nanowires to study chronic lymphocytic leukaemia and the involvement of the Wnt* signalling pathway [84] by silencing target genes using siRNA. In the same paper, they studied injection efficiency for a range of primary mouse and human immune cells, both adherent and non-adherent. Immune cells are not readily transfected without triggering an immune response, changing their behaviour. By tailoring the physical dimensions of their nanowires to suit each specific type of immune cell, Park et al. managed to transfect a wide range of immune cells without an immune response [84]. This systematic development of nanowire substrates to enable the injection of primary immune cells laid the foundation for the work of Yosef et al. [142] Yosef et al. used these nanowires to inject siRNA into murine T-cells in order to map out the genetic network regulating differentiation into T_H17 cells, discovering 46 new regulatory genes and finding two opposing regulatory pathways. In another study, these silicon nanowires were used to administer an inhibitor of the enzyme Polo-like kinase to study its effects on the antiviral in bone-marrow derived dendritic cells (BMDCs) [139].

---

* Wnt is a cellular signalling pathway which is important for cell proliferation, migration and differentiation.

This multitude of demonstrations of successful injection systems, summarized in Figure 3.1 and

Table 3.1 (p. 44-45), firmly establishes high aspect ratio, vertical nanostructures as a promising injection tool for cell biology, worth exploring further. The nanostructures offer important advantages over traditional injection techniques. Compared to microinjection, the physical injection method these nanostructures most closely resemble, the nanowires offer a vastly increased throughput with thousands of cells being automatically injected at once compared to the manual one-by-one approach common for microinjection. The nanowire systems display a similar versatility in the range of injected compounds, one of the great advantages of microinjection compared to e.g. viral or lipofection based injection systems.

However, the nanowires still suffer from one disadvantage compared to microinjection. The injection mechanism is of a one-shot nature: the compound(s) to be injected into the cells are injected when the cells adhere to the surface. There is no control over when the cargo is delivered, and it is not possible to deliver compounds at timed intervals or different compounds at different time points. Microinjection offers not only this kind of experimental control but also the possibility to retrieve material from within the cells. One of the aims of this thesis is to improve the versatility of nanowire-based injection systems by creating hollow nanotubes with fluidic connections, thereby adding the time resolved injection and the biopsy capability offered by microinjection, while keeping the simple, automated, high throughput ability of the nanowire-based systems.

Nanotubes with fluidic connections

As outlined in the previous section, one of the drawbacks the wide range of nano-based injection systems share is their one-shot nature: they are loaded with compounds that cross the cell membrane when the cells are seeded on the substrate. One of the aims of this thesis is to address this issue by creating nanotubes, as described in Paper I. If achieved, this will add temporal control, such as delayed injections or multiple, serial injections, as well as the ability to retrieve material from within the cells. To achieve this, we envision converting our GaP nanowires into hollow oxide nanotubes and connecting these to a microfluidic channel, a work begun in Paper I.
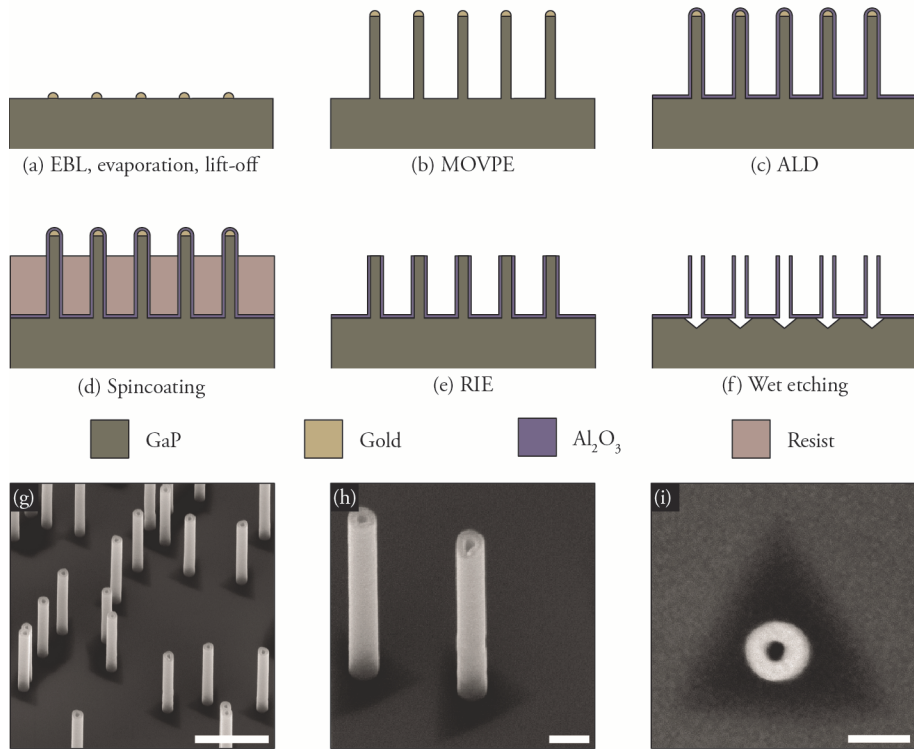
Figure 3.2 Fabrication of our oxide nanotubes (Paper I). Nanowires are grown from gold nanoparticles (a-b) and covered in aluminium oxide using ALD (c). The lower regions of the nanowires are covered in resist (d) and the protruding tips are removed using RIE (e), exposing the semiconductor core, which is selectively removed using wet etching (f). SEM images showing the oxide nanotubes (g-i). The dark triangular areas at the base of the nanotubes are created by anisotropic wet etching of the GaP substrate. Scale bars are 1 µm (g) and 200 nm (h-i). Tilt 30° (g, h) and 0° (i).

This fabrication process relied on techniques that are no longer available in our cleanroom and advanced epitaxial growth so the alternative fabrication method in Paper I (Figure 3.2) was developed. One adaptation we implemented was a change of nanowire material, replacing the GaAs/AlInP core shell nanowires with the bio-compatible GaP nanowires used for our other biology-related projects [19], [21], [22], [48], [109], [143], [144]. The epitaxial AlInP shell was replaced with an aluminium oxide ALD coating after sputtered SiO_x proved too soft to withstand the resist layer (the nanowires would bend and RIE could not be used to expose the GaP core). To create the through-wafer connection, we attempted to use RIE. However, the etch rate proved to not be controllable to the degree needed to form the thin membrane. The same etch time would occasionally create a hole through the entire substrate and occasionally only reach halfway through. With no good method to monitor etch depth *in situ*, the fabrication was unpredictable and other options needed to be explored.
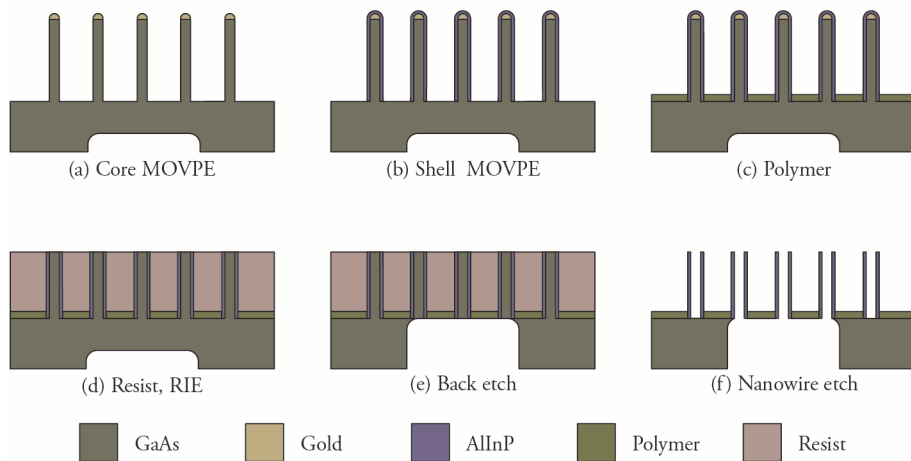
Figure 3.3 Nanotube fabrication as explored in our pilot project, creating a suspended membrane with nanosyringes [134]. GaAs nanowires were grown on a substrate with an indentation in the back (a). By changing growth conditions, a shell of AlInP was grown around the GaAs (b). The nanowires were then embedded in a polymer (c). A resist layer was used to protect the nanowires while removing the tips using RIE (d). Wet etching was used to convert the backside indentation into a through-wafer connection (e). Finally, the GaAs nanowires were etched and the resist was removed, leaving AlInP nanotubes in a polymer membrane (f).

Subsurface microchannel

When the initially explored suspended membrane fabrication failed, Jason Beech suggested an alternative. When the GaP nanowires are removed by wet etching, the etchant will attack and dissolve the GaP substrate as well. This can be seen as dark triangular areas underneath the nanotubes in the SEM images in Figure 3.2 (the triangular areas indicating an anisotropic etching process, i.e. preferential etching of specific crystal planes). Beech's suggestion was to position the nanotubes in an array that would cause these triangular cavities to overlap, thus linking to form a continuous microchannel connecting all nanotubes on the surface (Figure 3.4 a). This was achieved using EBL to control the spatial distribution of the gold seed particles used to control growth of the sacrificial GaP nanowires and extending the wet etching step to increase the size of the cavities forming under the nanotubes. The resulting arrays of nanotubes with their subsurface microchannel can be seen in Figure 3.4 b-c.
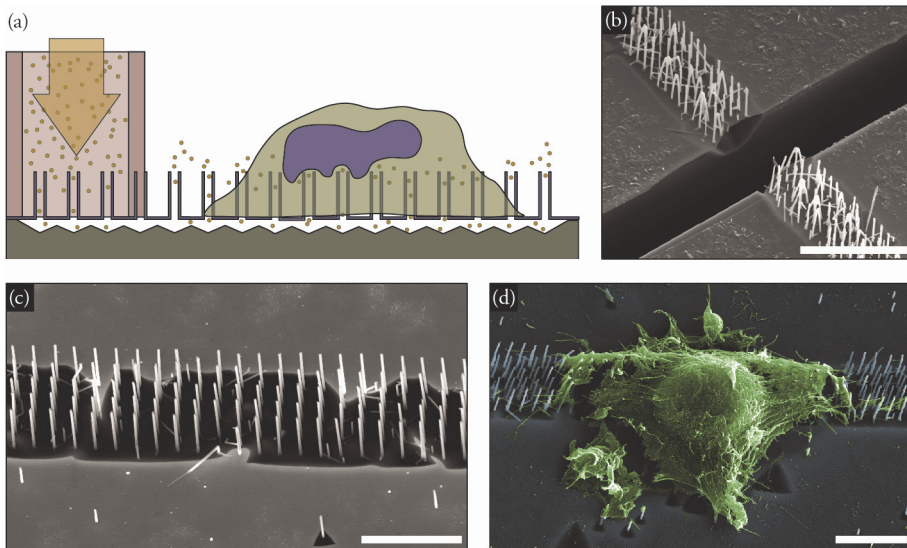
Figure 3.4 Sketch showing our proposed arrays of oxide nanotubes connected by subsurface microchannel (a) presented in Paper I. SEM images show or arrays of nanotubes with the subsurface microchannel (dark area) (b-d). Scale bars are 10 μm (b) and 5 μm (c-d). Tilt 30°.

To test the fluidic transport capability of the channel, we separated the centimetre long nanotube array into two halves by blocking the surface with a strand of glue. A fluorescent dye dissolved in ethanol was added to one side of the barrier (Figure 3.5 a) and fluorescence microscopy was used to observe the dye enter the channels on the other side of the physical barrier, by means of capillary wetting (Figure 3.5 b). As a further test, we added fluorescently labelled DNA to one side of the barrier and used electrophoresis to pull the DNA through the microchannel (Figure 3.5 c). These initial fluidics experiments proved that our fabrication method was successful. However, in order to connect the device to the pumps that are used to control the flow in microfluidic devices, we had to interface the nanotubes and their delicate microchannel with the macroscopic world. We attempted to achieve this by adopting the normal approach used for PDMS-based microfluidics: simply gluing a silicon tube onto the channel (Figure 3.4 a). This approach proved to be too harsh and damaged the microscopic channels and the devices inevitably broke. We think the breakage occurred by the channels both collapsing and being filled with glue, thus losing their fluid transport capabilities. We have a few ideas on how to successfully interface our nanotubes with conventional microfluidics such as using UV-lithography to reinforce the channels or further explore the through-wafer membrane etching. While considering alternate solutions, we published Paper I and have since focused on furthering our knowledge of how cells interact with nanostructures, knowledge crucial to nanowire-based cell applications.
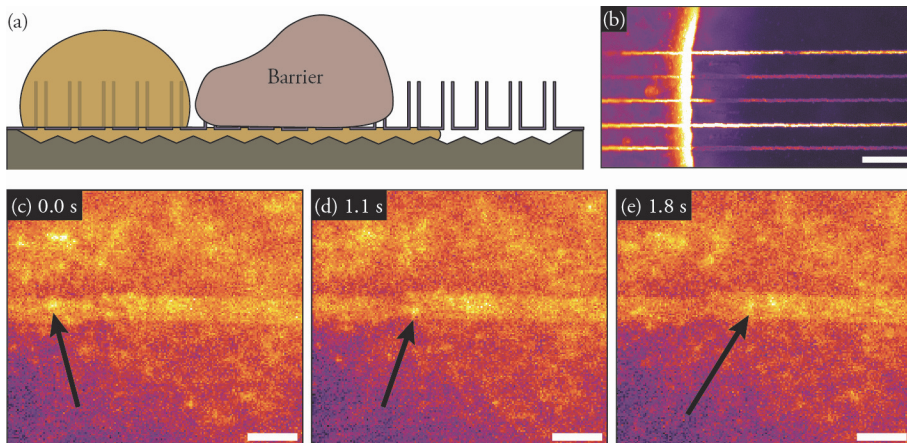
Figure 3.5 Demonstration of the liquid transport capabilities offered by our subsurface microchannel. A physical barrier (brown) separated the channel into two halves, forcing a fluorescent liquid (orange) to move through the channel rather than across the surface (a). Fluorescence microscopy image showing how 5 parallel channels are filled with the fluorescent dye (b). Using the same setup, we could observe as DNA moved through the microchannel (black arrow), with flow driven by evaporation of liquid on one side of the barrier. Scale bars are 100 μm (b) and 10 μm (c-e).

Nanosyringes in literature

Nanosyringes are a quickly developing technique and while our work with oxide nanotubes and the subsurface microchannel was undergoing review and revisions, two other groups published results based on similar devices. Peer working in Sivan's group fabricated a membrane containing silicon oxide nanotubes by using RIE to create EBL defined through-wafer connections in a silicon substrate [27]. The wafer was oxidized and selective dry etching could be used to etch back the silicon substrate, exposing silicon oxide nanotubes. Cells were cultured on top of the oxide nanotubes and fluorescently labelled dextran and DNA coding for red fluorescent protein were successfully introduced into cells with the help of saponins, a molecular family of surfactants. VanDersarl in Melosh's lab based their fabrication method on a commercially available porous polycarbonate filter which was covered in aluminium oxide using ALD [133], the isotropic deposition ensuring the interior of the pores was coated as well as the top surface. The top oxide layer was removed using RIE and selective oxygen plasma etching was used to etch down the porous membrane, exposing the Al_2O_3 coated pore-walls. Using this simple, inexpensive approach, VanDersarl could readily produce large (several cm²) sheets covered with oxide nanotubes. Since the sheets were based on flexible filters, they were very durable and, more importantly, they already had holes through the substrate, i.e. there is fluidic access to the back of the nanotubes from the beginning. To finalize their device, VanDersarl et al. sandwiched the nanotube-containing membrane between two PDMS pieces, the top

piece containing a cell culture chamber and the bottom containing a microfluidic channel, capable of directing molecules to be injected into cells with spatial and temporal control. Using this device, they performed successful injection of dyes, ions and plasmid DNA and demonstrated sequential delivery. In a recent publication, the group improved the injection reliance of their system by integrating a transparent electrode made from indium tin oxide into the channel below the nanotube membrane [28]. This electrode, paired with a platinum electrode above the cells, allowed for every effective, local electroporation using the nanotubes as electrodes. This enabled the creation of temporary membrane pores that would quickly close after injection. Using this improved setup, they managed to inject dyes and plasmid DNA into cells, 24 h apart. They also demonstrated that the created pores closed within 10 min, which can be very beneficial for cell viability. The improvement this second version of their device offered highlights one weakness in the first device. It appears that creating a stable membrane penetration is not readily achieved, which is also highlighted by Peer et al.'s use of a surfactant to aid injection experiments. The question of whether nanowires and similar structures spontaneously penetrate the cell membrane in mammalian cells is a hot topic in this field and will be addressed in detail in Section 4.6 in the next chapter.

3.3 Chapter summary

This chapter has described some of the many promising cell biological applications based around nanowires and similar vertical nanostructures. Focus has been around injection systems, from the first proof of principle injections in 2003 [113] to the most recent work where these structures have been used to shed light on important biological questions [84], [142]. In Paper I, we started to address some of the limitations of these static systems by using nanotubes with fluidic transport to allow temporal control and the retrieval of intracellular material. This large interest in using nanowires in cell biological applications warrants the question: *"How do cells respond to nanowires?"* - A question which will be the focus of the next chapter.

Table 3.1 A summary of injection experiments based on vertical nanowires and related structures. The physical dimensions of the nanowires are density (ρ), length (L) and diameter ($\varnothing$). Different groups have often used different units (such as nanowires mm^{-2} or nanowires per cell). In these cases the units have been converted with as much fidelity as possible. Regrettably, all relevant information was not always obtainable in all of the publications.

Year	Group	substrate	ρ [μm^{-2}]	L [μm]	$\varnothing$ [nm]	Cell type(s)	Injected molecule(s)	Comments
						Epitaxial nanowires		
2007	Kim et al.[20]	Si nanowires	2-3 nano-wires per cell	6	90	HEK293	DNA	1% efficiency
2010	Shalek et al. [26]	Si nanowires	N/A	N/A	N/A	HeLa, prim. rat neurons, prim.hum. fibroblasts	Proteins, peptides, DNA, dyes, drugs, siRNA	95-100% delivery efficiency Used random and ordered arrays
2011	Chevrier et al. [139]	Si nanowires	N/A	N/A	N/A	BMDC	Enzyme inhibitor	Decipher signalling network for antiviral response
2012	Shalek et al. [84]	Si nanowires	0.19-1	1-3	<150	Immune cells, Leukaemia	siRNA	Non adherent cells Extensive functional study Nanowires tailored for each cell type
2013	Yosef et al. [142]	Si nanowires	N/A	N/A	N/A	Murine TH17	siRNA	Extensive genetic mapping

Vertical, high aspect ratio nanostructures

Year	Reference	Material				Cell	Cargo	Notes
2003	McKnight et al. [113]	Carbon nanofibers	0.04	7	30 (tip)	CHO	DNA	Cells centrifuged or pushed onto array. Stable or transient transfections
2008	Mann et al. [136]	Carbon nanofibers	0.0025-0.04	10-17	100 (tip)	CHO	siRNA	
2009	Park et al. [132]	Carbon tubes	77	0.04-0.16	50 (outer)	NIH3T3, human stem cells	Quantum dots, DNA,	
2013	Mumm et al. [81]	CuO nanowires in PDMS	N/A	0.5-5	100-150	HeLa, HEK293	GFP DNA	1% efficiency

Nanotube based fluidic injection systems

Year	Reference	Material				Cell	Cargo	Notes
2011	VanDersarl et al. [133]	Al2O3 nanotubes	0.1-1	1-2	100-750	HeLa, CHO	DNA, dyes, ions	Serial injection demonstrated
2012	Persson et al.	Al2O3 nanotubes	1	4	180 (outer)	none	none	Paper I. No successful injection
2012	Peer et al. [27]	SiO2 nanotubes	0.04	5	500 (outer)	HEK293	Fluorescent dextran, plasmid DNA	Injections aided by surfactant 70% injection rate
2013	Xie et al. [28]	Al2O3 nanotubes	0.2	1.5	250	HEK293, CHO	Dyes, plasmid DNA	Electrode for electroporation. 67-95% efficiency

4 Cell and nanowire interactions

In the previous chapter, several applications based on the interactions between cells and nanowires were described, with focus on the injection application we have been exploring (Paper I). For these applications to find wide spread use, the basic cell-nanowire interactions need to be understood in detail. The literature concerning cell behaviour and viability is growing, but studies dedicated to the interaction between cells and nanowires (i.e. no application directly studied) are few. (Cell interactions with other nanotopographies such as grooves, rough surfaces, pores and fibres are studied extensively [106], [107] but fall outside the scope of this thesis.)

This chapter will give an overview of studies that have started to shed light on cell-nanowire interactions and put our work into context (Paper II-IV). In Papers II and IV, we studied basic cell behaviour like migration and division for cells cultured on nanowires of different length or density, in order to understand these interactions in detail. With increased understanding, new applications can be developed and existing nanowire-based methods can be improved by minimizing unintentional cell perturbations. To improve future studies of cell-nanowire interactions, we developed inherently fluorescent nanowires for improved imaging (Paper III).

One obstacle arises when surveying the literature in order to try to understand how cells interact with nanowires. The range of cell types studied is very wide, from primary non-adherent immune cells [84] and cancer [26], [81] to immortal kidney cells [81], [85], fibroblasts [79], [145], [146] and neurons [26], [85], [147] (Appendix 1 can be used as a reference list). The range of nanostructures is similarly diverse with everything from very sparse, random patterns of short nanopyramids [79] to densely packed, ordered arrays of 100 nm diameter tips [145] and, of course, vertical, epitaxial semiconductor nanowires [26], [84], [85], some of which are seen in Figure 3.1. Another issue is the substrates used as controls. Very often, cells are compared to control substrates of the same material as the nanowires are made from which is good practice, reducing suspicions of chemical effects contributing to the results. However, tissue culture substrates such as polystyrene (PS) or glass which are typically used should also be used additional controls as cell behaviour can differ between glass, PS and semiconductor surfaces (e.g. deviating morphologies or different migration behaviour) on these substrates as on the semiconductor surface, as we (Paper II and IV) and others [19], [83], [143] have reported.

4.1 Methods to study cell-nanowire interactions

Studying cell behaviour and cell responses to different stimuli is one of the most fundamental aspects of cell biological research and hence a large library of different methods has been developed to probe cell behaviour. Methods range from extremely simple, like estimating number of cells, to advanced methods like cataloguing the amount of specific proteins present in the cells [148]. However, many of the existing techniques rely on a few prerequisites that are not readily met for nanowire-based cell cultures. These prerequisites often include a transparent substrate and/or a large number of cells (which translates into a large surface area). It is often useful or even compulsory to detach the cells from the substrate they are cultured on, something which is not readily achievable for cells cultured on nanowires, depending on the nanowire dimensions. Some groups report successful trypsinization [26], [81], [133] while at least one group utilizes the strong adhesion to prevent cells from detaching [82]. Successful trypsinization seems to be dependent on the physical dimensions of the nanowires; we found it to be possible to detach cells cultured on 1.5 μm long nanowires but not on 6.7 μm long nanowires (diameter 80 nm, density 1 nanowire μm^{-2}, results not published).

These limitations leaves one, very versatile method: fluorescence microscopy. Fluorescence microscopy uses adherent cells (no need to detach them) and data collection is based on photography (small surfaces, a few mm^2 are sufficient). In almost all implementations, fluorescence microscopy does not require a transparent sample. Fluorescence based microscopy is extremely versatile owing to the specificity and functionality of the many dyes that have been developed, as outlined in Chapter 2.

Another commonly used tool to study cell-nanowire interactions is SEM. One of the drawbacks of optical microscopy (such as fluorescence microscopy) is that the nanowire structure and orientation are smaller than what can be resolved using optical microscopy (typically 200-300 nm). Therefore optical studies are commonly complemented with SEM, where the nanowires are readily resolvable. Thus, the direct physical interactions between cells and nanowires can be observed in detail.

4.2 Nanowire effects on cell morphology

The morphology of cells refers to their overall physical characteristics, as observed in a microscope. Commonly studied cell lines show diverse morphologies which can tell us about their well-being and function. For instance, migratory cells tend to be spread out with relation to each other and have an elongated shape with a flat, broad edge (lamellipodia) in the direction of migration whereas endothelial cells usually grow in

patches and are more symmetrical. Investigating the morphology of cells is one of the very first observations done to determine if the cells are responding with a morphological change to an insult, be it a treatment, a bacterial infection or non-optimal pH [39]. If the cells do not appear normal, something might be wrong though the reverse is not necessarily true.

Since assessment of cell morphology is such a readily available experiment, it is one of the entry points into studying cell interactions with nanowires. The observation is in fact so routine that few authors comment on cell morphology and those that do, often merely state that the morphology looks healthy, normal or unchanged [26], [81], [84], [85] compared to controls (tissue culture plastic, glass or a flat control of their particular material). Some authors report smaller and rounder cells [19], [79]–[81], [145], [146], smaller, rounder and elongated [145] or show other morphological deviations [143], compared to controls.

With the variety of cell types, nanotopographies, materials and experimental design approaches, any different morphologies reported might be attributed to a wide range of factors such as different cell types responding differently as well as different topographical structures combined with different material stiffness and surface chemistry. In studies where a single type of nanostructure and a single cell line has been used, it is easier to draw conclusions on how specific aspects of the nanowires influence cell morphology. Based on this approach, different effects from physical nanostructure dimensions have been reported with relation to length (refs [79], [143], [145] and Paper II) as well as nanowire spacing (ref [23], [83] and Paper IV).

Some cell types such as neurons appear to prefer growing on semiconductor nanowire substrates compared to flat semiconductor controls, as demonstrated by an increased amount of axonal protrusions, both for dorsal root ganglion neurons [19] and retinal neurons [143]. Piret et al. studied the effects of nanowire dimensions and found that, for their retinal neurons, 4 µm long nanowires were optimal to promote axonal outgrowth [143]. They also found that some of the associated cells, such as astrocytes, showed very different morphologies when cultured on nanowires compared to flat GaP while glial cells did not exhibit any substrate-induced changes in morphologies, demonstrating a cell type dependent response to nanowires.

In Papers II and IV, we found a correlation between the physical dimensions of nanowires and the morphology of the cells (mouse fibroblasts, L929). In Paper II we found that, when cultured on 1.5 µm long nanowires (diameter 80 nm, density 1 nanowire µm^{-2}), the cells appeared fairly normal compared to cells on planar GaP substrates and tissue culture plastic, albeit they were somewhat more rounded (Figure 4.1 a-c). On 6.7 µm long nanowires (same diameter and density), cells developed into very large abnormal cells with morphologies very different from those on flat controls

49

and short nanowires (Figure 4.1 d-e). This was attributed to the cells failing to divide on these substrates (see Section 4.4). Apart from the atypically shaped cells, we also noted a very large heterogeneity in the morphologies; some cells would appear almost normal whereas others were very deformed.

In Paper IV, we varied the average inter-nanowire distance, keeping length and diameter constant (diameter 80 nm, length 4 μm). Here we found that for a low density (0.1 nanowires μm^{-2}), the cells would develop irregular morphologies with long protrusions, in rare cases up to 200 μm. Often they would have several, jagged protrusions (Figure 4.1 f). Again, this was attributed to an inability to migrate and, using phase holographic time-lapse microscopy (Section 0), we could observe as immobile cells would adopt these abnormal morphologies (see Supportive Movie S11[*]). When the cells were cultured on high density nanowire arrays (4 μm^{-2}), the cells were motile and adopted morphologies similar to the flat control substrates (Figure 4.1 e).

---

[*] The supporting material is described in Appendix 2 and can be found online: http://bit.ly/Persson2014.
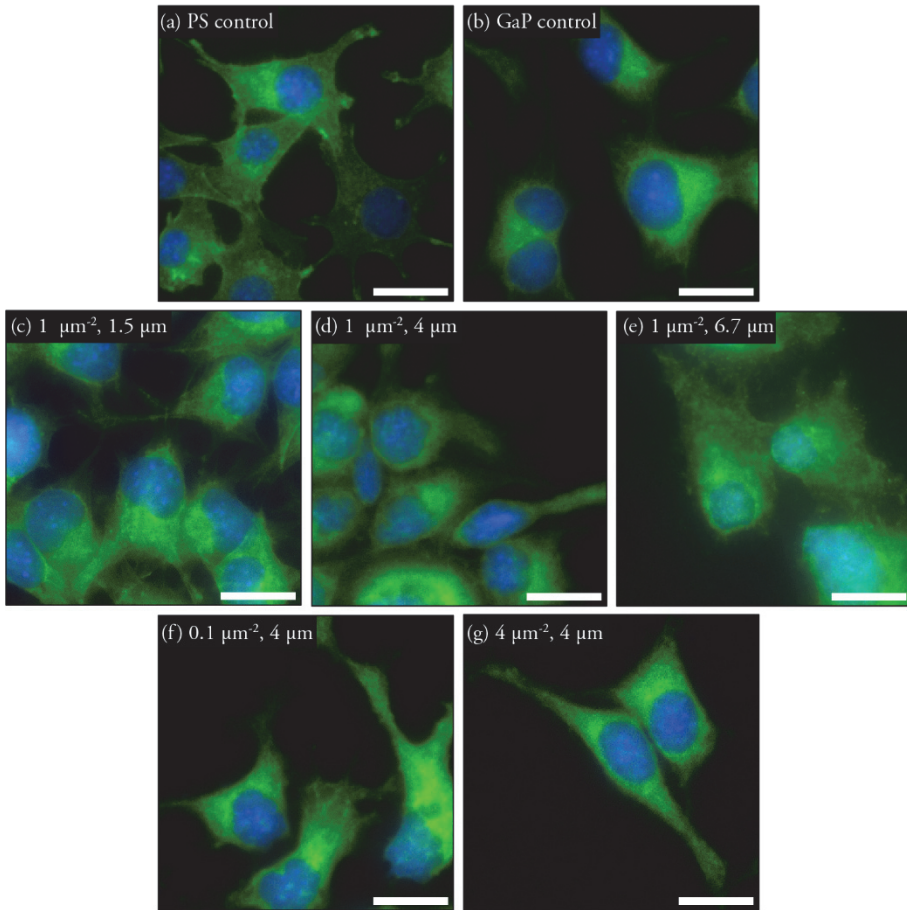
Figure 4.1 A variety in the morphology of fibroblasts can be seen for cells cultured on nanowires depending on the density and lengths of nanowires. Actin is labelled with FITC-conjugated phalloidin (green) and nucleic DNA is labelled with bisbenzimide (blue). Scale bars are 20 μm.

Figure 4.2 (The following two pages). Selection of SEM images showing L929 on GaP nanowires. For high densities, cells experience a bed of nails effect and reside on the tips of the nanowires (a, h-i). For lower densities, the cells adhere to the substrate between the nanowires, with the nanowires seemingly penetrating into the cells (b-g, j). For particularly low densities (here 0.1 μm-2), the nanowires will even emerge from the top of the cells (f-g). The same can sometimes be observed for higher densities, particularly for long nanowires (d, e). Sometimes these nanowires appear membrane clad (g, j), sometimes they penetrate through the membrane (e) and sometimes they appear as small bumps, just barely visible (i). When cultured on nanowires, cells can be seen to grab onto the structures and pull on these, deflecting the nanowires (c, j). The nanowires in the images have different physical dimensions. All have a diameter of 80 nm but density varies between 0.1 (f-g), 1 (b-e, j), 5 (h-i) and 10 (a) nanowires μm-2. The nanowire length also varies, from 1.5 (b-c) to 4 (a, f-j) and 6.7 μm (d-e). Scale bars are 10 μm (a, b, d, f, h), 2 μm (c, e, i-j), and 500 nm (g). Tilt is 30° (b-i) or 54° (a).

53
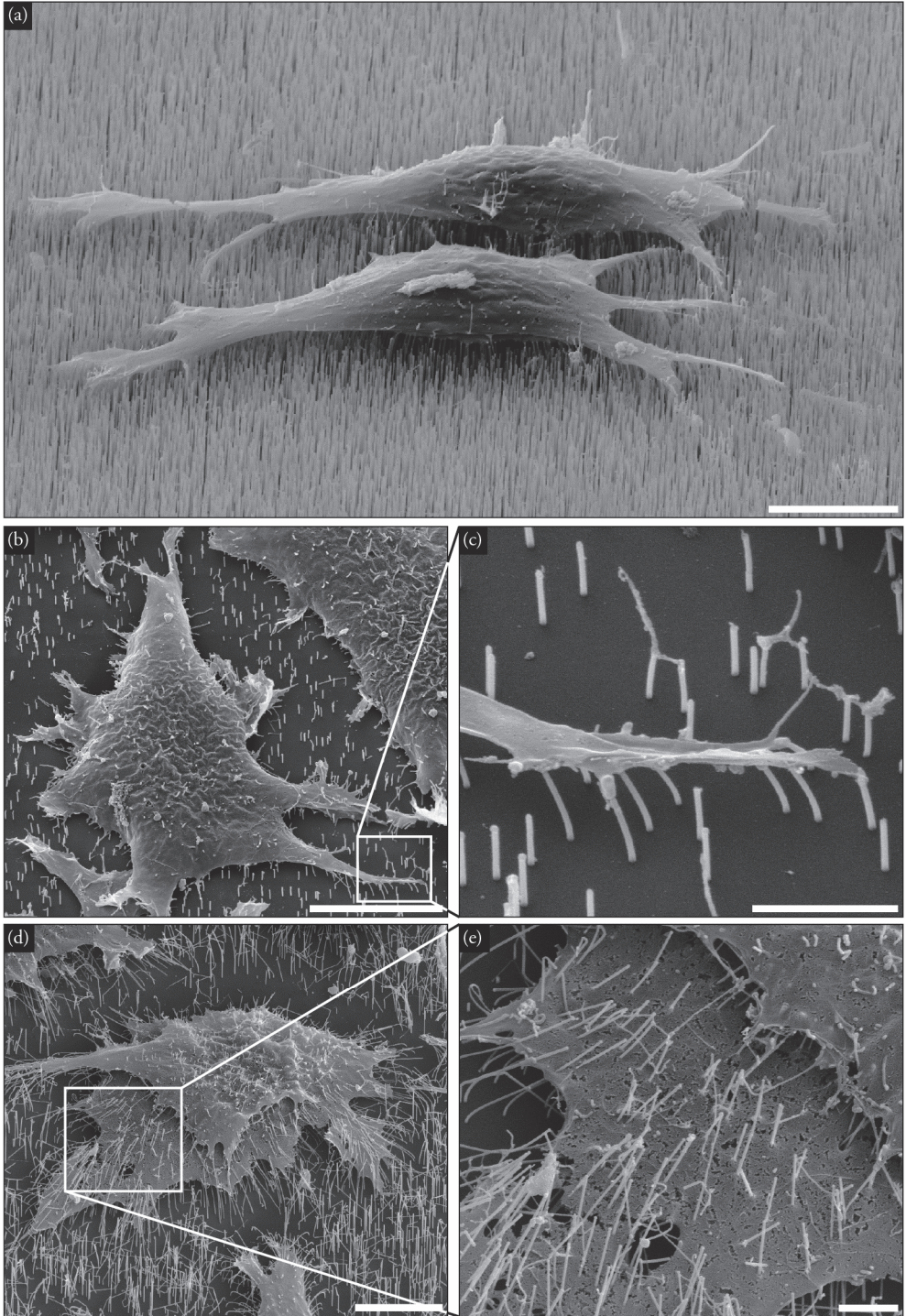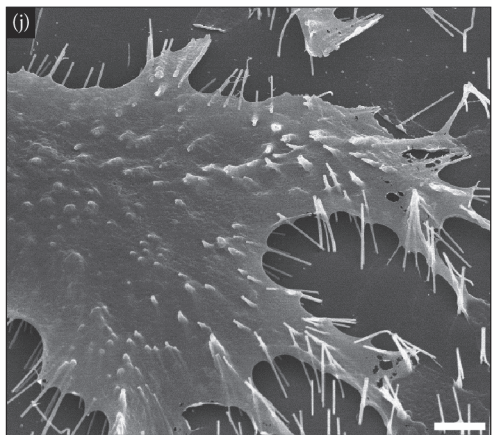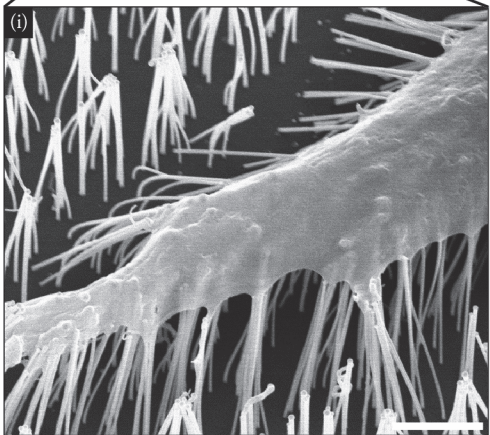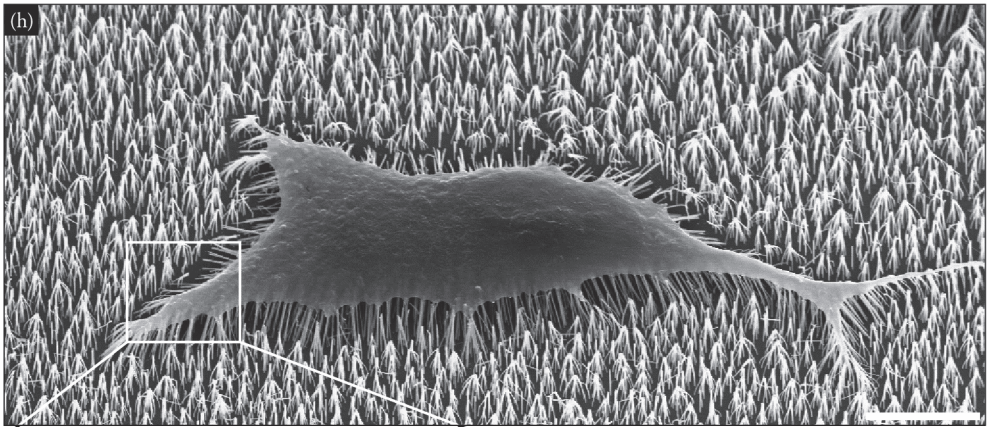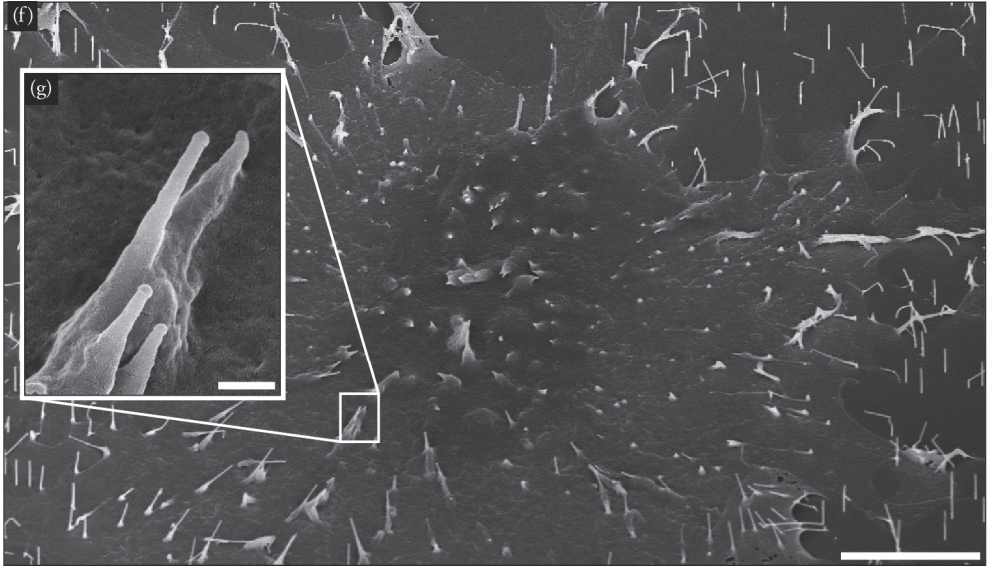
Scanning electron microscopy

When working with nanowires, it is often of interest to complement studies based on optical microscopy with SEM data to resolve the nanowires. Using SEM, several groups have reported on the close interactions between cells and nanowires (see for instance refs [19], [20], [23], [85]). In fact, these close interactions are often what spark researchers' imagination to try and develop cell biological applications based on nanowires in the first place.

When cultured on nanowires, cells will either sit on the flat surface between the nanowires (Figure 4.2 b, d-h) with the nanowires seemingly penetrating deep into the cells or they will reside on top of the structures, if the nanowires are placed densely enough. Nanowires can often be observed as protrusions on the top side of the cells (Figure 4.2 d-g, i-j). In most cases these protrusions are membrane bound but will sometimes appear to penetrate through the membrane (Figure 4.2 d-e). This is likely an artefact from the dehydration step in sample preparation, during which the cell membrane often cracks and cannot be taken as an indication of nanowires penetrating the cell membrane in living cells (more on this in section 4.6). Another feature often observed is cell protrusions adhering to the nanowires and bending these toward the cell. This is likely a behaviour related to the cells' natural disposition to adhere to and pull on the substrate on which they are cultured [149]. Though this nanowire deflection has been observed in live cells [110], the dehydration process necessary for SEM imaging (see Chapter 2) can cause cells to shrink and exaggerate nanowire bending.

4.3 Nanowires affect cell migration

Cell migration is an important, physiological characteristic of many different cell types. *In vivo*, cells migrate during foetal development, angiogenesis[*], construction of connective tissue and cells of the immune system migrate to sites of infection or physical damage. Deregulated migration is linked to many autoimmune diseases such as type 1 diabetes [150], and is one of the hallmarks of cancer [151], [152], enabling cancer cells to spread throughout a patient's body in a process called metastasis. As such, migration, and especially changes in migration behaviour, is often studied *in vitro* using time-lapse microscopy. In Papers II and IV we employed phase holographic microscopy to conduct time-lapse imaging of cells cultured on nanowires with either

---

[*] Angiogenesis is the process by which new blood vessels are formed as protrusions from already existing vessels.

varying length (Paper II) or varying density (Paper IV). In Paper II, we found that increasing nanowire length reduces cell motility (see Supporting Material*). In Paper IV we found that, if density is increased to the point where cells adhere to the nanowire tips (Figure 4.2 a, h-i), cells are able to migrate.

Studies of cell migration on nanostructured surfaces are rare, owing to the difficulty in imaging cells on these substrates without staining them (as discussed in relation to phase holographic microscopy in (Chapter 2). To circumvent this issue, Mumm et al. [81] and Fletcher et al. [153] have embedded their nanostructures in transparent substrates compatible with standard transmitted light based microscopy methods. However, neither performed time-lapse imaging. Hanson et al. used Pt nanopillars on a transparent quartz substrate to image neurons once every 24 h and concluded that the cells migrated until they were in contact with the nanopillars where they became immobilized [147]. Transparent substrates paired with transmitted light microscopy is not the only means of carrying out time-lapse microscopy. Apart from labelling cells (see section on phototoxicity in Chapter 2), a reflective substrate made from e.g. silicon can be used in connection with white light transmitted through the objective. With this approach, Łopacińska et al. studied migrating mouse fibroblasts (NIH3T3) on silicon surfaces with varying nanotopographies [79]. One of their surfaces was similar to the epitaxial nanowires studied in this thesis (diameter 700/200 nm (base/tip),length 3 μm, density 0.04 nanowires μm^{-2},)and for this substrate they reported a two-fold increase in cell motility (measured as μm/min) compared to flat silicon. The cells on this surface not only moved faster but in a more randomized pattern, seen as a two-fold reduction in persistence length.

One of the advantages of our nanowire system is the large bandgap energy of GaP, meaning it is transparent to light of wavelengths above 549 nm, as discussed in Chapter 2. Worth noticing is that this is a fairly unique property for GaP as most other semiconductor substrates have much lower band gap energies, making them non-transparent to visible light. The commercial implementation of phase holographic microscopy supplied by the company Phase Holographic Imaging (PHI AB, Lund, Sweden) utilizes a long wave length laser (633 nm) which can pass through our GaP substrates, if double side polished wafers are used (single side polished wafers have a rough surface which scatters the light). This method enables long term imaging (96+ hours) of cells in their natural state (no staining) and was used extensively in Paper II and Paper IV to image mouse fibroblasts (L929) on substrates with nanowires.

---

* The supporting material is described in Appendix 2 and can be found online: http://bit.ly/Persson2014.

We found that when cultured on nanowires (diameter 80 nm, density 1 nanowire μm^{-2}) with varying length (1.5, 4 and 6.7 μm) (Paper II), the cells would display a length dependent migration pattern (Figure 4.3 a-c, Supporting Material, movies S1-3[*]). On short (1.5 μm) nanowires, the cells would move at a high rate and cover distances similar to that on plastic control surfaces (Figure 4.5). For medium length nanowires (3.8 μm), the motility was reduced and for the longest nanowires (6.7 μm), motility was practically non-existent. We attributed this to the cells being entangled by the longer nanowires which appear to be protruding into the cells as judged from SEM images (Figure 4.2**Fel! Hittar inte referenskälla.** d-e). This would also explain why the cells on the much shorter nanowires seemed largely unhindered (Figure 4.2 b-c).

In Paper IV, we used a constant nanowire length and diameter (diameter 80 nm, length 4 μm) and varied the nanowire density (Figure 4.3 d-f, Supporting Material, movies S6-8). Here we found that on average 50-100 nanowires per cell were sufficient to prevent cells from moving (density 0.1 μm^{-2}) (Figure 4.3 d, Supporting Material, movie S6). For these low density substrates, we also observed a different mode of migration compared to flat controls (PS and GaP). The cell migration occurred during short intervals following cell division and at all other times the cells remain stationary (Figure 4.5, Supporting Material, movie S12). We interpret this as the cells being entangled and prevented from moving by the nanowires, but upon division, during which the cells roll into spheres and reduce their adhesion to the substrate, one or both of the daughter cells might become disentangled from the nanowires and migrate. This movement is short and we attribute the immobilization to the cells once more becoming entangled by nanowires. When the cells were cultured on dense samples (4 nanowires μm-2) they would adhere to the top of the nanowires (Figure 4.2 h-i) and were able to migrate (Figure 4.3 f, Supporting Material, movie S8).

---

[*] The supporting material is described in Appendix 2 and can be found online: http://bit.ly/Persson2014.

(a) 1 μm⁻², 1.5 μm (b) 1 μm⁻², 3.8 μm (c) 1 μm⁻², 6.7 μm

(d) 0.1 μm⁻², 4 μm (e) 1 μm⁻², 4 μm (f) 4 μm⁻², 4 μm
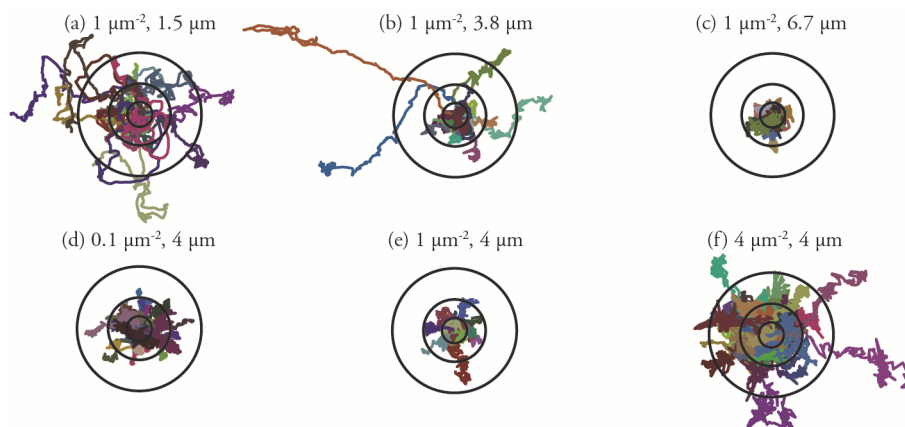
Figure 4.3 Time-lapse traces for L929 on different nanowire substrates from paper II (a-c) & IV (d-f). Note that two slightly different experimental procedures were followed. In Paper II, the cells were incubated for 24 h on the substrates prior to imaging and then tracked for 20 h while in Paper IV, the cells were tracked for the first 24 h just after seeding. The concentric circles have radii of 10, 25 and 50 μm. The movies from which some of these tracks were extracted can be found in the Supporting Material[*], Movie S1-3 and S6-8.

(a) PS ctrl (b) GaP ctrl (c) PS ctrl (d) GaP ctrl
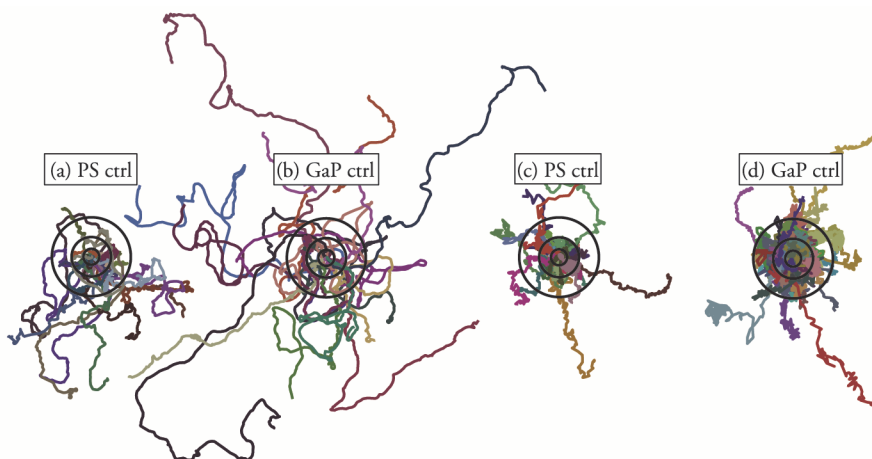
Figure 4.4 Time-lapse traces for L929 on control substrates (PS and GaP) used in paper II (a-b) & IV (c-d). The concentric circles have radii of 10, 25 and 50 μm. The movies from which some of these tracks were extracted can be found in the Supporting Material[*], Movie S4-5 and S9-10.

---

[*] The supporting material is described in Appendix 2 and can be found online: http://bit.ly/Persson2014.
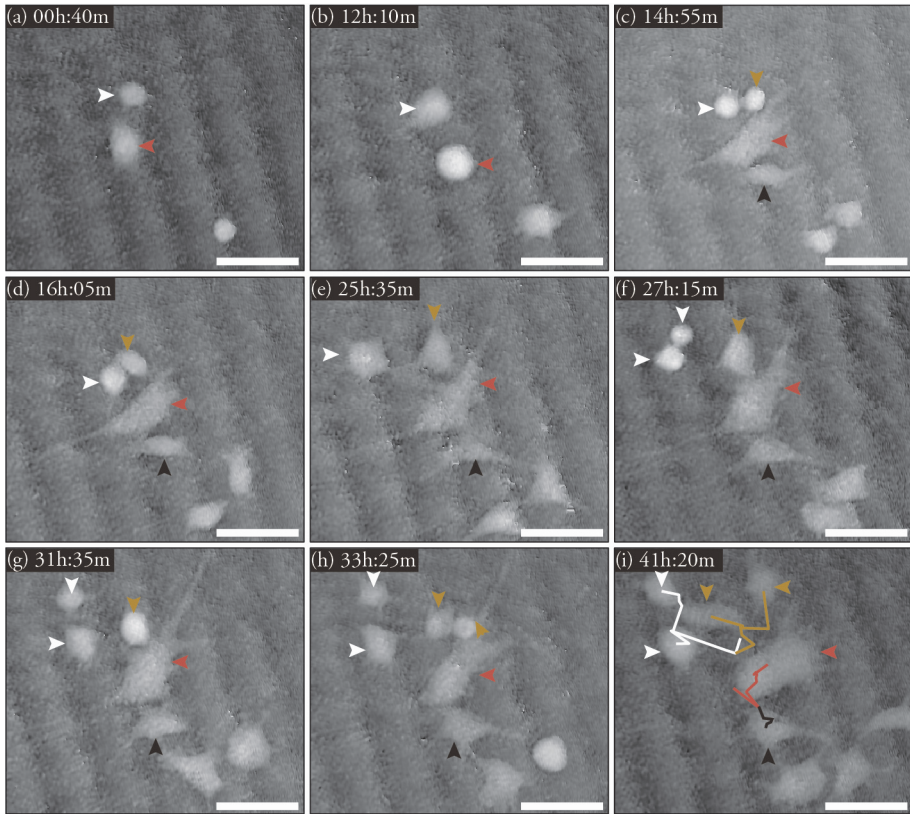
Figure 4.5 Cell migration on low density nanowire substrates (diameter 80 nm, length 4 μm, density 0.1 nanowires μm^{-2}). Frames from Supporting Material, movie S12[*]. Cells remain stationary until they divide. Following division one or both daughter cells might become migratory. Here, the cell labelled with a white arrow divides (b) and the daughter cell labelled with a white migrates some distance before re-adhering. Meanwhile the daughter cell labelled with a yellow arrow remains stationary after division. The final frame (i) shows the tracks two of the cells in (a) have taken, including their daughter cells. Scale bar 50 μm. Time stamp refers to time after seeding.

4.4 Nanowire effects on cell proliferation and division

As an organism grows and as cells age and wear out, new cells need to be produced, a task achieved by cell proliferation both *in vivo* and *in vitro*. Division and proliferation are very important aspects of cell culturing and the rate at which cells proliferate is often used in toxicity studies to investigate whether a compound is toxic or not. For cells on nanostructured surfaces, few papers comment on cell proliferation and often qualitative terms are used. Shalek et al. observe a reduction in rate of cell proliferation for HeLa cells on silicon nanowires (no dimensions given) compared to cells on glass coverslips [26]. Berthing et al. report a similar survival rate for cells (HEK293 and F11) when cultured on InAs nanowires (diameter 100-300 nm, length 1-3 μm, density 0.3 nanowires $μm^{-2}$) compared to flat controls (InAs and glass) [85]. The survival rate was estimated using the membrane impermeable dye EthD-1 to label dead cells while living cells were identified by their enzymatic activity using calcein AM (Chapter 2).

In Paper II and IV, we studied cell proliferation quantitatively by measuring cell number as a function of both time and the physical properties of the nanowires ( ). In Paper II we varied the nanowire length (1.5, 4 and 6.7 μm) while keeping diameter (80 nm) and density (1 nanowire $μm^{-2}$) constant. In Paper IV we varied the diameter (0.1, 1 and 4 nanowires $μm^{-2}$), keeping diameter (80 nm) and length (4 μm) constant. Combining the results from these papers, we see that long nanowires (6.7 μm) or dense arrays (4 $μm^{-2}$) greatly reduce cell proliferation rate whereas shorter nanowires (diameter 80 nm, length 1.5-3.8 μm, density 1 $μm^{-2}$) or sparse arrays (diameter 80 nm, length 3.8 μm, density 0.1-1 $μm^{-2}$) affect the proliferation to a lesser extent (although a reduction compared to flat controls (GaP and PS) can still be seen). In contrast Peer et al., the only other group to study time-resolved cell number for cells on similar, vertical nanostructures, did not find any difference in cell proliferation between cells (HEK293) cultured on their nanosyringe substrates (outer diameter 500 nm, length 5 μm, density 0.04 nanowires $μm^{-2}$) and cells cultured on flat controls (cell culture plates and silicon) [27]. This difference might be explained by the low density. As seen in Paper IV, a lower nanowire density has a lower impact on cell proliferation. Alternately, the larger diameter of Peer et al.'s nanowires results in stiffer nanowires which might lead to reduced interference with cell division (further discussed under the heading *nuclear invagination* on pp. 66-68).
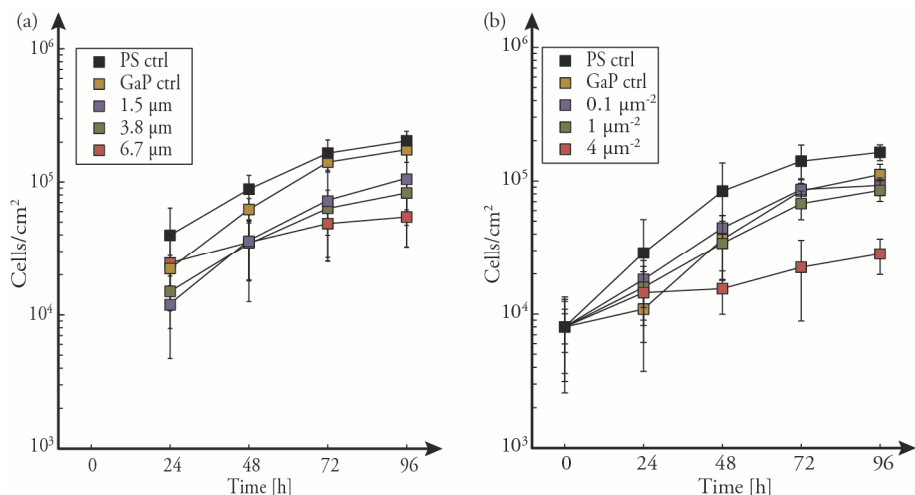
Figure 4.6 Cell proliferation data presented in Paper II (a) and Paper IV (b). Mouse fibroblasts (L929) were cultured on nanowire substrates (see legend), flat GaP and PS control for 96 h. Every 24 h the samples were imaged using phase holographic microscopy and cell number was determined.

Instead of measuring the number of cells directly, the mitochondrial reduction capacity (related to oxygen turnover) can be determined using e.g. AlamarBlue™ (Chapter 2) or MTT[*]. The reducing capacity of the cell culture is supposed to be proportional to the cell number. Using AlamarBlue™ reduction as a proxy for cell number, Choi et al. report a length dependant reduction in cell number for human primary fibroblasts cultured on ordered nanoneedle arrays (tip diameter 10 nm, density 19 μm^{-2}) up to 80 h in culture [145]. Cells on their short structures (50-100 nm and 200-300 nm) showed a lower reduction compared to cells on their longer structures (500-600 nm). For human liver cells (HepG2 and LX-2), Qi et al. reported a slight reduction in cell number on their silicon nanowires (random etched structures, length 20 µm, cells on top of nanostructures) compared to the same cells cultured on flat silicon [154]. Using MTT, Łopacińska et al. found a reduced metabolic activity for cells (NIH3T3) cultured on their silicon nanostructures (diameter 700/200 nm (base/tip), length 3 µm, density 0.04 μm^{-2}) compared to PS but an increased activity compared to flat silicon [79]. Note that, while this measured activity is connected to the number of cells, certain stressful situations may affect respiration without changing the cell number [155]. In fact, L929 cells cultured on our nanowires show an increase in cell respiration (Paper II). Here we used the AlamarBlue™ assay and normalised the fluorescence signal to cell number (determined by manual counting). In practice, this means that the

---

[*] MTT, or 3-(4,5-dimethylthiazol-2-yl)-2,5-diphenyltetrazolium bromide, is a water-soluble salt. Upon reduction by cellular enzymes, it will turn insoluble, precipitating out of solution. Measuring the absorption gives an indication of the level of metabolic activity in the cell culture [174].

changes in activity observed by Choi et al., Qi et al. and Łopacińska et al. might be attributed to either changes in cell number, changes in metabolism or both. If our findings are transferable to their cell lines and nanostructures, then there is indeed a decrease in cell number for their substrates and cell lines as well.

Division

Except for Berthing et al, who did not find any changes in cell viability [85], , most publications point to a reduction in proliferation rate for cells cultured on nanowire substrates compared to flat controls [26], [27], [79], [145], [154] (Papers II and IV). This reduction in cell number could arise from different sources such as an increased cell death on nanowire substrates, a longer cell cycle, cells detaching from the substrate or cells failing to divide. If the cell number increases on a sample (compared to the seeding density), all of these mechanisms are connected to cell division. That is, if an increased cell death, for example, would be the explanation for reduced cell number compared to controls, there is still division occurring as the number of cells increases. If only a single time point is measured and the cell number is found to be lower than for control samples, then it is not certain that division is occurring. Note that the total number of cells is confirmed to increase in our work (Papers II and IV) and that of Peer et al. [27], as in those cases the same samples were imaged at several time points. In cases where a reduced cell proliferation is found by measuring cell respiration [79], [145], [154], it is not certain whether cell number actually decreases at a lower rate or if the cells exhibit a reduced respiration, though it seems likely that the cell number does increase (as respiration likely increases (Paper II)).

To discern the cause of reduced cell number, time-lapse microscopy can be employed to witness any division events. In our work with time-lapse imaging, we have observed a high rate of failed cell division for cells cultured on nanowires. This was especially prevalent for cells cultured on our long nanowires (diameter 80 nm, length 6.7 μm, density 1 nanowire μm^{-2}) in Paper II.

Figure 4.7 shows how division errors are caused by the nanowire substrate, in this case leading to interrupted division and asymmetrical daughter cells (Supporting Material, movie S13[*]). In paper II, we found that these interrupted divisions were most common for cells cultured on the longest nanowires (6.7 μm) and barely occurred on the shortest nanowires studied (1.5 μm). When we instead kept length and diameter constant (diameter 80 nm, length 4 μm) and varied density1. (0.1, 1 and 4 nanowires μm^{-2}) (Paper IV), we saw similar interrupted division events, but to a lesser extent than for cells cultured on the long nanowires.

---

[*] The supporting material is described in Appendix 2 and can be found online:
http://bit.ly/Persson2014.
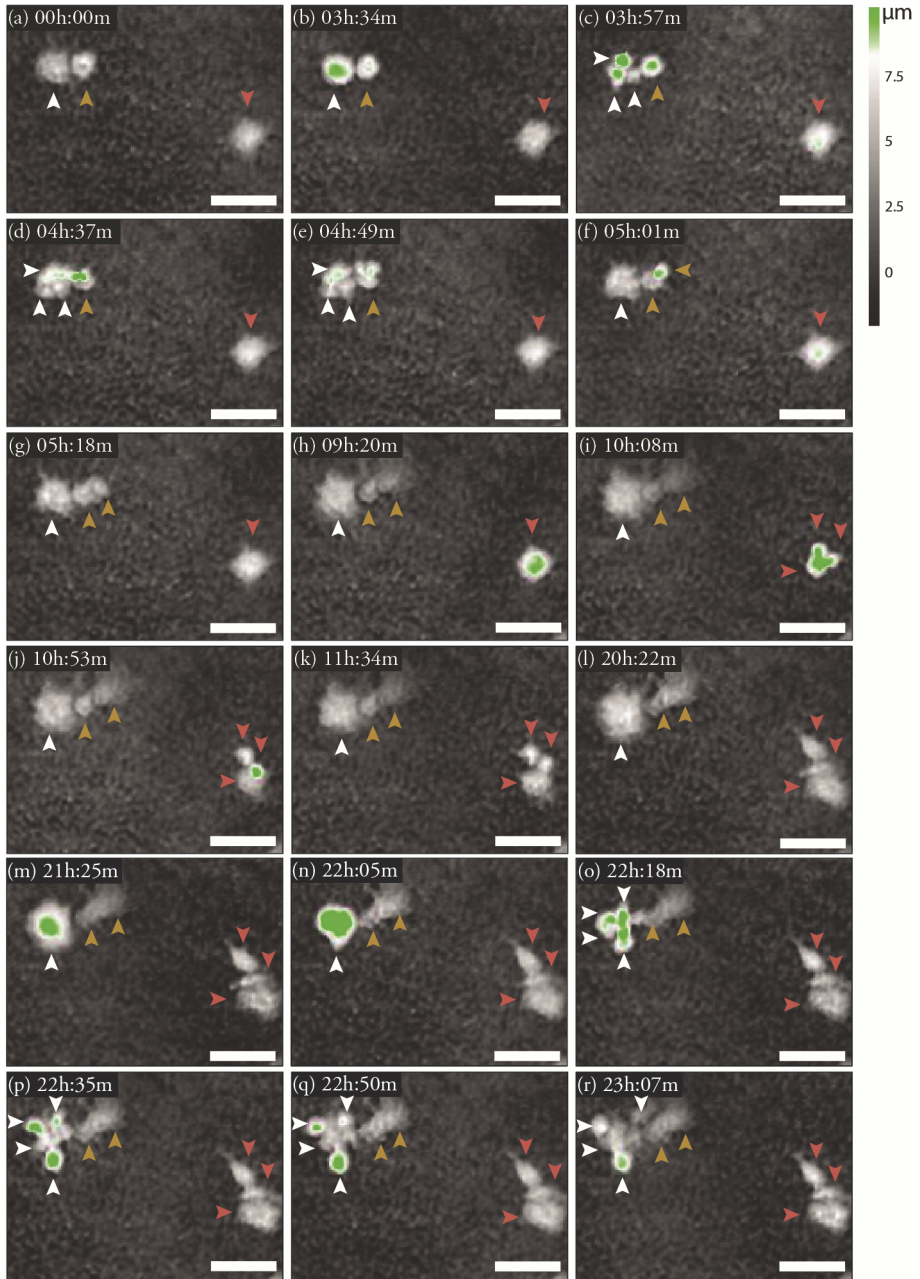
Figure 4.7 (Opposite) Selection of frames from movie S13 (Supporting Material*) from Paper II, showing how mouse fibroblasts fail to divide when cultured on long nanowires (diameter 80 nm, length 6.7 μm, density 1 nanowire μm⁻²). In these frames, three different types of erroneous division are observed. The cell marked with yellow arrowheads undergoes a fairly successful division event (f-g), although the resulting daughters are of different sizes. The cell marked with a red arrowhead divides into three daughter cells (h-k) of different sizes while the cell labelled with a white arrowhead first fails to divide (a-g) and subsequently divides into four daughter cells of different sizes (m-r). Height information is colour coded to highlight cells that are rolled up in preparation for division (see legend). Scale bars are 50 μm.

Nuclear morphology

The time-lapse observations of failed division events outlined above motivate further investigations. By labelling the cell nuclei and examining the cells using fluorescence microscopy, we observed irregularities in nuclear shape imposed by nanowires. Irregularities included unusual nuclear morphologies, abnormally large nuclei and multiple nuclei in single cells (Papers II and IV). Since it is often not possible to distinguish a cell with multiple, completely separate nuclei from a cell with a single nucleus with double or more DNA content, we chose not to distinguish between the two. The term *multinuclear* used in Paper II does not necessarily mean that a cell is confirmed to have two separate nuclei but rather that, judging from the nucleus' size and morphology, it likely has two or more times the DNA content of a healthy cell. In paper IV we replaced the term *multinuclear* with *aberrant nuclei* to clarify this.

The aberrant nuclear morphology is likely caused by cells completing the cell cycle, but failing to undergo the final stages of division, reforming as one large cell with double DNA content (

Figure 4.7 b-g, white arrow). The nuclear envelope similarly reforms and either two new nuclei or one large, deformed nucleus with double DNA content is formed. Several cells have more than two nuclei which indicates they have not only failed division once but several times, with a completed cell cycle in between the attempts (Figure 4.8). This indicates that the cell cycle is reset after the failed division attempt and that there is no signalling blocking cell cycle progression. In Paper II, we quantified the occurrence of cells with aberrant nuclei (referred to as multinuclear cells in Paper II) as a function of nanowire length and found that cells cultured on long nanowires (diameter 80 nm, length 6.7 μm, density 1 nanowire μm⁻²) displayed a much greater proportion of aberrant nuclei compared to cells on short nanowires (1.5 μm) (Figure 4.9 a). In Paper IV, we found a trend indicating a density dependence as well: cells on the dense substrates (diameter 80 nm, length 4 μm, density 4 nanowires μm⁻²) displayed

---

*The supporting material is described in Appendix 2 and can be found online:
http://bit.ly/Persson2014.

a larger proportion of cells with aberrant nuclei compared to lower density substrates (0.1 nanowires μm^{-2}) (Figure 4.9 b).
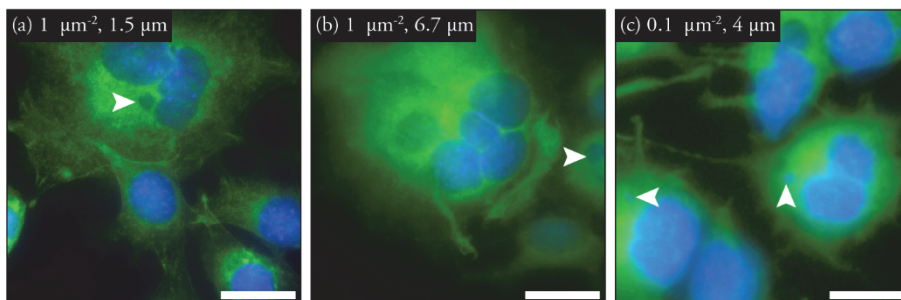
Figure 4.8 When cultured on nanowires, L929 cells can obtain multiple nuclei or nuclei with aberrant morphologies, regardless if they are cultured on short (a) or long nanowires (b) or low density nanowire arrays (c). Cells are also frequently observed to acquire micronuclei, here labelled with white arrows. Actin is labelled with FITC-conjugated phalloidin (green) and nucleic DNA is labelled with bisbenzimide (blue). Scale bars are 20 μm.
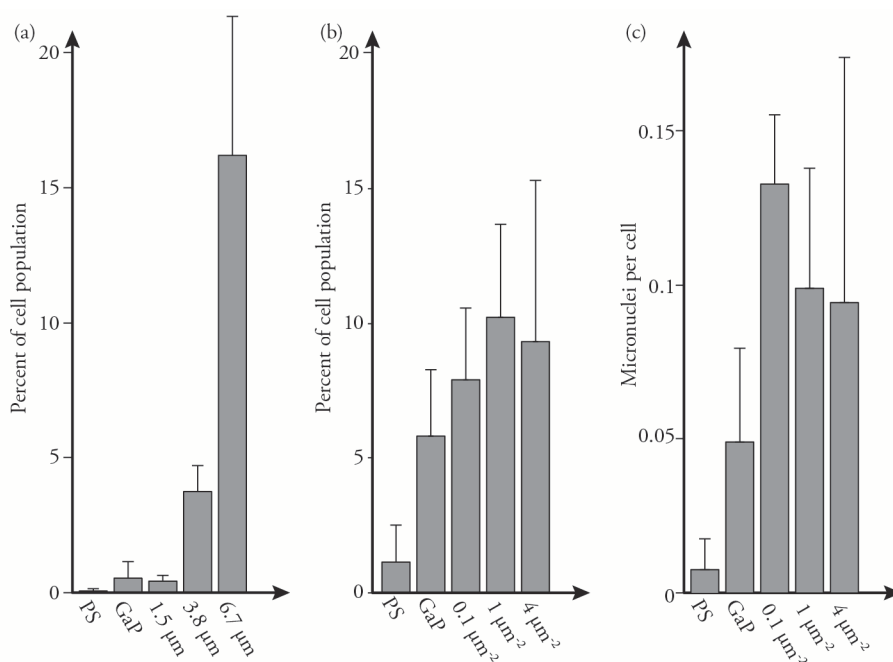
Figure 4.9 The occurrence of aberrant nuclear morphologies show trends of increasing with nanowire length (a) (Paper II) and with nanowire density (b) (Paper IV). In Paper IV, the occurrence of micronuclei was quantified as a function of nanowire density (c). The difference in occurrence of aberrant nuclear

morphologies can in part be explained by the different protocols used: in Paper II, cells were cultured for 72 h prior to quantification and in Paper IV, an incubation time of 96 h was used.
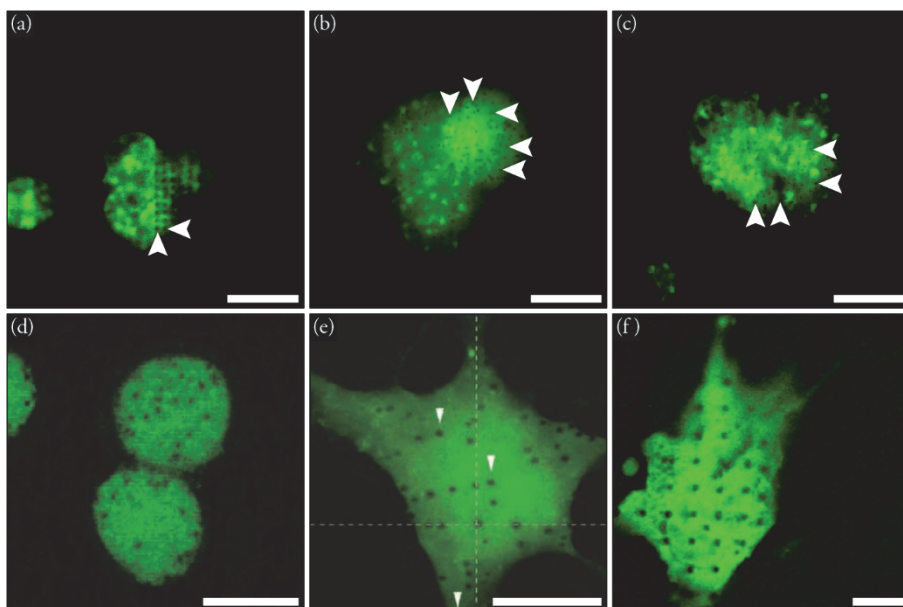
Figure 4.10 Fluorescence images showing how nanowires appear as black dots in both cell nuclei (a-d) and in the cell cytosol (e-f). When cultured on the oxide nanotubes in Paper I, these black dots are arranged in the same square pattern as the nanotubes causing them (a) in the nucleus of L929 cells. The same dots are observed for cells cultured on GaP nanowires (here, diameter 80 nm, length 6.7 μm, density 1 nanowire μm^{-2}) (b-c). These L929 cell nuclei display around 50 such black dots, some of which are labelled with white arrows. Similar dark dots are also described in literature[*] both for nuclei [20] (c) and cytosol [27], [85] (d, e).

---

[*] Copyright statement for Figure 4.10. (d): Reprinted with permission from [20], © 2007 ACS. (e) Reprinted with permission from [85], © 2011 John Wiley and Sons. (f) Reprinted with permission from [27], © 2012 ACS.

Nuclear invagination

Judging from the SEM images of cells on nanowires (Figure 4.2 b, d, f-g, and j), it is not surprising that nanowires do interfere with division. From these pictures it appears that the nanowires are penetrating straight into the cell interior, for cells cultured on nanowire arrays with low densities (≤1 nanowire μm^{-2} for diameters of 80 nm, applies to L929 cells). Using fluorescence microscopy, several groups have reported on nanowires penetrating deep into the cell cytosol and even the nucleus, observed as dark dots in an otherwise bright cell (Figure 4.10) [20], [27], [84]–[86] and Papers I and II.

Seeing how nanowires protrude into cells and possibly even the nucleus, interrupting cell movement and causing division to fail repeatedly, raises questions about how the cells can tolerate this insult and still progress through the cell cycle. Here it is useful to image the interior of cells cultured on nanowires. This can be achieved using confocal microscopy but resolution is typically poor and detailed interactions between the sub-resolution nanowires and specific parts of cells are hard to achieve. In the specific case of division, it would be very interesting to study the physical relationship between the nucleus and the nanowires. Using FIB tomography (Chapter 2), our collaborators Carsten Købler and Kristian Mølhave at Denmark's Technical University, created cross sectional SEM images showing the nuclei of L929 cells cultured on our GaP nanowires as described in Paper II (Figure 4.11). The images revealed that the nuclear membrane is not penetrated by the nanowires, but rather invaginates to accommodate the intruding structures. This invagination, which would be seen as black dots in fluorescently labelled nuclei (Figure 4.10), was observed for cells cultured both on short nanowires (diameter 80 nm, length 1.5 μm, density 1 nanowire μm^{-2}) and long nanowires (diameter 80 nm, length 6.7 μm, density 1 nanowire μm^{-2}). For cells on the long nanowires, these invaginations could obtain extreme proportions, sometimes even creating tunnels through the entire nucleus. Similar results but with less extreme nuclear folding, were obtained by Mumm et al. using transmission electron microscopy (TEM) [81] to study HeLa cells on their PDMS-coated CuO nanowires. Similar invaginations and even trans-nuclear tubes have been observed in living cells [156] and have been reported to co-localize with drug-carrying nanoparticles [157].

Figure 4.11 (Opposite)Using FIB tomography Carsten Købler, DTU, created cross sectional SEM images of L929 cells cultured on short (1.5 μm) (a-d) and long (6.7 μm) nanowires (e-h) (Paper II). Electron microscopy dyes (osmium tetroxide and uranyl acetate, see Chapter 2) make it possible to observe the nuclear membrane (M_{nuc}) and the cell membrane (M_{cell}) as thin, white lines. From these images it is evident that the nuclear membrane is intact and forms invaginations to prevent the nucleus (Nuc) from being penetrated by the nanowires (NW). This mechanism works for cells cultured on both short and long nanowires, even for a cell with three nuclei as shown here. Labels in the figure show the cytoplasm (CP) and DNA dense regions (asterisks). Scale bars are 1 μm. Images have been rescaled to correct for tilt.

(a) Short nanowires

(e) Long nanowires
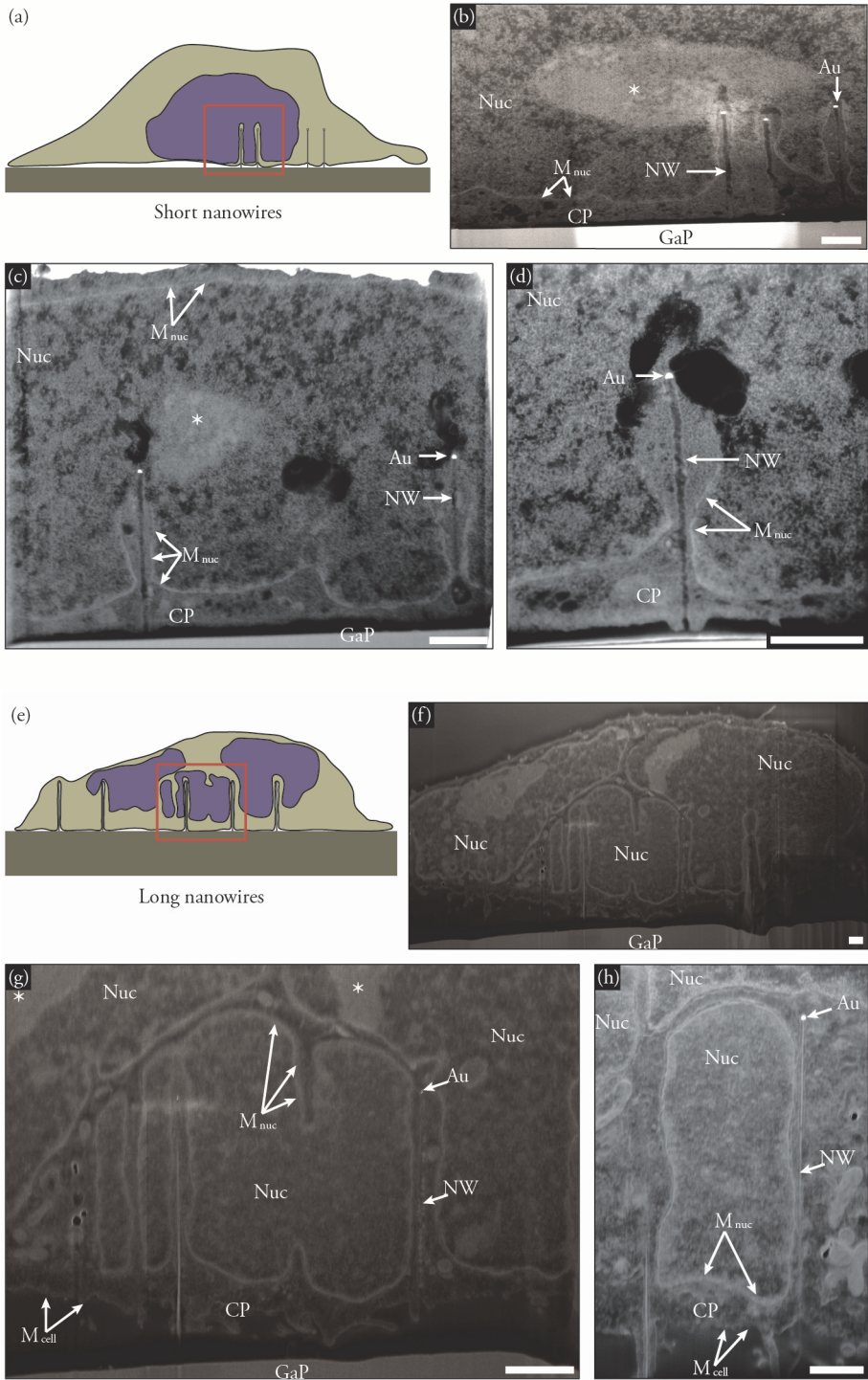
The invagination mechanism the nuclei use to avoid the nanowire intrusions explains, to some extent, how cells can appear healthy when nanowires seem to penetrate into the nucleus; the nuclear envelope is not penetrated and there is no direct contact between the nanowires and the DNA. However, during cell division, the nuclear envelope dissolves and the nanowires will be able to directly interfere with the DNA. When the nuclear envelope dissolves, the DNA has already been condensed into chromosomes and will bind to microtubule filaments, forming the mitotic spindle. In a healthy cell, the chromosomes will be lined up and separated to opposite sides of the cell before the cell divides into two daughter cells [32]. When the cell cytosol and nucleus are interspersed with nanowires, this chromosome separation is likely obstructed. In Paper IV, we present evidence of the formation of micronuclei (Figure 4.8 c and Figure 4.9 c) which might be caused by erroneous chromosome separation. Here we found an increase in micronuclei for cells cultured on sparse (0.1 nanowires μm^{-2}) compared to denser arrays (4 nanowires μm^{-2}) which would fit with the hypothesis that nanowires interfere with chromosomal separation (as the cells cultured on denser arrays adhere to the tips of the nanowires rather than engulfing these). Alternately, the micronuclei can be caused by an increased ROS generation in cells on nanowires [158], [159]. An increase in ROS levels can also cause incomplete nuclear separation [158] and might therefore help explain the occurrence of cells with aberrant nuclei (Figure 4.8, Figure 4.9). If the nanowires do mechanically interfere with cell division, this might explain the observation of Peer et al. that cells proliferate more slowly on their nanosyringe substrate (outer diameter 500 nm, length 5 μm, density 0.04 nanowires μm^{-2}) [27]. It might be that their much thicker, stiffer nanostructures remain stationary as the cell components are moving around them whereas our thin, flexible structures bend and follow the cell movement.

4.5 Nanowire effects on intracellular mechanisms

Studying cell morphology, migration and proliferation shows the overall behaviour of cells but does not reveal the underlying mechanisms. Though numerous methods to study these mechanisms exist for cells cultured in standard culture vessels, studies on nanowire substrates are often confined to using fluorescence microscopy (Section 4.1). By using specialised fluorophores that react to their surroundings (Section 2.2), it is possible to study molecular mechanisms for cells on nanowire substrates. Using some of these functional dyes, we have observed increased cell respiration, ROS generation and dsDNA breaks for cells on nanowires, and in particular on long nanowires (Paper II). Membrane impermeable dyes like PI and EthD-1 have been used to verify cell membrane integrity [28], [79]–[85] while calcein AM has been used to verify intact enzymatic activity in cells on different nanostructured surfaces [26], [28], [79], [81], [83], [85], [86]. As outlined in Section 4.4, AlamarBlue™ and MTT have been used as a proxy for cell number [79], [145], [154].

In Paper II, we measured the fluorescence intensity of AlamarBlue™ and normalised it to the number of cells in culture. We found that the cells (L929) showed an increased AlamarBlue™ reduction (interpreted as cell respiration) when cultured on nanowires compared to flat controls (GaP and PS) (Figure 4.12 a). This increase was length dependent: cells on longer nanowires (diameter 80 nm, length 6.7 μm, density 1 nanowire μm^{-2}) had a higher respiration rate compared to cells on short nanowires (1.5 μm). Increased cell respiration can be an indication of increased stress, as the cells increase their oxygen turnover in order to generate more energy for cellular processes to occur at a higher rate [155].

With the increased oxygen consumption, there is a risk of increasing the concentration of ROS to dangerous levels, where the ROS will not be destroyed by the cellular ROS scavenging system and might cause damage to DNA and proteins [160]. By using carboxy-H2DCFDA to label cell with a high ROS content (Figure 4.12 c), we could observe an increase in ROS generation following the behaviour observed for cell respiration, i.e. an increase with increasing nanowire length (Figure 4.12 b). By using antibodies to label γ-H2AX (indicative of dsDNA repair), we observed a trend of increasing dsDNA breaks for cells cultured on longer nanowires compared to shorter (Figure 4.12 d-g).

By using large surface areas to obtain high cell numbers and lysing cells *in situ* (removing the need for trypsinization), SanMartin et al. extracted and quantified the mRNA content of mouse cortical stem cells cultured on HfO coated nanowires (diameter 80 nm, length 5 μm, density 1 nanowire μm^{-2}) [161]. By mapping the expression levels of the entire genome, they observed altered expression levels for only 34 genes on nanowire substrates compared to flat controls (HfO). These genes, involved mainly in cell adhesion, morphology and metabolism, showed only minor changes, with a 1-2.4 fold up regulation on nanowire substrates. Relying on real time, quantitative PCR* to chart gene expression for HeLa cells cultured on nanowires, Shalek et al. report no changes in expression levels for five genes required for basic cell functions, compared to cells cultured in well plates [26]. In their continued work, Shalek et al. used the same approach to quantify the expression of 300 genes involved in the immune response, again finding no significant changes when comparing their cells cultured on nanowires with immune cells cultured on glass substrates [84].

---

* PCR, polymerase chain reaction, is a DNA amplification technique relying on DNA polymerase (responsible for *in vivo* DNA replication) to increase the amount of DNA in a sample.
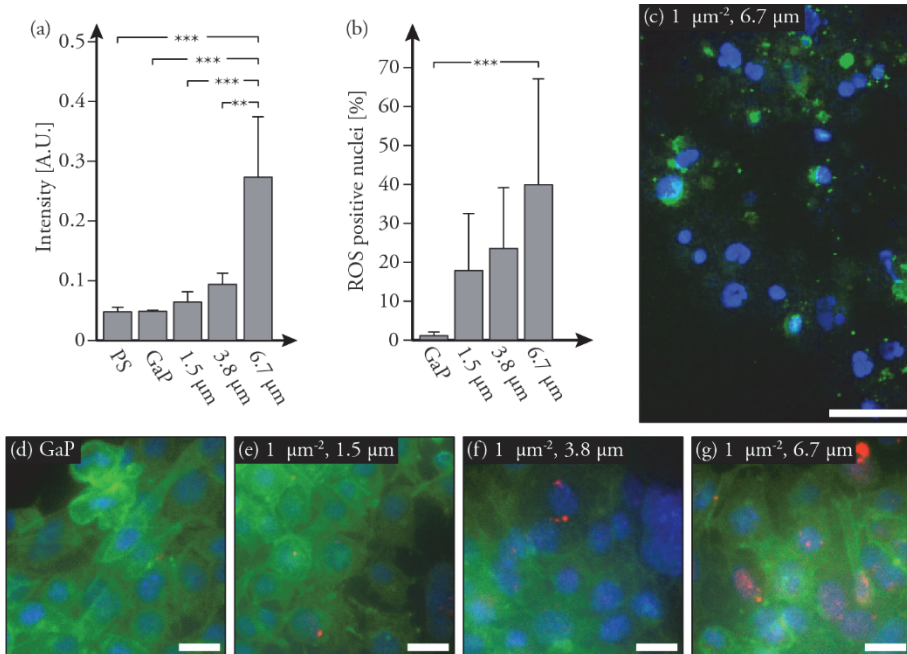
Figure 4.12 Cell respiration, as assessed using AlamarBlue reduction, increases with increasing nanowire length (a). ROS generation was found to increase as a function of increasing nanowire length (b) by using the dye carboxy-H2DCFDA to label cells with a high ROS content (c). Here L929 cells cultured on long nanowires counterstained with bisbenzimide (blue) are shown. In Paper II, we could also observe a trend of increasing DNA repair with increasing nanowire length (d-g). This was achieved by using antibodies to stain cells for γ-H2AX (red). Cells were also stained using FITC-phalloidin (green) and bisbenzimide (blue). Scale bars are 100 μm (c) and 20 μm (d-g).

4.6 Nanowire membrane penetration

For nanowire-based cell injections and other applications, it is of interest to know if and under what circumstances nanowires penetrate the cell membrane. Several reports show successful injections [20], [26]–[28], [84], [113], [132], [133], [135]–[139], indicating spontaneous penetration. Other groups show that membrane impermeable dyes do not enter cells [79]–[82], [85], indicating an intact cell membrane. In some cases, special procedures have been developed to ensure direct nanowire-cytosol contact, such as electroporation [24], [28], surface functionalization [20], [25] or the addition of surfactants [27], also supporting the notion that the membrane is not spontaneously penetrated.

Recent studies have supplied direct observation of intact cell membranes using TEM [81], [162] and confocal microscopy [81], [86]. Berthing et al. showed an intact cell membrane for HEK293 cells cultured on up to 11 μm long nanowires (diameter 90-110 nm, density 0.02-0.1 nanowires μm^{-2}) (both uncoated InAs and coated with aminosilanes for increased injection rate [20]) [86]. A hydrophobic surface treatment (polyethyleneimine) increased membrane penetration to 7% for the 11 μm long nanowires but had no effect on the shorter nanowires (2 and 6 μm).

By injecting GFP quenching Co^{2+} ions, Xu et al. quantified the spontaneous penetration of nanostraws (diameter 100 nm, length 1 μm, density 0.3 nanostraws μm^{-2}) into CHO cells, finding a penetration rate of 6% for untreated alumina and 7% and 12% for nanostraws coated with adhesion-promoting polyornithine and fibronectin, respectively [138]. Xie et al. developed a model to predict cell membrane penetration, taking nanowire dimensions (diameter, length and density), cell stiffness and buoyancy into account [163]. They found that gravitational penetration typically requires diameters below 20 nm and that penetration mediated through cell adhesion forces is much more likely. Increasing nanowire length, reducing diameter or density increases the probability for adhesion mediated penetration.

Supported lipid bilayers (SLBs), created by lipid vesicles to rupturing on a surface, self-assembling into a bilayer, are often used as a model for the cell membrane [164]. To improve our understanding of the interactions between nanowires and the cell membrane, we developed a protocol to create continuous, fluid SLBs on SiOx coated GaP nanowires [165]. We found that the SLBs conformed to the nanowire morphology and we showed the possibility to use this system to study interactions between nanowires and membrane-bound proteins and tethered vesicles. Since membrane curvature is known to affect cell membrane function [166], [167], it is of interest to study how the nanowire-imposed curvature affects SLBs conforming to this substrate. Using this model system, we can learn how membrane-bound proteins and the mechanical properties of SLBs, and, by extension, the cell membrane are affected.

4.7 Imaging nanowires using optical microscopy

Since studies of cell-nanowire interactions rely heavily on microscopy (Section 4.1), imaging nanowires in an optical microscope is very useful. However, the nanowires are smaller than the resolution limit in optical microscopy and hence diffraction will cause them to appear as 200-300nm large circular objects. In order to image the nanowires, one of three strategies is often employed: either the nanowires need to reflect light, or they are modified to emit light, or everything else is made to emit light.

Using a laser scanning confocal microscope, it is filters can be chosen to allow the excitation laser to reach the detector. Any light reflected by the nanowires will be collected and the nanowires are visualised (Figure 4.13 a) [21], [86], [144], [168]. This approach is straightforward and requires no preparation, but some nanowires are harder to visualize than others, depending on size and material. Another drawback is that the substrate will reflect a lot of light, i.e. not only nanowires are visualised.

It is possible to use fluorescent dyes to label the nanowires by exploiting proteins that bind to nanowires and in turn label these [22], [110], [169] (Figure 4.13 d). One protein previously used in this fashion is laminin which has the advantage of preferentially binding to nanowires over the flat surface between them [169]. One drawback with this approach is the need to alter the surface of the nanowires. Apart from the extra sample preparation steps, coating a substrate with proteins drastically changes cell interactions compared to the native surface [170]. Sometimes this can be useful to promote cell adhesion and tailor interactions [171], [172],but sometimes the native surface might be of greater interest. A similar, dye dependent approach circumventing this surface treatment is to use dyes that stain the cells' cytosol, causing nanowires to appear as dark pillars in an otherwise bright cell [81], [85], [86] (Figure 4.13 b). Alternately, a fluorophore can be added to the liquid surrounding the cells, causing both cells and nanowires to be visualized through dye exclusion [85] (Figure 4.13 c).

Fluorescent GaInP nanowires

To improve upon existing optical imaging of nanowires, we developed inherently fluorescent GaInP nanowire heterostructures (Paper III) (Figure 4.13 e). The new fluorescent nanowires, improve image quality compared to using laser reflection [21], [86], [144], [168] or dye exclusion [81], [85], [86] and remove the need for coating nanowires with proteins [22], [110], [169] labelling the cytosol or the surrounding liquid. A further advantage of the GaInP nanowires is the increased photostability compared to organic dyes (Figure 4.14 b). The GaInP nanowires are also uniquely fluorescent; in the case of nonspecific labelling of all surfaces or the cells/liquid, everything solid will emit light or remain dark and in the case of laser scattering, many objects might scatter light, especially when imaging nanowires on a substrate or in tissue. With our GaInP nanowires, only the GaInP part of the nanowires will actually emit light, increasing the certainty that the structures imaged are indeed nanowires. We also showed that it is possible to tailor emission wavelength and intensity by varying the concentration of the precursor trimethyl-indium (TMIn) during growth (Figure 4.14 c).
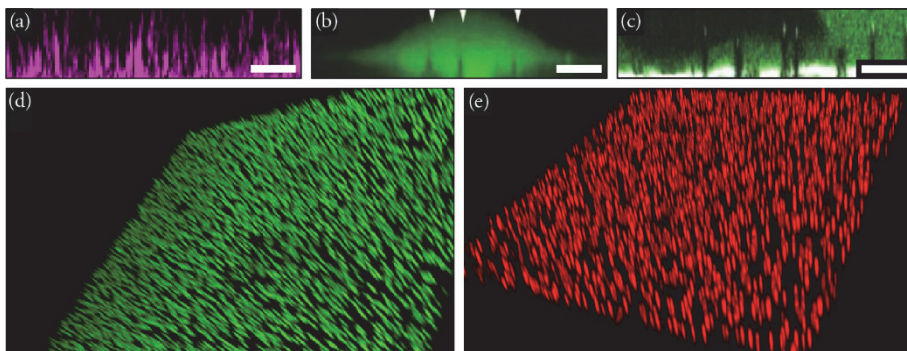
Figure 4.13 Nanowires can be visualised using fluorescence microscopy by laser scattering (a), staining the cell cytosol* (b) [85] or the surrounding medium (c) [85]. Alternately, a protein such as laminin can be absorbed to the nanowires and subsequently labelled (d) [169]. In Paper III, we developed inherently fluorescent GaInP nanowires to circumvent the need for labelling the cell or medium or unnecessary surface modifications (c, e). Scale bars are 5 μm (a-c). The confocal 3D renderings show areas of 143x143 μm (d) or 50x50 μm.

In Paper III, we added a further functionality to our nanowires by introducing several fluorescent segments separated by non-fluorescent segments, (Figure 4.15). For studies using suspended nanowires, this versatile barcode system is very useful, making it possible to use different numbers of segments to encode information about surface treatment, nanowire dimensions and administration route. It is for instance possible to coat single segment nanowires with proteins or an oxide layer and subject dual segment nanowires to another modification. The two sets of nanowires can then be administered to the same cell culture or test animal, making it possible to study any differences with regards to nanowire location based on surface treatment.

---

* Copyright statement for Figure 4.13. (a-b) Reprinted with permission from [85], © 2011, John Wiley and Sons. (d): Reprinted from [169] under Creative Commons (CC BY-NC-SA 3.0).
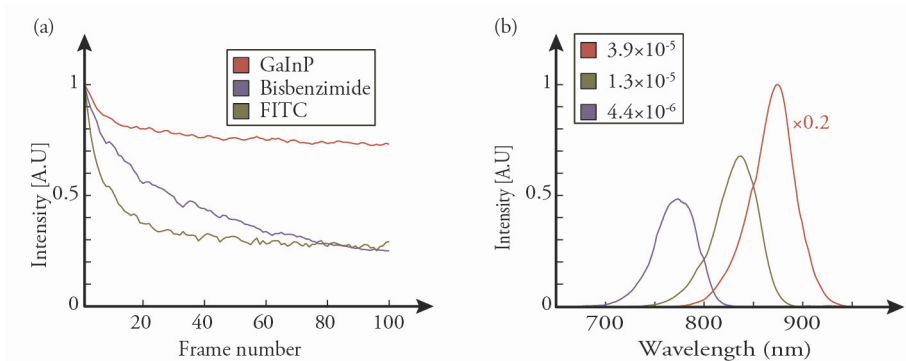
Figure 4.14 Demonstration of the photostability of the newly developed fluorescent GaInP nanowires (a) (Paper III). A sample with fluorescently labelled cells was continuously imaged using CLSM and total intensity in each channel was plotted as a function of frame number. Emission spectra for GaInP showing how varying the molar fraction of the precursor TMIn (legend) during growth affects emission wavelength and intensity (b). The spectrum for the highest molar fraction has been rescaled by a factor of 0.2.
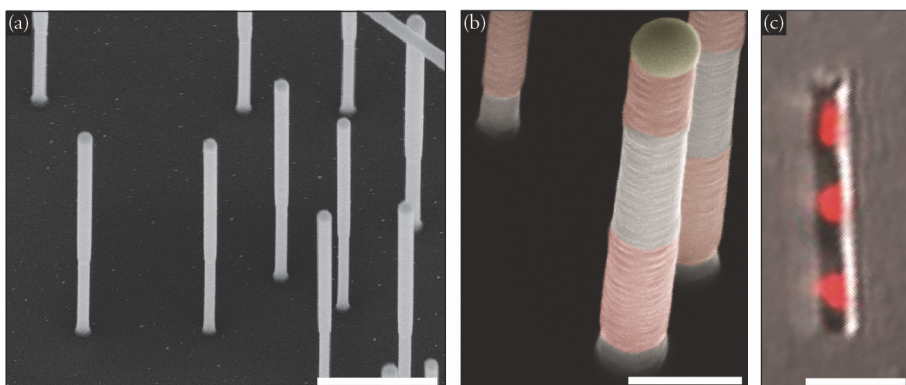
Figure 4.15 GaInP nanowires in SEM (a). The narrow base is made from GaP. SEM of barcode nanowires, where fluorescent GaInP segments (false colour red) are separated by non-fluorescent GaP segments (b). CLSM image of barcode GaInP nanowire with three fluorescent segments using laser reflection (grey) and fluorescence imaging (red). Scale bars are 1 μm (a), 250 nm (b) and 2 μm (c). Tilt is 30° (a-b).

4.8 Chapter summary

This chapter has dealt with the interactions between cells and nanowires, combining our results in Paper II and IV with studies from the community, in an effort to further understand these interactions and thereby improve nanowire-based applications in cell biology. These studies are very diverse and lack standardisation; different groups use different kinds of similar, vertical high aspect ratio nanostructures and focus on different cell lines. Since the field is so new, there are no standardised experimental procedures and different groups rely on different protocols and methods to measure the same aspects of cell behaviour. The large variation in methods and investigated systems makes it difficult to compare results between papers. With this in mind, if all adherent, immortal mammalian cell lines can be compared to one another, a few general conclusions regarding cells cultured on nanowire substrates can be drawn:

- Cells closely interact with nanowires by adhering to them and pulling on the nanowires, as often observed using SEM.

- Depending on nanowire density, cells will either reside on top like a fakir on a bed-of-nails or the cells will reside on the substrate between the nanowires, with the nanowires protruding deep into the cells.

- The nanowires are likely membrane bound even if they appear to penetrate straight through the cells, with direct observation of membrane around nanowires and reports where protocols have been developed to ensure penetration. Even the cell nucleus appears to be intact and adopts its morphology to avoid the nanowires.

- Cells cultured on nanowires show an intact enzymatic activity and retain the ability to produce proteins, while no or minor changes in mRNA content are reported.

- Nanowires reduce cell proliferation rate.

Apart from these frequent observations, we have further observed that nanowires interfere with cell division, resulting in cells with aberrant nuclear morphologies. We also found that cell motility is reduced for increasing nanowire lengths and that 50 nanowires (density 0.1 nanowires μm^{-2}) are enough to immobilise cells. If nanowire density is increased (in this case to 4 μm^{-2}), the cells will adhere to the tips of the nanowires and migrate as normal. We also observed that the reduction in cell proliferation rate, reported by us and others, has both a length dependence (reduced rate for longer nanowires) and density dependence (reduced rate for denser samples, including cells experiencing the bed-of-nails effect). We have also observed an increase in cell respiration, leading to increased ROS generation and DNA damage, with greater effects for cells on long nanowires compared to short nanowires.

From these observations, a few guidelines can be constructed for minimising cell perturbations from nanowires. In our studies, some of the detrimental effects stem from cell division. By limiting the time the cells are interfaced with the nanowires to below the average cell cycle time, these effects could be minimised. Using synchronised cells can increase the time allowed for cell culture (as all cells will divide simultaneously). Mitosis blocking compounds could potentially be used as well. If possible, the nanowire length should also be limited though this might not always be an option, since longer nanowires show a theoretical increase in membrane penetration efficiency. If membrane penetration is crucial, this can be achieved by increasing nanowire length or decreasing diameter as well as density. Alternately, the nanowires can be treated with different compounds to increase penetration rate. Another issue is the generation of ROS which can potentially be reduced by limiting the time the cells are cultured on the nanowires. If this is not an option, ROS scavenging compounds such as curcumin [173] could potentially be used to aid the natural ROS scavenging system of the cells.

Studying cell nanowire interactions

This chapter has also dealt with methods to study cells on nanowires, establishing that fluorescence microscopy takes a leading role due to the problems related to detaching cells from nanowire substrates and the low number of cells. Therefore it is important to visualise nanowires using optical microscopy and in Paper III, we developed inherently fluorescent nanowires to improve on existing methods involves laser scattering or staining nanowires via adsorption of proteins or staining the cell cytosol or medium. We also demonstrate the possibility to create barcode nanowires, with multiple fluorescent segments for systematic studies of e.g. effects of surface treatment or administration route. These new nanowires will be valuable for future studies, where we can learn even more about cell-nanowire interactions to improve nanowire-based applications in cell biology.

5 Summary of papers

The content of Papers I-IV included in this thesis have been discussed and put into context in Chapters 3 and 4 and are summarized here for convenience.

I. Vertical oxide nanotubes connected by subsurface microchannels

In Paper I we worked toward a functional cell injection system based on oxide nanotubes connected to a microfluidic system. We developed a fabrication protocol that enabled us to fabricate devices where oxide nanotubes were connected by a microfluidic channel, capable of transporting liquid and DNA. When the device is fully operational, it will be possible to conduct serial injections in a time resolved manner to single cells on a chip and to perform nano-biopsies, the retrieval of intracellular material.

II. Fibroblasts cultured on nanowires exhibit low motility, impaired cell division, and DNA Damage

For nanowires to find widespread application in cell biological research problems, the full extent of the interactions between cells and nanowires must be understood. In Paper II we used time-lapse imaging to study cell migration and division on nanowire substrates. We also investigated cell proliferation rate, respiration and generation of ROS as well as DNA damage. By varying the nanowire length (1.5, 4 and 6.7 μm) while keeping diameter (80 nm) and density (1 nanowire μm^{-2}) constant, we observed a length dependant decrease in proliferation rate and motility. For long nanowires we could observe an increased number of failed cell divisions resulting in large cells with aberrant nuclear morphologies. Furthermore, for cells cultured on long nanowires we found an increase in cell respiration which led to an increase in ROS content, inducing DNA strand breaks. Using FIB tomography we observed how cell nuclei would fold and create tunnels in an effort to avoid direct contact between DNA and nanowires.

III. Fluorescent nanowire heterostructures as a versatile tool for biology applications

Working toward improving future studies of cell-nanowire interactions, in Paper III we developed an MOVPE recipe to grow inherently fluorescent GaInP nanowires. These nanowires can replace current methods used to image nanowires in optical microscopy, improving lateral resolution and removing the need for sample modification. The emission wavelength and intensity of the GaInP nanowires can be tuned by varying the indium content and the nanowires show a greater photostability than organic dyes. We also demonstrated the possibility to create striped nanowires with alternating fluorescent and non-fluorescent segments. These barcode heterostructures can be used to label and track different nanowires, for instance with different surface treatments or different administration routes, in a single cell or organism.

IV. From immobilized cells to motile cells on a bed of nails: effects of vertical nanowire array density on cell behaviour

In Paper IV, we continued on the work started in Paper II, where we studied the cell behaviour on nanowire substrates with varying nanowire length. Here we instead kept length (4 μm) and diameter (80 nm) constant while varying nanowire density (0.1, 1 and 4 nanowires $μm^{-2}$). Time-lapse microscopy revealed that cells were immobilised on the samples with low and intermediate density (0.1 and 1 nanowires $μm^{-2}$). On the highest density sample, the cells would adhere to the tips of the nanowires and were able to migrate. Cell proliferation rate showed an opposite behaviour: on the dense arrays proliferation was markedly lower than for cells on low and intermediate density substrates. Studies of nuclear morphology revealed an increase in aberrant nuclei for cells on dense nanowire arrays compared to cells on the low and intermediate density substrates while micronucleus frequency showed an opposite trend: the number of micronuclei increased for the lowest density substrate.

6 Concluding remarks

This thesis has been devoted to exploring both interactions between nanowires and cells and the possible applications of these structures. The two aims of this thesis were:

Aim 1: Explore fundamental interactions between mammalian cells and nanowires to further the field of nanowire-based applications in cell biology by improving both device design and the interpretation of the results obtained.

Aim 2: Improve existing nanowire-based injection systems by exploring the use of nanotubes incorporated into a fluidic system for cell injection.

Papers II and IV dealt with the first aim of the thesis by employing a variety of microscopy-based investigations to study how cells behave when interfaced with nanowires of different lengths and surface densities. Time-lapse microscopy revealed that cells were largely immobilized and division was disrupted, leading to multinuclear cells. This immobilization was observed for cells interfaced with as few as 50-100 nanowires. We observed that below a certain density (in this case 2000 nanowires per cell) the cells would adhere to the substrate between the nanowires and seemingly be impaled by these, explaining the observed immobilization. Above this density, the cells would adhere to the tips of the nanowires and retain their motility. We also found that limiting the nanowire length to 1.5 μm (diameter 80 nm, density 1 nanowire μm^{-2}) greatly reduced the effects on motility and division. Using FIB tomography, we could observe cell nuclei evading nanowire penetration by folding, creating invaginations and sometimes even tunnels through the entire nucleus. Using a set of functional dyes further revealed that long (6.7 μm) nanowires caused excessive cell respiration leading to the generation of ROS and ultimately DNA damage. These effects were not as pronounced for cells cultured on the shorter nanowires.

Together, Paper II and Paper IV serve to guide scientists developing nanowire-based cell biological applications. The results show that, in order to minimize detrimental effects caused by the nanowires, one should limit the nanowire length as much as possible. If this is not an option, the time the cells are in contact with the substrate can be minimized, preferably to be below the cell cycle time since division is problematic and causes aberrant behaviour. To maximise the culture time, synchronised cells can be used. The results also show how cell motility can be intentionally influenced by

tailoring nanowire dimensions: for these fibroblasts as few as 50-100 nanowires per cell is enough to immobilize the majority of the cells. It takes around 2000 nanowires per cell to cause the bed-of-nails effect where cells can adhere to the tips of the nanowires, showing increased motility but decreased proliferation rate.

To improve future studies of the interactions between cells and nanowires, we developed intrinsically fluorescent GaInP nanowires, as described in Paper III. These nanowire heterostructures improve imaging conditions and replace the need for surface modifications which can alter cell behaviour. These nanowires make it possible to determine the exact number of nanowires interfaced with a single cell and the improved localization accuracy improves the possibility to study their spatial relation to subcellular structures and to use the nanowires for force measurements. By combining fluorescent and non-fluorescent segments to create a barcode system, it is possible to compare different surface treatments, time points or administration routes in one cell culture or organism in a single experiment.

The second aim of the thesis was addressed in Paper I where we developed a fabrication procedure to create oxide nanotubes connected to a microfluidic channel. We showed that the channel and nanotubes are capable of transporting dyes and DNA in a liquid, important steps toward a functioning nanosyringe device. Once this system is fully operational, it will offer several advantages over existing, related techniques. Compared to microinjection, it will offer automation with an increased injection throughput while reducing the level of user experience required. Compared to existing solid nanowire injection systems, the nanotubes with their incorporated microfluidic connection offer the advantage of repeated, time resolved injection and the possibility to retrieve material from the cells, offering great versatility to several experiments.

The results presented in this thesis will undoubtedly be useful for research groups across the world as they further develop cell biological methods based around semiconductor nanowires and similar nanostructures.

7 References

[1]   R. Booker and E. Boysen, *Nanotechnology for dummies*. Wiley Publishing, inc., 2005.

[2]   A. Tanner, J. Morrison, D. James, R. Fontaine, and P. Gamache, *Inside the iPhone 5s*. [Online]. Available: http://www.chipworks.com/en/technical-competitive-analysis/resources/blog/inside-the-iphone-5s/. [Accessed: 25-Jun-2014].

[3]   G. J. Nohynek, J. Lademann, C. Ribaud, and M. S. Roberts, *Grey goo on the skin? Nanotechnology, cosmetic and sunscreen safety*, Crit. Rev. Toxicol., Mar. 2007, vol. 37, no. 3, pp. 251–77.

[4]   C. M. Magin, S. P. Cooper, and A. B. Brennan, *Non-toxic antifouling strategies*, Mater. Today, Apr. 2010, vol. 13, no. 4, pp. 36–44.

[5]   P. M. Ajayan, L. S. Schadler, and P. V. Braun, *Nanocomposite science and technology*. John Wiley & Sons, 2006, p. 239.

[6]   R. S. Wagner and W. C. Ellis, *Vapor-Liquid-Solid Mechanism of Crystal Growth*, Appl. Phys. Lett., 1964, vol. 4, no. 5, pp. 89–90.

[7]   C. P. T. Svensson, T. Mårtensson, J. Trägårdh, C. Larsson, M. Rask, D. Hessman, L. Samuelson, and J. Ohlsson, *Monolithic GaAs/InGaP nanowire light emitting diodes on silicon*, Nanotechnology, Jul. 2008, vol. 19, no. 30, p. 305201 (6pp).

[8]   J. Wallentin, N. Anttu, D. Asoli, M. Huffman, I. Åberg, M. H. Magnusson, G. Siefer, P. Fuss-Kailuweit, F. Dimroth, B. Witzigmann, H. Q. Xu, L. Samuelson, K. Deppert, and M. T. Borgström, *InP nanowire array solar cells achieving 13.8% efficiency by exceeding the ray optics limit*, Science, Mar. 2013, vol. 339, no. 6123, pp. 1057–60.

[9]   B. Ganjipour, J. Wallentin, M. T. Borgström, L. Samuelson, and C. Thelander, *Tunnel field-effect transistors based on InP-GaAs heterostructure nanowires.*, ACS Nano, Apr. 2012, vol. 6, no. 4, pp. 3109–13.

[10]   P. M. Wu, J. Gooth, X. Zianni, S. F. Svensson, J. G. Gluschke, K. a Dick, C. Thelander, K. Nielsch, and H. Linke, *Large thermoelectric power factor enhancement observed in InAs nanowires.*, Nano Lett., Sep. 2013, vol. 13, no. 9, pp. 4080–6.

[11]   K. Storm, F. Halvardsson, M. Heurlin, D. Lindgren, A. Gustafsson, P. M. Wu, B. Monemar, and L. Samuelson, *Spatially resolved Hall effect measurement in a single semiconductor nanowire*, Nat. Nanotechnol., Nov. 2012, vol. 7, no. 11, pp. 718–22.

[12]   M. T. Deng, C. L. Yu, G. Y. Huang, M. Larsson, P. Caroff, and H. Q. Xu, *Anomalous zero-bias conductance peak in a Nb-InSb nanowire-Nb hybrid device*, Nano Lett., Dec. 2012, vol. 12, no. 12, pp. 6414–9.

[13]   L. P. Rokhinson, X. Liu, and J. K. Furdyna, *The fractional a.c. Josephson effect in a semiconductor–superconductor nanowire as a signature of Majorana particles*, Nat. Phys., Sep. 2012, vol. 8, no. 11, pp. 795–799.

[14]   T. J. Webster, M. C. Waid, J. L. McKenzie, R. L. Price, and J. U. Ejiofor, *Nano-biotechnology: carbon nanofibres as improved neural and orthopaedic implants*, Nanotechnology, Jan. 2004, vol. 15, no. 1, pp. 48–54.

[15]   M. E. Davis, Z. G. Chen, and D. M. Shin, *Nanoparticle therapeutics: an emerging treatment modality for cancer.*, Nat. Rev. Drug Discov., Sep. 2008, vol. 7, no. 9, pp. 771–82.

[16]   M. Ferrari, *Cancer nanotechnology: opportunities and challenges*, Nat. Rev. Cancer, Mar. 2005, vol. 5, no. 3, pp. 161–71.

[17]   W. J. Gradishar, S. Tjulandin, N. Davidson, H. Shaw, N. Desai, P. Bhar, M. Hawkins, and J. O'Shaughnessy, *Phase III trial of nanoparticle albumin-bound paclitaxel compared with polyethylated castor oil-based paclitaxel in women with breast cancer.*, J. Clin. Oncol., Nov. 2005, vol. 23, no. 31, pp. 7794–803.

[18]   N. A. Kotov, J. O. Winter, I. P. Clements, E. Jan, B. P. Timko, S. Campidelli, S. Pathak, A. Mazzatenta, C. M. Lieber, M. Prato, R. V Bellamkonda, G. A. Silva, N. W. S. Kam, F. Patolsky, and L. Ballerini, *Nanomaterials for neural interfaces*, Adv. Mater., 2009, vol. 21, no. 40, pp. 3970–4004.

[19]   W. Hällström, T. Mårtensson, C. Prinz, P. Gustavsson, L. Montelius, L. Samuelson, and M. Kanje, *Gallium phosphide nanowires as a substrate for cultured neurons*, Nano Lett., Oct. 2007, vol. 7, no. 10, pp. 2960–5.

[20]   W. Kim, J. K. Ng, M. E. Kunitake, B. R. Conklin, and P. Yang, *Interfacing silicon nanowires with mammalian cells*, J. Am. Chem. Soc., Jun. 2007, vol. 129, no. 23, pp. 7228–9.

[21]   C. Prinz, W. Hällström, T. Mårtensson, L. Samuelson, L. Montelius, and M. Kanje, *Axonal guidance on patterned free-standing nanowire surfaces*, Nanotechnology, Aug. 2008, vol. 19, no. 34, p. 345101(6pp).

[22]   W. Hällström, C. N. Prinz, D. Suyatin, L. Samuelson, L. Montelius, and M. Kanje, *Rectifying and sorting of regenerating axons by free-standing nanowire patterns: A highway for nerve fibers*, Langmuir, 2009, vol. 25, no. 8, pp. 4343–4346.

[23]   M. A. Bucaro, Y. Vasquez, B. D. Hatton, and J. Aizenberg, *Fine-tuning the degree of stem cell polarization and alignment on ordered arrays of high-aspect-ratio nanopillars*, ACS Nano, Jul. 2012, vol. 6, no. 7, pp. 6222–30.

[24]   J. T. Robinson, M. Jorgolli, A. K. Shalek, M. H. Yoon, R. S. Gertner, and H. Park, *Vertical nanowire electrode arrays as a scalable platform for intracellular interfacing to neuronal circuits*, Nat. Nanotechnol., 2012, vol. 7, no. 3, pp. 180–184.

[25]   X. Duan, R. Gao, P. Xie, T. Cohen-Karni, Q. Qing, H. S. Choe, B. Tian, X. Jiang, and C. M. Lieber, *Intracellular recordings of action potentials by an extracellular nanoscale field-effect transistor*, Nat. Nanotechnol., Mar. 2012, vol. 7, no. 3, pp. 174–179.

[26] A. K. Shalek, J. T. Robinson, E. S. Karp, J. S. Lee, D.-R. Ahn, M.-H. Yoon, A. Sutton, M. Jorgolli, R. S. Gertner, T. S. Gujral, G. MacBeath, E. G. Yang, and H. Park, *Vertical silicon nanowires as a universal platform for delivering biomolecules into living cells*, Proc. Natl. Acad. Sci. U. S. A., Feb. 2010, vol. 107, no. 5, pp. 1870–5.

[27] E. Peer, A. Artzy-Schnirman, L. Gepstein, and U. Sivan, *Hollow nanoneedle array and its utilization for repeated administration of biomolecules to the same cells*, ACS Nano, Jun. 2012, vol. 6, no. 6, pp. 4940–6.

[28] X. Xie, A. M. Xu, S. Leal-Ortiz, Y. Cao, C. C. Garner, and N. A. Melosh, *Nanostraw - electroporation system for highly efficient intracellular delivery and transfection*, ACS Nano, 2013, vol. 7, no. 5, pp. 4351–4358.

[29] G. P. C. Drummen, *Fluorescent probes and fluorescence (microscopy) techniques-illuminating biological and biomedical research*, Molecules, Jan. 2012, vol. 17, no. 12, pp. 14067–90.

[30] H. Gest, *The discovery of microorganisms by Robert Hooke and Antoni van Leeuwenhoek, fellows of the Royal Society*, Notes Rec. R. Soc. Lond., 2004, vol. 58, no. 2, pp. 187–201.

[31] R. Hooke, *Micrographia: or some physiological descriptions of minute bodies made by magnifying glasses with observations and inquiries thereupon*. London: Jo. Martyn and Ja. Allestry, 1665, p. 246.

[32] B. Alberts, D. Bray, K. Hopkin, A. Johnson, J. Lewis, M. Raff, K. Roberts, and P. Walter, *Essential cell biology*, 2nd ed. New York: Garland Science, 2004.

[33] S. Hoole, *The select works of Antony van Leeuwenhoek containing his microscopical discoveries*. London: G. Sidney, 1800, p. 372.

[34] *Royal Swedish Academy of Sciences, Press Release, 1986*, 9553. [Online]. Available: http://www.nobelprize.org/nobel_prizes/physics/laureates/1986/press.html. [Accessed: 25-Jun-2014].

[35] K. R. Porter, A. Claude, and E. F. Fullam, *A Study of tissue culture cells by electron microscopy*, J. Exp. Med., 1945, vol. 81, no. 3, pp. 233–246.

[36] E. B. Wilson, *The cell in development and inheritance*. Mcmillan & Co. ltd, 1897.

[37] Lister, *An extract of a letter of the same mr. Lister, written from York April 12. 1672 concerning animated horse-hairs; rectifying a vulgar error*, Philos. Trans., 1672, vol. 7, pp. 4064–4066.

[38] R. G. Harrison, M. J. Greenman, F. P. Mall, and C. M. Jackson, *Observations of the living developing nerve fiber*, Anat. Rec., Jun. 1907, vol. 1, no. 5, pp. 116–128.

[39] J. A. McAteer and J. M. Davis, *Basic cell culture technique and the maintenance of cell lines*, in *Basic Cell Culture*, 2nd ed., J. M. Davis, Ed. Oxford University Press, 2002, pp. 135–189.

[40] A. Carrel, *On the permanent life tf Tissues outside of the organism*, J. Exp. Med., May 1912, vol. 15, no. 5, pp. 516–528.

[41] Rebecca Skloot, *The immortal life of Henrietta Lacks*. London/GB: Pan Books Ltd, 2011.

[42]   W. F. Scherer, J. T. Syverton, and G. O. Gey, *Studies on the propagation in vitro of poliomyelitis viruses. IV. Viral multiplication in a stable strain of human malignant epithelial cells (strain HeLa) derived from an epidermoid carcinoma of the cervix*, J. Exp. Med., 1953, vol. 97, no. 5, pp. 695–710.

[43]   Z. Su, W. Zhou, and Y. Zhang, *New insight into the soot nanoparticles in a candle flame*, Chem. Commun. (Camb)., Apr. 2011, vol. 47, no. 16, pp. 4700–2.

[44]   G. S. May and S. M. Sze, *Fundamentals of semiconductor fabrication*. John Wiley & Sons, 2004.

[45]   K. Hiruma, M. Yazawa, K. Haraguchi, K. Ogawa, T. Katsuyama, M. Koguchi, and H. Kakibayashi, *GaAs free-standing quantum-size wires*, J. Appl. Phys., 1993, vol. 74, no. 5, pp. 3162–3171.

[46]   K. A. Dick, *A review of nanowire growth promoted by alloys and non-alloying elements with emphasis on Au-assisted III-V nanowires*, Prog. Cryst. Growth Charact. Mater., 2008, vol. 54, no. 3–4, pp. 138–173.

[47]   M. E. Messing, K. A. Dick, L. R. Wallenberg, and K. Deppert, *Generation of size-selected gold nanoparticles by spark discharge — for growth of epitaxial nanowires*, Gold Bull., 2009, vol. 42, no. 1, pp. 20–26.

[48]   D. B. Suyatin, W. Hällström, L. Samuelson, L. Montelius, C. N. Prinz, and M. Kanje, *Gallium phosphide nanowire arrays and their possible application in cellular force investigations*, J. Vac. Sci. Technol. B, 2009, vol. 27, no. 6, pp. 3092–3094.

[49]   W. Seifert, M. Borgström, K. Deppert, K. A. Dick, J. Johansson, M. W. Larsson, T. Mårtensson, N. Sköld, C. P. T. Svensson, B. A. Wacaser, L. R. Wallenberg, and L. Samuelson, *Growth of one-dimensional nanostructures in MOVPE*, J. Cryst. Growth, 2004, vol. 272, no. 1–4, pp. 211–220.

[50]   S. Hofmann, R. Sharma, C. T. Wirth, F. Cervantes-Sodi, C. Ducati, T. Kasama, R. E. Dunin-Borkowski, J. Drucker, P. Bennett, and J. Robertson, *Ledge-flow-controlled catalyst interface dynamics during Si nanowire growth.*, Nat. Mater., May 2008, vol. 7, no. 5, pp. 372–5.

[51]   S. Heun, B. Radha, D. Ercolani, G. U. Kulkarni, F. Rossi, V. Grillo, G. Salviati, F. Beltram, and L. Sorba, *Coexistence of vapor-liquid-solid and vapor-solid-solid growth modes in Pd-assisted InAs nanowires.*, Small, Sep. 2010, vol. 6, no. 17, pp. 1935–41.

[52]   K. Ikejiri, J. Noborisaka, S. Hara, J. Motohisa, and T. Fukui, *Mechanism of catalyst-free growth of GaAs nanowires by selective area MOVPE*, J. Cryst. Growth, Jan. 2007, vol. 298, pp. 616–619.

[53]   S. A. Fortuna and X. Li, *Metal-catalyzed semiconductor nanowires: a review on the control of growth directions*, Semicond. Sci. Technol., Feb. 2010, vol. 25, no. 2, p. 024005.

[54]   D. L. Smith, *Thin-film deposition, principles & practice*. Boston, MA: McGraw-Hill, 1995.

[55]   S. M. George, *Atomic layer deposition: an overview*, Chem. Rev., Jan. 2010, vol. 110, no. 1, pp. 111–31.

[56] R. L. Puurunen, *Surface chemistry of atomic layer deposition: A case study for the trimethylaluminum/water process*, J. Appl. Phys., 2005, vol. 97, no. 12, p. 121301.

[57] M. Leskelä and M. Ritala, *Atomic layer deposition (ALD): from precursors to thin film structures*, Thin Solid Films, Apr. 2002, vol. 409, no. 1, pp. 138–146.

[58] A. C. Dillon, A. W. Ott, J. D. Way, and S. M. George, *Surface chemistry of Al2O3 deposition using AlCH3 and H2O in a binary reaction sequence*, Surf. Sci., 1995, vol. 322, no. 1–3, pp. 230–242.

[59] M. D. Groner, F. H. Fabreguette, J. W. Elam, and S. M. George, *Low-temperature Al2O3 atomic layer deposition*, 2004, vol. 16, no. 4, pp. 639–645.

[60] S. Jakschik, U. Schroeder, T. Hecht, D. Krueger, G. Dollinger, A. Bergmaier, C. Luhmann, and J. W. Bartha, *Physical characterization of thin ALD–Al2O3 films*, Appl. Surf. Sci., Apr. 2003, vol. 211, no. 1–4, pp. 352–359.

[61] S. J. Pearton and D. R. Norton, *Dry etching of electronic oxides, polymers, and semiconductors*, Plasma Process. Polym., 2005, vol. 2, no. 1, pp. 16–37.

[62] H. Jansen, H. Gardeniers, M. De Boer, M. Elwenspoek, and J. Fluitman, *A survey on the reactive ion etching of silicon in microtechnology*, J. Micromechanics Microengineering, Mar. 1996, vol. 6, no. 1, pp. 14–28.

[63] M. Boufnichel, S. Aachboun, F. Grangeon, P. Lefaucheux, and P. Ranson, *Profile control of high aspect ratio trenches of silicon. I. Effect of process parameters on local bowing*, J. Vac. Sci. Technol. B, 2002, vol. 20, no. 4, pp. 1508–1513.

[64] A. Mölder, M. Sebesta, M. Gustafsson, L. Gisselson, a G. Wingren, and K. Alm, *Non-invasive, label-free cell counting and quantitative analysis of adherent cells using digital holography*, J. Microsc., Nov. 2008, vol. 232, no. 2, pp. 240–7.

[65] M. Gustafsson and M. Sebesta, *Refractometry of microscopic objects*, Appl. Opt., 2004, vol. 43, no. 25, pp. 4796–4801.

[66] M. R. Lorenz, G. D. Pettit, and R.C. Taylor, *Band gap of gallium phosphide from 0 to 900K and light emission from diodes at high temperatures*, Phys. Rev., 1968, vol. 171, no. 3, pp. 867–881.

[67] PHIAB, *Holomonitor M3, Technical specification*, 9654. [Online]. Available: http://phiab.se/products/holomonitor-m3. [Accessed: 06-Jul-2014].

[68] I. D. Johnson, *The molecular probes handbook*. Life Technologies Corporation, 2010.

[69] B. N. G. Giepmans, S. R. Adams, M. H. Ellisman, and R. Y. Tsien, *The fluorescent toolbox for assessing protein location and function*, Science, Apr. 2006, vol. 312, no. 5771, pp. 217–24.

[70] J. Zhang, R. E. Campbell, A. Y. Ting, and R. Y. Tsien, *Creating new fluorescent probes for cell biology*, Nat. Rev. Mol. Cell Biol., Dec. 2002, vol. 3, no. 12, pp. 906–18.

[71] R. Dixit and R. Cyr, *Cell damage and reactive oxygen species production induced by fluorescence microscopy: effect on mitosis and guidelines for non-invasive fluorescence microscopy*, Plant J., Oct. 2003, vol. 36, no. 2, pp. 280–290.

[72] J. W. Lichtman and J. Conchello, *Fluorescence microscopy*, 2005, vol. 2, no. 12, pp. 910–919.

[73]   R. A. Hoebe, C. H. Van Oven, T. W. J. Gadella, P. B. Dhonukshe, C. J. F. Van Noorden, and E. M. M. Manders, *Controlled light-exposure microscopy reduces photobleaching and phototoxicity in fluorescence live-cell imaging*, Nat. Biotechnol., Feb. 2007, vol. 25, no. 2, pp. 249–53.

[74]   E. Eruslanov and S. Kusmartsev, *Identification of ROS using oxidized DCFDA and flow-cytometry*, in *Advanced Protocols in Oxidative Stress II*, D. Armstrong, Ed. Humana Press, pp. 57–72.

[75]   J. O'Brien, I. Wilson, T. Orton, and F. Pognan, *Investigation of the Alamar Blue (resazurin) fluorescent dye for the assessment of mammalian cell cytotoxicity*, Eur. J. Biochem., Sep. 2000, vol. 267, no. 17, pp. 5421–6.

[76]   T. T. Paull, E. P. Rogakou, V. Yamazaki, C. U. Kirchgessner, M. Gellert, and W. M. Bonner, *A critical role for histone H2AX in recruitment of repair factors to nuclear foci after DNA damage*, Curr. Biol., Aug. 2000, vol. 10, no. 15, pp. 886–895.

[77]   B. Hudson, W. B. Upholt, J. Devinny, and J. Vinograd, *The use of an ethidium analogue in the dye-buoyant density procedure for the isolation of closed circular DNA: the variation of the superhelix density of mitochondrial DNA*, 1968, pp. 813–820.

[78]   S. A. Weston and C. R. Parish, *New fluorescent dyes for lymphocyte migration studies. Analysis by flow cytometry and fluorescence microscopy*, J. Immunol. Methods, Oct. 1990, vol. 133, no. 1, pp. 87–97.

[79]   J. M. Lopacinska, C. Gradinaru, R. Wierzbicki, C. Kobler, M. S. Schmidt, M. T. Madsen, M. Skolimowski, M. Dufva, H. Flyvbjerg, and K. Molhave, *Cell motility, morphology, viability and proliferation in response to nanotopography on silicon black*, Nanoscale, 2012, vol. 4, no. 12, pp. 3739–3745.

[80]   D.-J. Kim, J.-K. Seol, G. Lee, G.-S. Kim, and S.-K. Lee, *Cell adhesion and migration on nanopatterned substrates and their effects on cell-capture yield*, Nanotechnology, Oct. 2012, vol. 23, no. 39, p. 395102.

[81]   F. Mumm, K. M. M. Beckwith, S. Bonde, K. L. L. Martinez, and P. Sikorski, *A transparent nanowire-based cell impalement device suitable for detailed cell-nanowire interaction studies*, Small, 2013, vol. 9, no. 2, pp. 263–272.

[82]   Y.-R. Na, S. Y. Kim, J. T. Gaublomme, A. K. Shalek, M. Jorgolli, H. Park, and E. G. Yang, *Probing enzymatic activity inside living cells using a nanowire-cell "sandwich" assay*, Nano Lett., Jan. 2013, vol. 13, no. 1, pp. 153–8.

[83]   S. Bonde, T. Berthing, M. H. Madsen, T. K. Andersen, N. Buch-Månson, L. Guo, X. Li, F. Badique, K. Anselme, J. Nygård, and K. L. Martinez, *Tuning InAs nanowire density for HEK293 cell viability, adhesion, and morphology: Perspectives for nanowire-based biosensors*, ACS Appl. Mater. Interfaces, 2013, vol. 5, pp. 10510–10519.

[84]   A. K. Shalek, J. T. Gaublomme, L. L. Wang, N. Yosef, N. Chevrier, M. S. Andersen, J. T. Robinson, N. Pochet, D. Neuberg, R. S. Gertner, I. Amit, J. R. Brown, N. Hacohen, A. Regev, C. J. Wu, and H. Park, *Nanowire-mediated delivery enables functional interrogation of primary immune cells: Application to the analysis of chronic lymphocytic leukemia*, Nano Lett., 2012, vol. 12, no. 12, pp. 6498–6504.

[85] T. Berthing, S. Bonde, C. B. Sørensen, P. Utko, J. Nygård, and K. L. Martinez, *Intact mammalian cell function on semiconductor nanowire arrays: new perspectives for cell-based biosensing*, Small, Mar. 2011, vol. 7, no. 5, pp. 640–7.

[86] T. Berthing, S. Bonde, K. R. K. R. Rostgaard, M. H. M. H. Madsen, C. B. Sørensen, J. Nygård, K. L. K. L. Martinez, C. B. Sorensen, and J. Nygard, *Cell membrane conformation at vertical nanowire array interface revealed by fluorescence imaging*, Nanotechnology, Oct. 2012, vol. 23, no. 41, p. 415102 (8pp).

[87] M. W. Davidson and M. Abramowitz, *Optical microscopy*.

[88] M. J. Rust, M. Bates, and X. Zhuang, *imaging by stochastic optical reconstruction microscopy (STORM)*, 2006, vol. 3, no. 10, pp. 793–795.

[89] S. W. Hell and J. Wichmann, *Breaking the diffraction resolution limit by stimulated emission: stimulated-emission-depletion fluorescence microscopy*, Opt. Lett., Jun. 1994, vol. 19, no. 11, pp. 780–2.

[90] *Hitachi Launches World's Highest Resolution FE-SEM*, *Nanotechnology Now*, 9656. [Online]. Available: http://www.nanotech-now.com/news.cgi?story_id=42612. [Accessed: 28-Jul-2014].

[91] A. Bogner, P.-H. Jouneau, G. Thollet, D. Basset, and C. Gauthier, *A history of scanning electron microscopy developments: towards "wet-STEM" imaging*, Micron, Jan. 2007, vol. 38, no. 4, pp. 390–401.

[92] JEOL, *A Guide to Scanning Electron Microscopy*.

[93] J. J. Bozzola and L. D. Russel, *Electron microscopy: Principles and techniques for biologists*, 2nd ed. Jones & Bartlett Publishers, 1999.

[94] J. F. Hainfeld and F. R. Furuya, *A 1.4-nm gold cluster covalently attached to antibodies improves immunolabeling*, J. Histochem. Cytochem., Feb. 1992, vol. 40, no. 2, pp. 177–184.

[95] V. G. M. Sivel, J. Van den Brand, W. R. Wang, H. Mohdadi, F. D. Tichelaar, P. F. a Alkemade, and H. W. Zandbergen, *Application of the dual-beam FIB/SEM to metals research*, J. Microsc., Jun. 2004, vol. 214, no. Pt 3, pp. 237–45.

[96] D. J. Stokes, F. Morrissey, and B. H. Lich, *A new approach to studying biological and soft materials using focused ion beam scanning electron microscopy (FIB SEM)*, J. Phys. Conf. Ser., Feb. 2006, vol. 26, pp. 50–53.

[97] D. Drobne, M. Milani, A. Zrimec, V. Leser, and M. Berden Zrimec, *Electron and ion imaging of gland cells using the FIB/SEM system*, J. Microsc., 2005, vol. 219, pp. 29–35.

[98] K. A. . Elliget, R. I. Frehsney, N. E. Fusening, I. M. Greenfield, C. Guguen-Guillouzu, J. F. Lechner, C. Paraskeva, E. K. Parkinson, and D. M. Peehl, *Culture of epithelial cells*. Wiley-Liss, 1992.

[99] C. MacDonald, *Primary culture and the establishment of cell lines*, in *Basic cell culture*, 2nd ed., J. M. Davis, Ed. Oxford University Press, 2002, pp. 191–225.

[100] K. K. Sanford, W. R. Earle, and G. D. Likely, *The growth in vitro of single isolated tissue cells*, J. Natl. Cancer Inst., Dec. 1948, vol. 9, no. 3, pp. 229–46.

[101] T. Kinsman, *A technique for generating colour scanning electron microscope images*, *In Focus*, pp. 24–43, 2014.

[102] M. Safi, M. Yan, M.-A. Guedeau-Boudeville, H. Conjeaud, V. Garnier-Thibaud, N. Boggetto, A. Baeza-Squiban, F. Niedergang, D. Averbeck, and J.-F. Berret, *Interactions between magnetic nanowires and living cells: uptake, toxicity, and degradation*, ACS Nano, Jul. 2011, vol. 5, no. 7, pp. 5354–64.

[103] F. Peng, Y. Su, X. Wei, Y. Lu, Y. Zhou, Y. Zhong, S.-T. Lee, and Y. He, *Silicon-nanowire-based nanocarriers with ultrahigh drug-loading capacity for in vitro and in vivo cancer therapy.*, Angew. Chem. Int. Ed. Engl., Jan. 2013, vol. 52, no. 5, pp. 1457–61.

[104] N. H. Kwon, M. F. Beaux, C. Ebert, L. Wang, B. E. Lassiter, Y. H. Park, D. N. McIlroy, C. J. Hovde, and G. a Bohach, *Nanowire-based delivery of Escherichia coli O157 shiga toxin 1 A subunit into human and bovine cells.*, Nano Lett., Sep. 2007, vol. 7, no. 9, pp. 2718–23.

[105] Y. Su, X. Wei, F. Peng, Y. Zhong, Y. Lu, S. Su, T. Xu, S.-T. Lee, and Y. He, *Gold nanoparticles-decorated silicon nanowires as highly efficient near-infrared hyperthermia agents for cancer cells destruction*, Nano Lett., May 2012, vol. 12, no. 4, pp. 1845–50.

[106] C. J. Bettinger, R. Langer, and J. T. Borenstein, *Engineering substrate topography at the micro- and nanoscale to control cell function.*, Angew. Chem. Int. Ed. Engl., Jan. 2009, vol. 48, no. 30, pp. 5406–15.

[107] E. Martínez, E. Engel, J. A. Planell, and J. Samitier, *Effects of artificial micro- and nano-structured surfaces on cell behaviour*, Ann. Anat., Jan. 2009, vol. 191, no. 1, pp. 126–35.

[108] K.-Y. Lee, I. Kim, S.-E. Kim, D.-W. Jeong, J.-J. Kim, H. Rhim, J.-P. Ahn, S.-H. Park, and H.-J. Choi, *Vertical nanowire probes for intracellular signaling of living cells*, Nanoscale Res. Lett., Jan. 2014, vol. 9, no. 1, p. 56.

[109] F. Johansson, W. Hällström, P. Gustavsson, L. Wallman, C. Prinz, L. Montelius, and M. Kanje, *Nanomodified surfaces and guidance of nerve cell processes*, J. Vac. Sci. Technol. B, 2008, vol. 26, no. 6, pp. 2558–2561.

[110] W. Hällström, M. Lexholm, D. B. Suyatin, G. Hammarin, D. Hessman, L. Samuelson, L. Montelius, M. Kanje, and C. N. Prinz, *Fifteen-piconewton force detection from neural growth cones using nanowire arrays*, Nano Lett., 2010, vol. 10, no. 3, pp. 782–787.

[111] C. W. Kuo, J. Y. Shiu, F. C. Chien, S. M. Tsai, D. Y. Chueh, and P. L. Chen, *Polymeric nanopillar arrays for cell traction force measurements*, Electrophoresis, 2010, vol. 31, no. 18, pp. 3152–3158.

[112] J. L. Tan, J. Tien, D. M. Pirone, D. S. Gray, K. Bhadriraju, and C. S. Chen, *Cells lying on a bed of microneedles: An approach to isolate mechanical force*, Proc. Natl. Acad. Sci. U. S. A., 2003, vol. 100, no. 4, pp. 1484–1489.

[113] T. E. McKnight, A. V Melechko, G. D. Griffin, M. A. Guillorn, V. I. Merkulov, F. Serna, D. K. Hensley, M. J. Doktycz, D. H. Lowndes, and M. L. Simpson, *Intracellular integration of synthetic nanostructures with viable cells for controlled biochemical manipulation*, Nanotechnology, May 2003, vol. 14, no. 5, pp. 551–556.

[114] H. Xia, Q. Mao, H. L. Paulson, and B. L. Davidson, *siRNA-mediated gene silencing in vitro and in vivo*, Nat. Biotechnol., Oct. 2002, vol. 20, no. 10, pp. 1006–10.

[115] M. Ehrenberg and J. L. McGrath, *Binding between particles and proteins in extracts: implications for microrheology and toxicity*, Acta Biomater., May 2005, vol. 1, no. 3, pp. 305–15.

[116] Y. L. Wang, *Fluorescent analog cytochemistry: tracing functional protein components in living cells*, Methods Cell Biol., Jan. 1989, vol. 29, pp. 1–12.

[117] C. M. Waterman-Storer, A. Desai, J. C. Bulinski, and E. D. Salmon, *Fluorescent speckle microscopy, a method to visualize the dynamics of protein assemblies in living cells*, Curr. Biol., Nov. 1998, vol. 8, no. 22, pp. 1227–30.

[118] D. J. Stephens and R. Pepperkok, *The many ways to cross the plasma membrane*, Proc. Natl. Acad. Sci. U. S. A., Apr. 2001, vol. 98, no. 8, pp. 4295–8.

[119] Y. Zhang and L. C. Yu, *Single-cell microinjection technology in cell biology*, Bioessays, 2008, vol. 30, no. 6, pp. 606–610.

[120] R. E. Kingston, *Introduction of DNA into mammalian cells*, in *Current protocols in molecular biology*, John Wiley & Sons, Inc., 1991.

[121] P. L. Felgner, T. R. Gadek, M. Holm, R. Roman, H. W. Chan, M. Wenz, J. P. Northrop, G. M. Ringold, and M. Danielsen, *Lipofection: a highly efficient, lipid-mediated DNA-transfection procedure*, Proc. Natl. Acad. Sci. U. S. A., Dec. 1987, vol. 84, no. 21, pp. 7413–7.

[122] E. A. Baker, M. W. Vaughn, and D. L. Haviland, *Choices in transfection methodologies: Transfection efficiency should not be the sole criterion*, Focus (Madison)., 2000, vol. 22, pp. 31–33.

[123] T. Y. Tsong, *Electroporation of cell membranes*, Biophys. J., Aug. 1991, vol. 60, no. 2, pp. 297–306.

[124] M. Graessmann and A. Graessmann, *Microinjection of tissue culture cells*, in *Methods in Enzymology, Vol 101*, vol. 101, no. 1980, Academic Press Inc., 1983, pp. 482–492.

[125] H. Matsuoka, T. Komazaki, Y. Mukai, M. Shibusawa, H. Akane, A. Chaki, N. Uetake, and M. Saito, *High throughput easy microinjection with a single-cell manipulation supporting robot*, J. Biotechnol., 2005, vol. 116, no. 2, pp. 185–194.

[126] A. Adamo and K. F. Jensen, *Microfluidic based single cell microinjection*, Lab Chip, 2008, vol. 8, no. 8, pp. 1258–1261.

[127] D. V McAllister, M. G. Allen, and M. R. Prausnitz, *Microfabricated microneedles for gene and drug delivery*, Annu. Rev. Biomed. Eng., 2000, vol. 2, pp. 289–313.

[128] K. Chun, G. Hashiguchi, H. Toshiyoshi, H. Fujita, Y. Kikuchi, J. Ishikawa, Y. Murakami, and E. Tamiya, *An array of hollow microcapillaries for the controlled injection of genetic materials into animal/plant cells*, Mems '99 Twelfth IEEE Int. Conf. Micro Electro Mech. Syst. Tech. Dig., 1999, pp. 406–411.

[129] A. Meister, M. Gabi, P. Behr, P. Studer, J. Vörös, P. Niedermann, J. Bitterli, J. Polesel-Maris, M. Liley, H. Heinzelmann, and T. Zambelli, *FluidFM: combining atomic force microscopy and nanofluidics in a universal liquid delivery system for single cell applications and beyond*, Nano Lett., Jun. 2009, vol. 9, no. 6, pp. 2501–7.

[130]   M. G. Schrlau, E. M. Falls, B. L. Ziober, and H. H. Bau, *Carbon nanopipettes for cell probes and intracellular injection*, Nanotechnology, 2008, vol. 19, no. 1, p. 015101 (4pp).

[131]   X. Chen, A. Kis, A. Zettl, and C. R. Bertozzi, *A cell nanoinjector based on carbon nanotubes*, Proc. Natl. Acad. Sci. U. S. A., 2007, vol. 104, no. 20, pp. 8218–8222.

[132]   S. Park, Y.-S. Kim, W. B. Kim, and S. Jon, *Carbon Nanosyringe Array as a Platform for Intracellular Delivery*, Nano Lett., 2009, vol. 9, no. 4, pp. 1325–1329.

[133]   J. J. VanDersarl, A. M. Xu, and N. A. Melosh, *Nanostraws for direct fluidic intracellular access*, Nano Lett., Aug. 2012, vol. 12, no. 8, pp. 3881–6.

[134]   N. Sköld, W. Hällström, H. Persson, L. Montelius, M. Kanje, L. Samuelson, C. N. Prinz, and J. O. Tegenfeldt, *Nanofluidics in hollow nanowires*, Nanotechnology, 2010, vol. 21, no. 15, pp. 155301–155304.

[135]   D. B. Peckys, A. V Melechko, M. L. Simpson, and T. E. McKnight, *Immobilization and release strategies for DNA delivery using carbon nanofiber arrays and self-assembled monolayers*, Nanotechnology, 2009, vol. 20, no. 14, p. 145304 (8pp).

[136]   D. G. J. Mann, T. E. McKnight, J. T. McPherson, P. R. Hoyt, A. V Melechko, M. L. Simpson, and G. S. Sayler, *Inducible RNA interference-mediated gene silencing using nanostructured gene delivery arrays*, ACS Nano, 2008, vol. 2, no. 1, pp. 69–76.

[137]   T. E. McKnight, A. V. Melechko, D. K. Hensley, D. G. J. Mann, G. D. Griffin, and M. L. Simpson, *Tracking gene expression after DNA delivery using spatially indexed nanofiber arrays*, Nano Lett., Jul. 2004, vol. 4, no. 7, pp. 1213–1219.

[138]   A. M. Xu, A. Aalipour, S. Leal-Ortiz, A. H. Mekhdjian, X. Xie, A. R. Dunn, C. C. Garner, and N. A. Melosh, *Quantification of nanowire penetration into living cells*, Nat. Commun., Apr. 2014, vol. 5, pp. 1–8.

[139]   N. Chevrier, P. Mertins, M. N. Artyomov, A. K. Shalek, M. Iannacone, M. F. Ciaccio, I. Gat-Viks, E. Tonti, M. M. DeGrace, K. R. Clauser, M. Garber, T. M. Eisenhaure, N. Yosef, J. Robinson, A. Sutton, M. S. Andersen, D. E. Root, U. von Andrian, R. B. Jones, H. Park, S. A. Carr, A. Regev, I. Amit, and N. Hacohen, *Systematic discovery of TLR signaling components delineates viral-sensing circuits.*, Cell, Nov. 2011, vol. 147, no. 4, pp. 853–67.

[140]   D. B. Peckys, N. de Jonge, M. L. Simpson, and T. E. McKnight, *End-specific strategies of attachment of long double stranded DNA onto gold-coated nanofiber arrays*, Nanotechnology, Oct. 2008, vol. 19, no. 43, p. 435301 (9pp).

[141]   R. C. Pearce, J. G. Railsback, B. D. Anderson, M. F. Sarac, T. E. McKnight, J. B. Tracy, and A. V Melechko, *Transfer of vertically aligned carbon nano fibers to polydimethylsiloxane (PDMS) while maintaining their alignment and impalefection functionality*, ACS Appl. Mater. Interfaces, 2013, vol. 5, pp. 878–882.

[142]   N. Yosef, A. K. Shalek, J. T. Gaublomme, H. Jin, Y. Lee, A. Awasthi, C. Wu, K. Karwacz, S. Xiao, M. Jorgolli, D. Gennert, R. Satija, A. Shakya, D. Y. Lu, J. J. Trombetta, M. R. Pillai, P. J. Ratcliffe, M. L. Coleman, M. Bix, D. Tantin, H. Park, V. K. Kuchroo, and A. Regev, *Dynamic regulatory network controlling TH17 cell differentiation*, Nature, Apr. 2013, vol. 496, no. 7446, pp. 461–8.

[143] G. Piret, M. T. Perez, and C. N. Prinz, *Neurite outgrowth and synaptophysin expression of postnatal CNS neurons on GaP nanowire arrays in long-term retinal cell culture*, Biomaterials, 2013, vol. 34, no. 4, pp. 875–887.

[144] C. E. Linsmeier, C. N. Prinz, L. M. E. Pettersson, P. Caroff, L. Samuelson, J. Schouenborg, L. Montelius, and N. Danielsen, *Nanowire biocompatibility in the brain - looking for anNeedle in a 3D stack*, Nano Lett., 2009, vol. 9, no. 12, pp. 4184–4190.

[145] C. H. Choi, S. H. Hagvall, B. M. Wu, J. C. Y. Dunn, R. E. Beygui, and C. J. Kim, *Cell interaction with three-dimensional sharp-tip nanotopography*, Biomaterials, 2007, vol. 28, no. 9, pp. 1672–1679.

[146] Q. Ha, G. Yang, Z. Ao, D. Han, F. Iu, and S. Wang, *Rapid fibroblast activation in mammalian cells induced by silicon nanowire arrays*, Nanoscale, 2014, vol. 6, no. 14, pp. 8318–25.

[147] C. Xie, L. Hanson, W. J. Xie, Z. L. Lin, B. X. Cui, and Y. Cui, *Noninvasive neuron pinning with nanopillar arrays*, Nano Lett., 2010, vol. 10, no. 10, pp. 4020–4024.

[148] H. Towbin, T. Staehelin, and J. Gordon, *Electrophoretic transfer of proteins from polyacrylamide gels to nitrocellulose sheets: procedure and some applications.*, Proc. Natl. Acad. Sci. U. S. A., Jan. 1979, vol. 76, no. 9, pp. 4350–4354.

[149] B. Geiger, J. P. Spatz, and A. D. Bershadsky, *Environmental sensing through focal adhesions*, Nat. Rev. Mol. Cell Biol., 2009, vol. 10, no. 1, pp. 21–33.

[150] C. R. Mackay, *Moving targets: cell migration inhibitors as new anti-inflammatory therapies*, Nat. Immunol., Sep. 2008, vol. 9, no. 9, pp. 988–98.

[151] D. Hanahan and R. A. Weinberg, *The hallmarks of cancer*, Cell, 2000, vol. 100, no. 1, pp. 57–70.

[152] D. Hanahan and R. A. Weinberg, *Hallmarks of Cancer: The Next Generation*, Cell, 2011, vol. 144, no. 5, pp. 646–674.

[153] B. L. Fletcher, T. E. McKnight, A. V. Melechko, D. K. Hensley, D. K. Thomas, M. N. Ericso, and M. L. Simpson, *Transfer of flexible arrays of vertically aligned carbon nanofiber electrodes to temperature-sensitive substrates*, Adv. Mater., Jul. 2006, vol. 18, no. 13, pp. 1689–1694.

[154] S. Qi, C. Yi, S. Ji, C.-C. Fong, and M. Yang, *Cell adhesion and spreading behavior on vertically aligned silicon nanowire arrays*, ACS Appl. Mater. Interfaces, Jan. 2009, vol. 1, no. 1, pp. 30–4.

[155] C. M. Holst and S. M. Oredsson, *Comparison of three cytotoxicity tests in the evaluation of the cytotoxicity of a spermine analogue on human breast cancer cell lines*, Toxicol. Vitr., Apr. 2005, vol. 19, no. 3, pp. 379–87.

[156] M. Fricker, M. Hollinshead, N. White, and D. Vaux, *Interphase nuclei of many mammalian cell types contain deep, dynamic, tubular membrane-bound invaginations of the nuclear envelope*, J. Cell Biol., 1997, vol. 136, no. 3, pp. 531–544.

[157] D. H. M. Dam, J. H. Lee, P. N. Sisco, D. T. Co, M. Zhang, M. R. Wasielewski, and T. W. Odom, *Direct observation of nanoparticle-cancer cell nucleus interactions*, ACS Nano, 2012, vol. 6, no. 4, pp. 3318–3326.

[158] M. Fenech, M. Kirsch-Volders, a T. Natarajan, J. Surralles, J. W. Crott, J. Parry, H. Norppa, D. a Eastmond, J. D. Tucker, and P. Thomas, *Molecular mechanisms of micronucleus, nucleoplasmic bridge and nuclear bud formation in mammalian and human cells*, Mutagenesis, Jan. 2011, vol. 26, no. 1, pp. 125–32.

[159] L. Luzhna, P. Kathiria, and O. Kovalchuk, *Micronuclei in genotoxicity assessment: from genetics to epigenetics and beyond*, Front. Genet., Jan. 2013, vol. 4, p. 131 (17 pp).

[160] A. Wright, W. a Bubb, C. L. Hawkins, and M. J. Davies, *Singlet oxygen-mediated protein oxidation: evidence for the formation of reactive side chain peroxides on tyrosine residues*, Photochem. Photobiol., Jul. 2002, vol. 76, no. 1, pp. 35–46.

[161] A. SanMartin, F. Johansson, L. Samuelson, and C. N. Prinz, *Microarray analysis reveals moderate gene expression changes in cortical neural stem cells cultured on nanowire arrays*, J. Nanosci. Nanotechnol., Jul. 2014, vol. 14, no. 7, pp. 4880–4885.

[162] L. Hanson, Z. C. Lin, C. Xie, Y. Cui, and B. Cui, *Characterization of the cell-nanopillar interface by transmission electron microscopy*, Nano Lett., Nov. 2012, vol. 12, no. 11, pp. 5815–20.

[163] X. Xie, A. M. Xu, M. R. Angle, N. Tayebi, P. Verma, and N. A. Melosh, *Mechanical model of vertical nanowire cell penetration*, Nano Lett., Dec. 2013, vol. 13, no. 12, pp. 6002–8.

[164] E. T. Castellana and P. S. Cremer, *Solid supported lipid bilayers: From biophysical studies to sensor design*, Surf. Sci. Rep., 2006, vol. 61, no. 10, pp. 429–444.

[165] A. P. Dabkowska, C. Niman, G. Piret, H. Persson, H. P. Wacklin, H. Linke, C. Prinz, and T. Nylander, *Fluid and highly curved model membranes on vertical nanowire arrays.*, Nano Lett., Jun. 2014.

[166] H. T. McMahon and J. L. Gallop, *Membrane curvature and mechanisms of dynamic cell membrane remodelling*, Nature, Dec. 2005, vol. 438, no. 7068, pp. 590–6.

[167] R. Parthasarathy, C. Yu, and J. T. Groves, *Curvature-modulated phase separation in lipid bilayer membranes*, Langmuir, May 2006, vol. 22, no. 11, pp. 5095–9.

[168] K. Adolfsson, M. Schneider, G. Hammarin, U. Hacker, and C. N. Prinz, *Ingestion of gallium phosphide nanowires has no adverse effect on Drosophila tissue function*, Nanotechnology, 2013, vol. 24, no. 28, p. 285101 (7pp).

[169] G. Hammarin, H. Persson, A. P. Dabkowska, and C. N. Prinz, *Enhanced laminin adsorption on nanowires compared to flat surfaces*, Colloids Surfaces B Biointerfaces, 2014, vol. 122, pp. 85–89.

[170] C. J. Wilson, R. E. Clegg, D. I. Leavesley, and M. J. Pearcy, *Mediation of biomaterial-cell interactions by adsorbed proteins: a review*, Tissue Eng., 2005, vol. 11, no. 1–2, pp. 1–18.

[171] F. Greve, S. Frerker, A. G. Bittermann, C. Burkhardt, A. Hierlemann, and H. Hall, *Molecular design and characterization of the neuron-microelectrode array interface*, Biomaterials, 2007, vol. 28, no. 35, pp. 5246–5258.

[172] A. Blau, *Cell adhesion promotion strategies for signal transduction enhancement in microelectrode array in vitro electrophysiology: An introductory overview and critical discussion*, Curr. Opin. Colloid Interface Sci., Oct. 2013, vol. 18, no. 5, pp. 481–492.

[173]   A. Barzegar and A. a Moosavi-Movahedi, *Intracellular ROS protection efficiency and free radical-scavenging activity of curcumin*, PLoS One, Jan. 2011, vol. 6, no. 10, p. e26012 (7 pp).

[174]   M. V Berridge, P. M. Herst, and A. S. Tan, *Tetrazolium dyes as tools in cell biology: new insights into their cellular reduction*, Biotechnol. Annu. Rev., Jan. 2005, vol. 11, no. 05, pp. 127–52.

Appendix 1 – cell lines

This reference sheet summarizes some of the different cell lines frequently referred to in this thesis.

Cell line	Cell type
CHO	Chinese hamster ovary cells
F11	Rat embryonic dorsal root ganglion cells
HEK293	Human embryonic kidney cells
HeLa	Human cervical cancer cells
HEP-G2	Human liver carcinoma cells
L929	Mouse fibroblasts
LX-2	Human hepatic stellate cells
NIH3T3	Mouse embryonic fibroblasts

Appendix 2 – supporting material

There is supporting material available online for this thesis which can be found at http://bit.ly/Persson2014. This material consists of time-lapse movies of L929 fibroblasts on GaP nanowires and controls (PS and planar GaP) from Paper II and Paper IV. All scale bars are 100 μm.

Title	Description	Source
Movie S1	GaP nanowires (diameter 80 nm, length 1.5 μm, density 1 nanowire μm^{-2}) Acquisition started 24 h after seeding.	Paper II
Movie S2	GaP nanowires (diameter 80 nm, length 4 μm, density 1 nanowire μm^{-2}) Acquisition started 24 h after seeding.	Paper II
Movie S3	GaP nanowires (diameter 80 nm, length 6.7 μm, density 1 nanowire μm^{-2}) Acquisition started 24 h after seeding.	Paper II
Movie S4	Polystyrene Acquisition started 24 h after seeding.	Paper II
Movie S5	GaP Acquisition started 24 h after seeding.	Paper II
Movie S6	GaP nanowires (diameter 80 nm, length 4 μm, density 0.1 nanowires μm^{-2}) Acquisition started 0 h after seeding.	Paper IV
Movie S7	GaP nanowires (diameter 80 nm, length 4 μm, density 1 nanowire μm^{-2}) Acquisition started 0 h after seeding.	Paper IV
Movie S8	GaP nanowires (diameter 80 nm, length 4 μm, density 4 nanowires μm^{-2}) Acquisition started 0 h after seeding.	Paper IV
Movie S9	Polystyrene Acquisition started 0 h after seeding.	Paper IV
Movie S10	GaP Acquisition started 0 h after seeding.	Paper IV
Movie S11	Cells adapting eccentric morphology. Acquisition started 0 h after seeding. GaP nanowires (diameter 80 nm, length 4 μm, density 0.1 nanowires μm^{-2})	Paper IV
Movie S12	Cell migration behaviour following division. Acquisition started 0 h after seeding. GaP nanowires (diameter 80 nm, length 4 μm, density 0.1 nanowires μm^{-2})	Paper IV
Movie S13	Problematic cell division. Acquisition started 24 h after seeding. GaP nanowires (diameter 80 nm, length 6.7 μm, density 1 nanowire μm^{-2})	Paper II